IMPLEMENTING SHAPE MEMORY POLYMERS IN INTERACTIVE 4D KIRIGAMI STRUCTURES

A Dissertation

by

JESSICA B. REESE

Submitted to the Graduate and Professional School of
Texas A&M University
in partial fulfillment of the requirements for the degree of

DOCTOR OF PHILOSOPHY

Chair of Committee,	Arun Srinivasa
Co-Chair of Committee,	Jinsil Hwaryoung Seo
Committee Members,	J.N. Reddy
	Vinayak Krishnamurthy
Head of Department,	Timothy Jacobs

August 2021

Major Subject: Interdisciplinary Engineering

ABSTRACT

The aim of this thesis is to explore the relative efficacy of a novel manufacturing process (called 4D kirigami) for creating foldable and deployable components out of thermally responsive multifunctional shape memory polymers (SMPs) sheets. This work focuses on thermally responsive SMPs that switch states at a glass transition temperature, T_g, with incorporated thermochromic and photochromic powders that change color in response to stimuli.

The work studies the efficacy of laser-cutting and CNC-machining for the creation of groove patterns in SMP sheets for folding. We found that the CNC-machining caused less damage in the heat affected zone immediately surrounding the folds. Using a heated tip atomic force microscope, we also found that laser-cutting the material caused a decrease in T_g. The work outlines parameters such as springback angle, recovery angle which informs the creation of advanced kirigami structures. Two prototypes were created using advanced kirigami by CNC milling a bi-layer SMP: an origami cube and pyramid.

We also investigate the creation of tangible interactive structures (using the 4D kirigami on SMP sheets described above) for learning and Do it yourself (DIY) assistive technology (AT) for aesthetics as well as for functionality. Two interactive artworks were created, as a teaching tool, to reveal the intricacies associated with natural phenomena. One artwork demonstrates the natural cycles of a flower unfolding. Another artwork demonstrates the stretching of a chromatophore through an auxetic SMP.

The work builds on tangible interactive design, by creating DIY AT. The work presents an orthotic prototype for stroke patients with hypertonia using SMP with thermochromic powder. The powder gives visual feedback as to the state change of the material allowing stroke patients to adjust their device on their own. The work looks at how a child could create DIY AT and outlines how crafting techniques were used to aid children in thinking through complex 2D to 3D design. Also, how children feel empowered by the process of designing DIY AT.

DEDICATION

To my husband, Jarrod, who encouraged me to persevere throughout the process and provided support to finish the course. To my parents who gave me confidence to continue trying despite setbacks. To my daughter Evangeline who was "good news" and an unexpected blessing during this process. To my unborn child that was miscarried, I cherish the short time I had with you while completing my PhD. To my son Elias, you bring laughter to everyone around you. To my new daughter, Winifred, may you feel loved and appreciated.

ACKNOWLEDGMENTS

I would like to thank my parents who guided me and provided emotional support throughout this difficult process. I would also like to thank my husband who helped encourage me and to create time for me to finish my dissertation work.

I am grateful to my advisor, Dr. Arun Srinivasa, for his guidance and encouragement to complete this work. I am also grateful for the guidance from my co-advisor, Dr. Jinsil Hwaryoung Seo, who has helped me increase the breadth of my knowledge and forced me to think in a different context. I would like to thank my committee members, Dr. J.N. Reddy and Dr. Vinayak Krishnamurthy for their willingness to provide encouragement and feedback that forced me to think through this material critically.

I appreciate Dr. Terry Creasy for allowing me to use his laboratory facilities and for taking time out of his schedule to help me troubleshoot issues with equipment and fabrication that arose during my dissertation work. I would like to thank Jim Titus in the Texas A&M Woodshop for helping with the CNC milling in Chaper 4. I am grateful to Zimo Wang for helping with the work related to the nano-AFM and building the Lasersaur. I would like to also thank Dr. Satish Bukkapatnam for allowing access to the nano-AFM. I would like to acknowledge use of the Soft Matter Facility and thank Dr. David Truong and Dr. Peiran Wei for assistance with the DSC measurements in Chapter 3.

I would like to thank all the student members of the MEEN 402-501 Senior Design Team, as well as, the members of the ENGR 491 "Smart Prosthetics" Aggie Challenge Team at Texas A&M University that helped in the case studies included in Chapter 6. I am also grateful to a local orthotist, Matthew Zurcher, CPO, LPO of Central Texas Orthotics and Prosthetics that helped provide feedback for the design for Orthorigami for stroke patients. I would also like to thank Visualization students Emily Gueldner, Annie Sungkajun, and Michael Copeland, who facilitated the Orthorigami workshops with children.

CONTRIBUTORS AND FUNDING SOURCES

Contributors

This work was supported by a dissertation committee consisting of Professor Arun Srinivasa (co-advisor) of the Department of Mechanical Engineering, Professor Jinsil Hwaryoung Seo (co-advisor) of the Department of Visualization, Professor J.N. Reddy of the Department of Mechanical Engineering, and Professor Nnf Vinayak of the Department of Mechanical Engineering. The data from the nano-AFM in Chapter 3 was collected by Zimo Wang. All other work conducted for the dissertation was completed by the student independently.

Funding Sources

Graduate study was supported by a fellowship from Texas A&M University.

NOMENCLATURE

AT	Assistive Technology
DSC	Differential Scanning Calorimetry
nTA	nanoscale thermal analysis
PPI	Pulses per Inch
SMP	Shape Memory Polymer
SMA	Shape Memory Alloy
T_g	Glass Transition Temperature
UHMWPE	Ultra High Molecular Weight Polyethylene
ρ	Density

TABLE OF CONTENTS

Page

LIST OF FIGURES

FIGURE Page

LIST OF TABLES

TABLE Page

1. INTRODUCTION, LITERATURE REVIEW, AND MOTIVATION

1.1 Review of Shape Memory Polymers

Shape memory polymers (SMPs) are thermoset or thermoplastic materials that have the ability to “remember" a permanent shape. These polymers regain their permanent shape from a deformed shape when an external stimuli such as a chemical, thermal, photonic, or pH stimulus is applied. A representation of a thermally induced shape memory effect is given in Figure 1.1. Some examples of thermally induced SMPs are polyurethanes, polyurethanes with ionic or mesogenic components, block copolymers consisting of polyethyleneterephthalate and polyethyleneoxide, block copolymers containing polystyrene and polybutadiene, polyesterurethanes with methylenebis and butanediol [1].

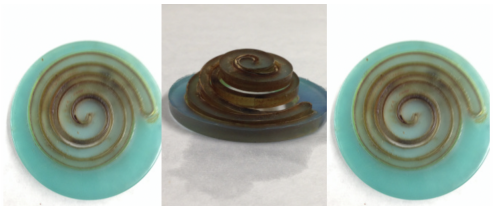

Figure 1.1: Shape memory cycle: (Left) SMP is in its permanent shape. (Middle) Heat is applied to heat the SMP above the T_g. In the heated state mechanical force is applied to stretch the SMP. The force is held while the SMP cools below the T_g. (Right) The SMP is heated above the T_g and returns to the permanent shape.

In the case of thermally induced SMPs, the mechanical properties change around a transition temperature, usually either the glass transition temperature or the melt temperature. Lendlein and Kelch state “that the shape memory effect is not related to a specific material property of single polymers; it rather results from a combination of the polymer structure and the polymer morphology together with the applied processing and programming technology" [1]. Within this framework, the processing occurs when the components of a SMP are mixed and poured into a mold to

cure, and its permanent shape is set. The programming takes place by applying an external force which allows the SMP to be deformed and locked into a temporary deformation state. Several authors have attempted to illustrate the mechanism behind SMPs at the molecular level. In particular to describe SMPs with covalently crosslinked networks, the analogy of a material containing “frozen" segments and “soft" or “switching" segments is used [26]. In this case, the chemical structure of the “frozen" segment creates an immobile link in the polymer network, while the flexible structure of the “soft" segment creates a reversible phase. Figure 1.2 represents this concept. In Figure 1.2, the large black dots represent strong covalent crosslinks attached to the corresponding “frozen" segments. The succeeding depiction is the material at the transition temperature with a mechanical force applied. The “soft" segments allow for the deformation shown in the figure due to degrees of freedom in their chemical structure. This shape is then locked in by lowering the temperature and subsequently removing the force. Once the material is heated again, the “soft" segments can go through a reversible phase transformation to return the material to the initial shape [26].

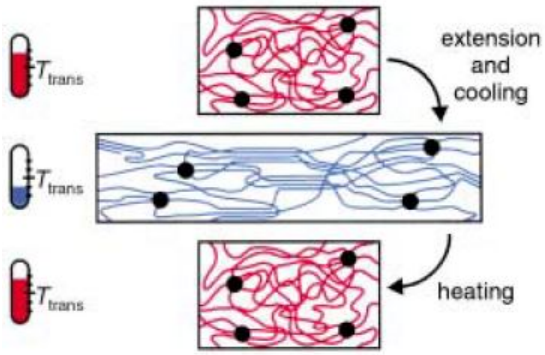

Figure 1.2: Representation of the molecular structure of the thermally induced shape memory effect [1].

1.2 Review of Applications of Shape Memory Polymers

Due to the duality of material at various phases, SMPs provide a unique amalgamation of properties that can be assets to a variety of applications. These materials are also usually low cost, low density, biocompatiable, and biodegradable. Despite these distinctive capabilities and advantages SMP materials provide to design, their initial discovery and wide use was gradual. The first patent of a shape memory effect occurred in 1941, but the first pronounced use of a SMPs was in the 1960s with polyethylene used in heat-shrinkable tubing and films [27]. Significant research in this subject began to take prominence starting the 1980s. Figures 1.3-1.4 represents the variety of uses of SMPs today and their various forms.

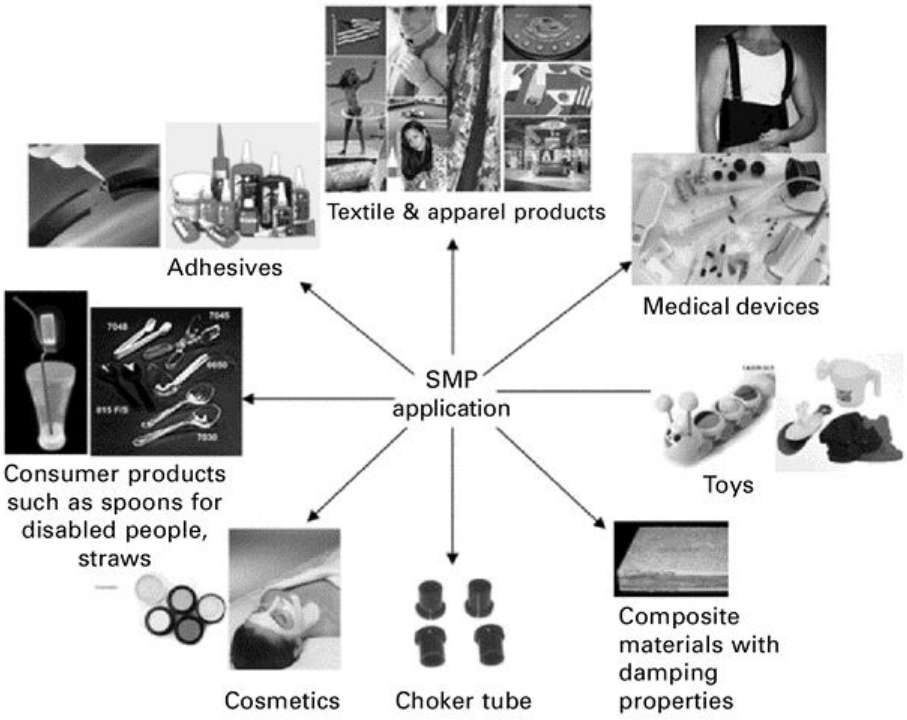

Figure 1.3: Applications of SMPs [2].

Since the 1980s, the development of different types of SMPs has largely been dominated by a small number of research groups tailoring SMPs for specific applications, including: biopoly-

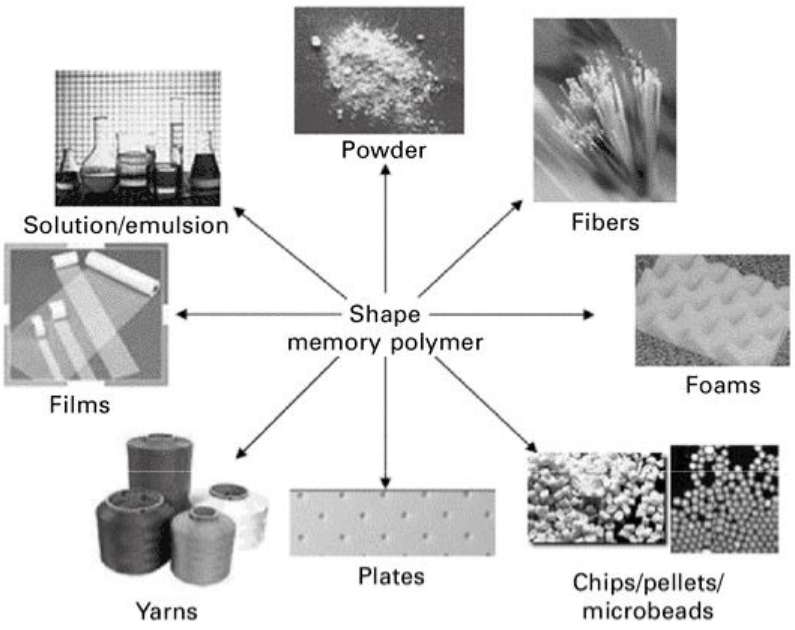

Figure 1.4: Application forms of SMPs [2].

mers, natural sources, composites and simulation, hydrogels, medical devices, liquid-crystal elastomers, and various other applications [27]. Lendlein and Langer's group worked in the area of biopolymers, particularly biodegradable SMP applicable to medical applications [27]. Their group fabricated a self-tightenable biodegradable suture from a SMP thermoplastic monofilament fiber [3]. This SMP suture is shown in Figure 1.5. Other areas for use of biopolymer SMPs include biodegradable catheters, smart stents, and orthodontic applications [27]. Larock and colleagues developed SMP from natural sources, specifically through copolymerization of natural oils, like fish oil and soybean oil. Both oil based SMPs provide tunable glass transition temperatures [28],[29]. In particular, the soybean oil based SMPs exhibit a high degree of control of shape memory properties based on chemical composition [29]. Gall and coworkers have focused on SMP composite and simulation systems for use in Biological MicroElectroMechanical Systems such as gripping/releasing systems employed in minimally invasive surgery [30]. Osada's group worked on shape memory hydrogels, which have application in the area of drug delivery systems, as a separation barrier that can adjust the volume of liquid absorbed, chemical valves that regulate

flow through expansion and contraction, and as an electrically driven worm-like muscle or “mobile" polymer [31]. Wilson and coworkers used SMP in medical device applications. Their work specifically focus on the actuation of SMP devices within the body or use of SMP devices for the relief of stress. They created an SMP dialysis needle adapter to relieve hemodynamic stress caused by flow impingement [32]. Buckley *et. al.* demonstrated the feasibility of inductively heated SMPs (loaded with nickel zinc ferrite ferromagnetic particles) for medical devices such as expandable stents and intravascular medical applications [33]. The researchers have also developed micro-actuator type SMPs for mechanically removing neurovascular occlusions which result in ischemic stroke [34]. Lehmann and researchers have worked on developing liquid-crystal elastomer material for mechno-electric applications like nanoscale transducers, sensors, actuators, motors, pumps, and medical microrobots [35]. Thomsen’s group also worked on liquid-crystal elastomers for application with artificial muscles [36]. Mather and Liu worked with other researchers for the use of SMPs in various other applications such as actuators and high temperature medical devices (artificial muscles, stents, and catheters) [37], [38], [39],[40]. Specifically, Rousseau and Mather created a main-chain siloxane based liquid crystal elastomer exhibiting shape memory effect to be used in soft actuator applications [37]. Mather and colleagues also investigated the use of norbornyl-polyhedral oligomeric silsesquioxane macromer hybrid copolymers. Their work has demonstrated that these hybrid copolymers would be useful in high temperature applications [39].

Despite the apparent advantage of SMP materials to certain applications, Lendlein and Kelch state that only a small number of applications have been implemented, since only a few SMPs have so far been investigated and even less are available on the market [1]. Also, there are still large strides to be made to streamline the use of SMPs, in particular, for thermal based SMPs, issues related to the constraint of transition temperature, modulus plateau, processing, and creep/fatigue life of the polymer [27].

1.3 Survey of Manufacturing Methods of SMP

In order to harness the advantages of SMPs for specific applications, such as stents, complex geometry is required. The question then arises how should these complex geometries be produced?

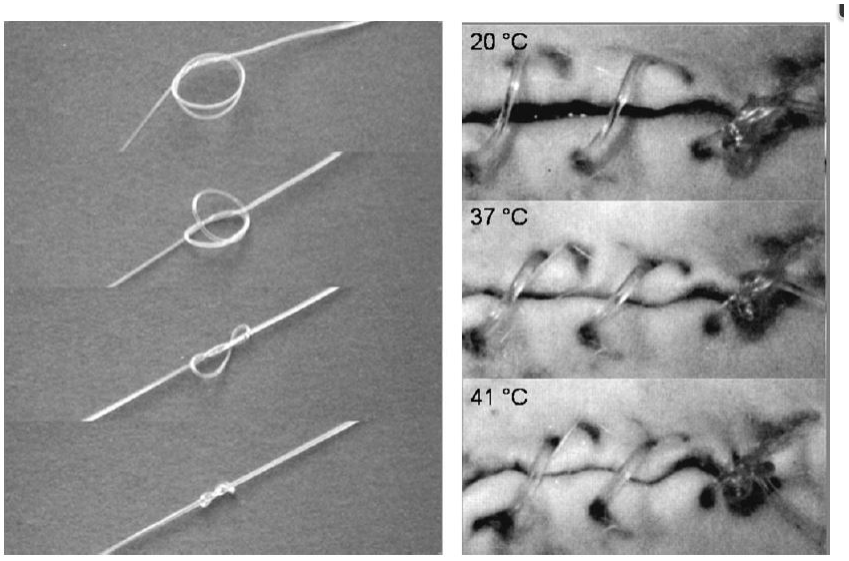

Figure 1.5: SMP suture self-tightening at elevated temperature [3].

Is it better to create complex geometry through individual molds or should traditional manufacturing techniques be employed to produce a variety of shapes without additional cost for molding?

These traditional manufacturing processes can be divided into two categories: additive and subtractive manufacturing processes. Additive manufacturing processes being those involving the deposition of material layer upon layer to create geometric shapes. Subtractive manufacturing processes create complex geometry through precise cutting away of material. A list of some common additive and subtractive manufacturing processes is presented in Table 1.1.

Additive manufacturing processes such as rapid prototyping and 3D printing have been around since the 1980s for industrial applications. Several additive manufacturing processes are available today, and they provide the ability to fabricate almost any shape that can be generated in a CAD model. Despite wide spread use, additive manufacturing processes are limited by design iteration speed. In the case of 3D printing, there is large freedom in the shapes produced; however, since objects are assembled from individual voxels the time required to build the volume makes the process slow compared to conventional manufacturing methods like forming and cutting [4],[41]. Another deficiency of additive manufacturing is that the part dimension is limited to the available printing space [42]. It is common to consider additive manufacturing as a way to create complex shapes

but due to the fact that these manufacturing processes are usually based on thermal deposition, there could be significant variations of transition temperatures and subsequent recovery properties of SMP when these are carried out.

Phenomena	Material Removal Processes	Material Addition Processes
Chemical Processes	Chemical Machining Electro-chemical machining	Stereo-Lithography (photo-polymerization) Laser-induced CVD
Thermo-physical Processes	Laser beam machining Plasma beam machining Electron beam machining Electro discharge machining	Selevtive laser sintering Plasma spraying Electron beam sintering Electro-discharge deposition
Liquid jet processes	Water jet machining	3D ink jet printing
Solid jet processes	Abravise machining	Powder jet laser cladding
Ultrasonic processes	Ultrasonic machining	

Table 1.1: Types of additive manufacturing processes.

1.4 Motivation and Objective: Kirigami, a New Way to Make Complex SMP Shapes

The present study seeks to leverage the properties of SMP combined with subtractive processing and subsequent thermally induced bending or folding (aka Kirigami) to create complex 3D geometries from 2D geometries. Mueller et al. pioneered this research with the use of laser-cutting acrylic sheets to create what she termed as “LaserOrigami." LaserOrigami allows users to laser-cut 3D structures by bending the workpiece rather than by means of joints, thereby eliminating the need for manual assembly [4]. This fabrication method works by taking a laser-cutter and applying a focused beam for a cut and defocusing the beam to increase the heat affected zone to bend the work piece. An example of the method is given in Figure 1.6. The main advantage of constructing a 3D structure from a 2D structure is that the iteration time is extremely short in comparison to additive manufacturing processes. However, according to Mueller et al. this process is subject to limitations. (1) LaserOrigami is limited to object shapes that can can constructed by cutting, folding, and stretching the material. (2) Works only with material that become compliant when heated

up. (3) Limited length of what can be bent or suspended in one piece. If a bend is too long, it cools down faster than the laser can heat it up. (4) Limited material thickness, again limited by the power of the laser [4]. Mueller et al. used acrylic sheets which have a unique behavior during laser processing. When acrylic is laser-cut the material boils off vapor of methyl methacrylate. Therefore, minimal material degradation occurs due to the process being purely a phase transformation to solid to liquid to vapor [8].

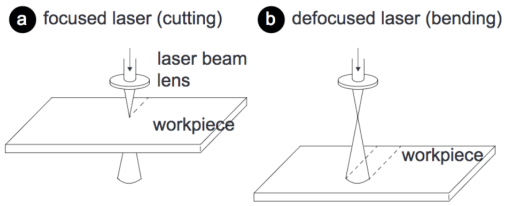

(a) LaserOrigami cuts the work piece by focusing the laser on the work piece and it bends by defocusing the laser.

(b) A pen holder created using LaserOrigami.

Figure 1.6: Using LaserOrigami to create a product [4].

The thermal switch of the SMP will provide a material that is compliant at elevated temperatures. However, direct application of the process Mueller et al. used to create origami from 2D structures will yield differing results. Mueller et al. employed acrylic which has a clear phase transformation, as explained earlier, under laser heating and bent due to gravitational force. Thermally induced SMPs have an entropic driving force within the SMP that will want to return the SMP to its permanent shape. Therefore, the SMP will not bend under its own weight. This work seeks to incorporate the ideas from the previous works by pairing the thermal properties of SMP with manufacturing processes and origami techniques to create an infinite number of 3D structures from the same 2D plate structure. In order to accomplish this goal, the 2D plate structure is cut using subtractive manufacturing processes and bent into the 3D structure. This work seeks to answer the to design 3D shapes from 2D sheets using SMP.

1.5 Research Questions

In order to design 3D shapes from 2D sheets using SMP, the work seeks to answer the following questions:

- Is it possible to create complex 3D structures from 2D SMP sheets using subtractive manufacturing processes?
- How does various manufacturing processes, such as laser-cutting, affect the material structure and performance?
- How do manufacturing processes, like laser-cutting, compare with more traditional milling and cutting in terms of property retention, material degradation, and performance?
- What structures can be created harnessing the origami nature of this design method? How can these structures be used in interactive design?
- How can DIY assistive technology (AT) be made using origami techniques?
- How children make and design with smart materials, specifically SMP? How children create and design with SMP to make DIY AT? How using SMP in design can affect children's creativity and confidence and provide a positive, enabling experience? What types of tools or fabrication or crafting technology aid children in design of DIY AT?

1.6 Structure of the Dissertation

The structure of this dissertation is as follows:

1. Chapter 1 gives an accordant background related to shape memory polymers, including behavior and applications. Also, the chapter contains the background related to manufacturing techniques and the motivation for the present study. The research question and the scope of the dissertation are given as well.

2. Chapter 2 discusses the chemical composition and reaction to create the SMP used in this research. The method of molding and curing the SMP is discussed. Furthermore, various methods of casting SMP sheets to make folding structures are covered.

3. Chapter 3 provides background with regards to laser-cutting, including basic information on parameters associated with the process and prior research on cutting of polymer materials. Also, this chapter includes experimental work look to assess the heat affected zone, T_g, and residual stress due to varying laser parameters.

4. Chapter 4 presents additional background on machining of polymeric materials, as well as, folding structures created using SMPs. This chapter specifies some results related to machining the SMP and depicts some folding structures created from machining.

5. Chapter 5 gives a review of prior artwork created using shape memory materials and a review of work in biomimicry. The end of the chapter presents two biomimicry inspired artistic applications using SMPs.

6. Chapter 6 explores the use of SMPs in orthotic devices. Specifically, the chapter reviews previous work related to DIY Assistive Technology (AT). The research looks at how to create DIY AT for stroke patients, for children that can be adjusted as the child grows, and how children design DIY AT.

7. Chapter 7 summarises the work presented in this dissertation and presents future work in relation to this work.

2. FABRICATION OF SMP MORPHABLE STRUCTURES

2.1 Chemical Structure of SMP

In order to design these "smart" origami structures, the formulation presented by Xie and Rousseau containing SMPs with modifiable glass transition temperatures was used. Xie and Rousseau created a tunable polymer structure by varying the mole ratios of neopentyl glycol diglydicyl ether (NGDE) and bisphenol A epoxy monomer (Epon 826) with the curing agent poly(propylene glycol) bis(2-aminopropyl) ether (Jeffamine D-230) [21]. The chemical structure of each of these components is given in Figures 2.1-2.3.

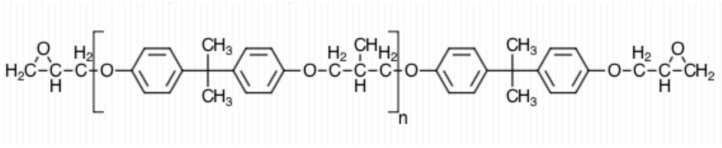

Figure 2.1: Structure of Epon 826 resin, n=0.085.

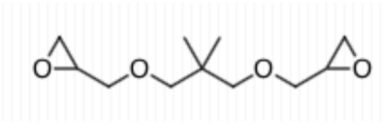

Figure 2.2: Structure of neopentyl glycol diglycidyl ether (NGDE).

The amine groups react through a ring opening poly-addition polymerization to create an amorphous thermoset network polymer. This reaction is given in Figure 2.4. Note that Jeffamine D-230 has a functionality of four, because it reacts with four epoxide groups, and NGDE and Epon 826 each have a functionality of two since each has one epoxide group on each end of the molecule for

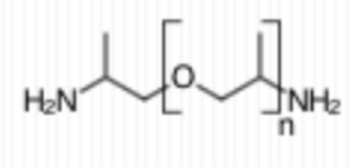

Figure 2.3: Structure of Jeffamine D-230 (n 2.5).

a total of two epoxide groups. This variation in functionality gives the mix ratio as one mole of Jeffamine D-230 to two moles of NGDE and Epon 826 combined.

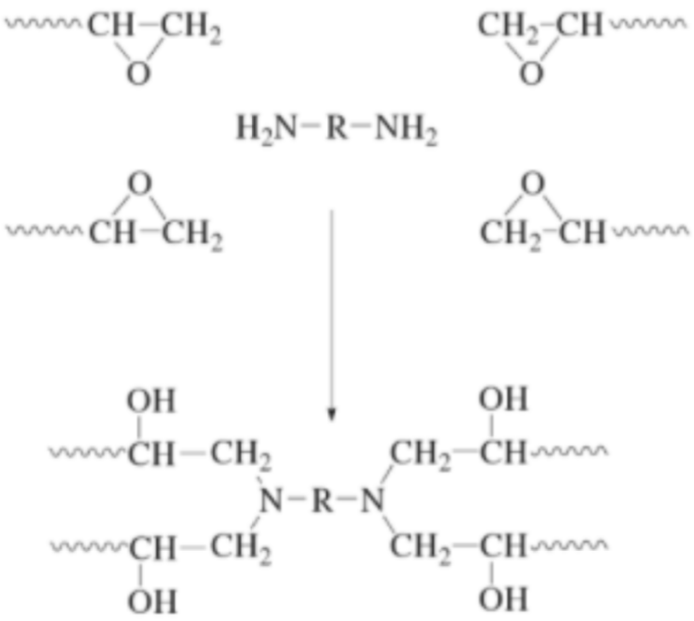

Figure 2.4: Poly-addition reaction of a diamine with epoxide groups [5].

The fully reacted polymer is given in Figure 2.5, where the nitrogen bond represents the location of the covalent crosslink within the structure. The NGDE and Epon 826 in between the crosslinks behave as either a “soft segment” or a “frozen segment” within the SMP. Epon 826 comprises the “frozen segments” due to the aromatic rings within the backbone. The “soft segments” come from the flexible aliphatic backbone of NGDE which increases the chain flexibility

by introducing rotational degrees of freedom, thus allowing for deformation above the T_g. By tailoring the proportion of chain flexibility, various SMP formulations can be made. The resulting formulations by Xie and Rousseasu and the associated T_gs are given in Table 2.1.

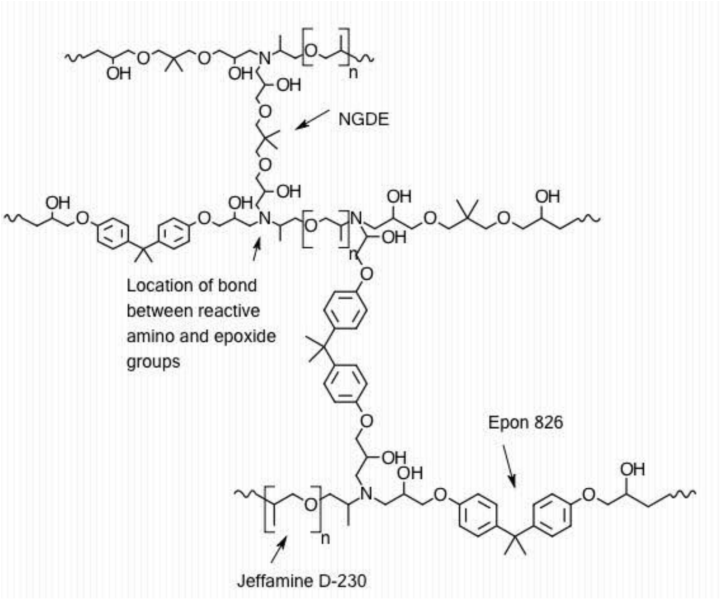

Figure 2.5: Chemical structure of the shape memory polymer.

Samples	Epon 826 (mol)	Jeffamine D-230 (mol)	NGDE	T_g (°C)
NGDE1	0.015	0.01	0.005	60-80
NGDE2	0.01	0.01	0.01	40-60
NGDE3	0.005	0.01	0.015	20-40
NGDE4	0	0.01	0.02	0-10

Table 2.1: Composition of the epoxy samples [21].

2.2 SMP Fabrication

In order to fabricate the shape memory polymer, a male mold was made from a 3D print of a solid model or milled out of an aluminum block. Each 3D printed mold was sanded and cleaned.

The aluminum molds were cleaned using compressed air or acetone. Next a female mold was made by casting silicone rubber, Mold Max 40, based on the volume of the Solid Works model, into the male mold and allowing the rubber to cure for 24 hours. An example of the male and associated female mold is given in Figure 2.6. Once, the silicone mold was cured, the SMP was made by selecting the desired T_g and converting the mole ratios given in Table 2.1 to volume or weight ratios using the properties given in Table 2.2.

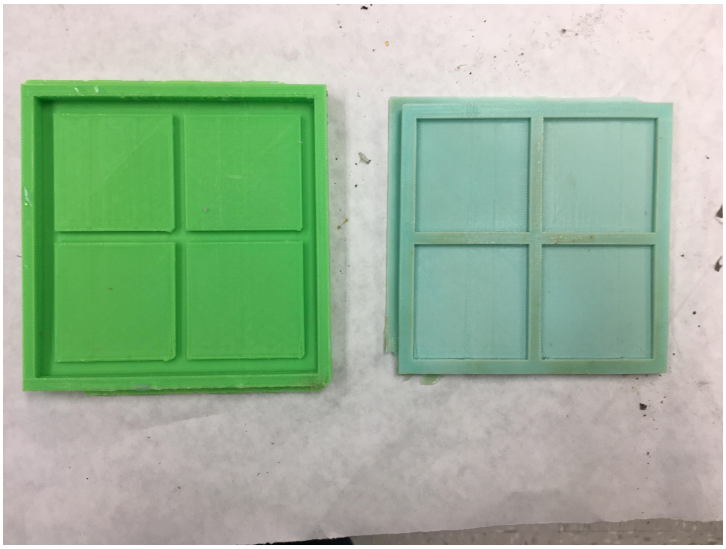

Figure 2.6: Male and female molds for casting SMP: (Left) ABS mold (Right) silicone mold.

Component	ρ **(g/ml)**	**Molar Mass (g/mol)**
Epon 826	1.16	364.055
Jeffamine D-230	0.948	230
NGDE	1.04	216

Table 2.2: Component properties of SMP.

To mix the samples, the following procedure was used:

1. Some Epon 826 was placed in a glass container and heated on a hot plate at 110°C until the viscosity was reduced and there was no appearance of bubbles in the mixture.

2. Based on the desired T_g the Jeffamine D-230 and NGDE were measured by weight in separate cups.

3. After the Epon 826 was sufficiently heated, the appropriate amount was measured and all three components were stirred together with a tongue depressor.

4. The mixture was placed under vacuum at 30 in Hg and vacuumed for 2 hours or until no bubbles remained.

5. The vacuumed mixture was poured slowly into the silicone mold, allowing the polymer to fold over itself and the inertia of the pouring to push the SMP to the outer edges of the mold. This pouring method ensured that any remaining bubbles in the mixture would be pushed to the outside of the mold.

6. The mold was cured for 1.5 hours at 100°C and then post-cured for 1 hour at 130°C in a convection oven.

7. The SMP was allowed to cool at room temperature and then de-molded.

The research wishes to explore how to use SMP in interactive design and to create wearable technology for users with disabilities. Therefore, color change was incorporated to provide an interactive visual component to incorporate into the design of interactive artworks and to provide the ability to sense when the material stiffness changed for those lacking a strong sense of touch. The color change was created by placing color changing powder and dye and incorporating it into the matrix. The appropriate amount of powder per the total volume of SMP was measured and added into the Jeffamine D-230 in Step 2. The amine/powder mixture was then sonicated. Then the components were mixed together according to Steps 2-7. These thermochromic and photochromic powders were purchased from Sparkfun, Solar Color Dust, and QRC Solutions. These powders are

called leuco-dyes, which reversibly switch from a colored state to a clear state due to an external stimulus causing the chemical structure to switch from one form to the next form.

Additionally, Castin' Craft dye purchased from Hobby Lobby was also employed. The dye was added to the NGDE in Step 2 and then components were mixed following the succeeding steps. An example of a blue thermochromic SMP with yellow dye incorporated into the matrix is shown in Figure 2.7.

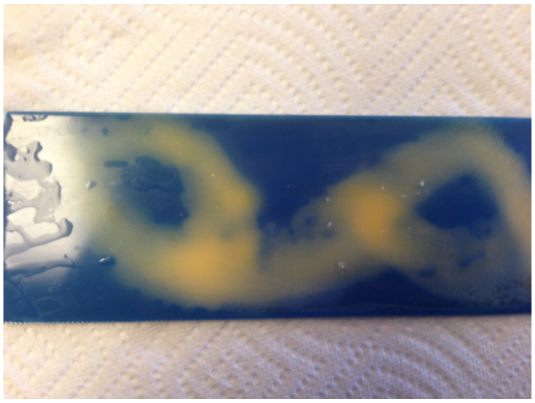

Figure 2.7: SMP with incorporated thermochromic powder and dye.

2.2.1 Fabrication of Large SMP Sheets Using Gravity Flow

To design morphable structures using subtractive manufacturing methods, the ability to cast a large SMP sheet is desired. Two methods of casting large SMP sheets were used. The first method exploited the self-leveling features of the epoxy. For this method an aluminum plate was prepared by cleaning the surface several times with acetone. Then yellow tacky tape was used to create the square boundary for the part. A second square creating an additional outer boundary was created using the tacky tape. A picture of the plate with the tacky tape is given in Figure 2.8. This method works, because as the epoxy heats up, the density of the epoxy becomes close to water, causing the epoxy to flow. The flow allows excess epoxy to move into the outer barrier, "dam", and the top surface in turn levels out. Next a mold release agent was applied to the plate. For the initial

trial a carnauba wax, Johnson's Paste Wax, was applied. The wax was applied by taking a small rolled ball of the wax and placing it in a cheesecloth. The cheesecloth was rolled in a circular motion across the desired mold area. The wax was allowed to set for a few minutes, then the excess was wiped from the area. The process was repeated for a minimum of four times. In later trials, Frekote 700-NC was used as the mold release agent, because it did not leave a residue on the SMP. The prepared plate was placed in the oven at 100°C for 30 minutes to pre-heat the plate. The SMP was poured into the center of the plate and allowed to overflow into the dam portion and cured according to the procedure given previously. Once the SMP was cured, the plate was removed from the oven and allowed to cool. The resulting plate was then carefully sheared off using a scraper and a hammer. An image of one of the plate made using this method is given in Figure 2.9. The limitations of this method were due to the fact that the minimum part thickness was determined by the thickness of the tacky tape. Further limitations, include issues with obtaining a level plate during curing. Also, it is difficult to extract the part from the aluminum plate, as small cracks in the part are created easily.

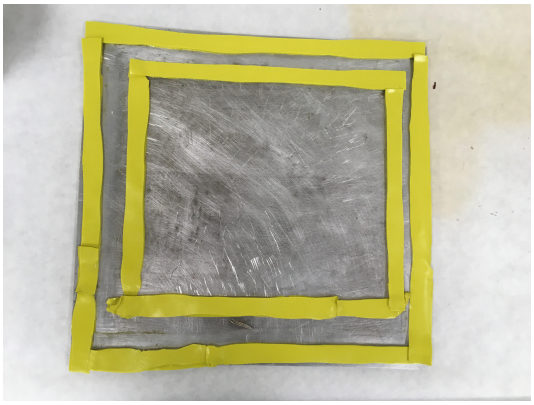

Figure 2.8: Prepared aluminum plate with tacky tape for sheet casting.

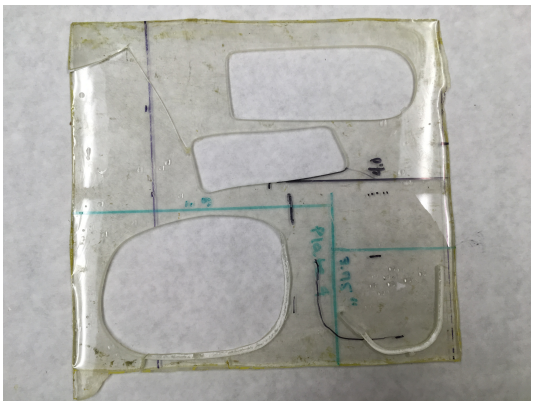

Figure 2.9: CNC machined SMP sheet created by self-leveling epoxy method.

2.2.2 Fabrication of Large SMP Sheets Using Injection Molding

Injection molding with pressure casting was also used to fabricate large SMP sheets. Pressure casting reduces the visibility of air bubbles, because when resin is placed under pressure, the air bubbles created in mixing shrink to the point which they are not visible. For the injection molded part, an aluminum clamshell mold was milled with a square cavity with rounded edges. Three additional bleeder pathways were added at the top of the cavity. This mold contained a hole to attach the port connection to the pressure pot. The other half of the mold was a flat sheet. These two halves were bolted together. In order to prepare the mold, the surfaces were cleaned with acetone. Next, Frekote 700-NC was applied as a release agent to the surface. The volume of SMP was calculated based on the volume required for the mold, plus the additional volume required for the tube connecting the pressure pot to mold. The components of the SMP were mixed in a vacuum mixer. The cup of SMP was placed in a modified Speedair 6Z899 2.5 gallon paint pressure tank. The pressure tank set at a height above the port. Plastic tubing was used to connect the pressure tank to the port in the mold. Wood dowels were used as a dipstick to check the if the resin had reached the top of the mold. Once pressure pot and mold were set-up, the tank was pressurized and the pressurized resin was allowed to flow into the mold until the dowels indicated the resin had reached the top of the mold. Next, the plastic tube was cut and tied up against the mold. The mold was set, remaining vertical, in the oven and cured at the cure cycle given earlier. Once, the

cure was complete, the mold was removed from the oven and allowed to cure at room temperature. The mold was then unscrewed and removed by shearing the plate from the mold using a flat head screwdriver. A picture of the final product is given in Figure 2.10.

Figure 2.10: SMP sheet made using injection molding with a pressure pot.

2.2.3 Fabrication of Layered SMP Sheets

The thrust of this work is the understanding of how to create 3D structures from 2D structures using origami techniques. Researchers have taken different approaches including additive/subtractive manufacturing, 2D sheets that wrinkle or bend, and 2D sheets that contain hinges [43]. Previous work in this area is discussed further in Chapter 4. This research seeks to create 3D structures from 2D structures using subtractive manufacturing, but also by incorporating hinges that allow for bending. To create a foldable SMP, using a living hinge, a layered SMP was created. This SMP was created using the procedure described in Xie *et. al.* which is a modification of the procedure given previously in this chapter [44]. In order to create a bilayer polymer, two varying T_gs were chosen and the appropriate ratios were measured and mixed according to steps 1-4. The first epoxy layer was poured into the mold as described in step 5 and cured at $100°$C for 40 minutes to create the first layer. The second layer was then poured on top of the first layer with the pouring as described in step 5 and cured at $100°$C for 40 minutes. The layers were then post-cured at $130°$C for 1 hour. A picture of the layered structure is given in Figure 2.11. Castin' Craft dye was incorporated into one of the layers to aide in differentiation of the two layers. Typically for

these structures the desire was to have a “hard” epoxy layer and a “soft” SMP layer. Therefore, the “soft” layer contained NGDE and in turn had shape memory properties. However, the “hard” layer was formed from the combination of Epon 826 and Jeffamine D-230 alone creating a single hard epoxy layer.

Figure 2.11: Layered SMP structure (T_g=50-60°C for the green layer and T_g=80-100°C for the clear layer).

3.1 Laser Processing Fundamentals

Laser machining of materials employs the use of a high speed x-y table with an intensely narrow heat zone due to the highly localized energy density of the laser. Specifically, the area heated by the laser is small with most of the heated material removed, generating low overall thermal degradation and input into the system [8]. A laser converts electrical energy into a high energy density beam of light, defined explicitly as *light amplification by the stimulated emission of radiation* or L.A.S.E.R. [45]. This process works by exciting an atom to a higher energy state through absorption of a photon. For the case of stimulated emission, the atom absorbs two photons with the second photon of the same energy as the preceding photon. This second photon causes the atom to emit a photon of the same energy, wavelength, phase, and polarisation as itself. Hence, creating a coherent light source [6]. The process of photon emission is illustrated in Figure 3.1.

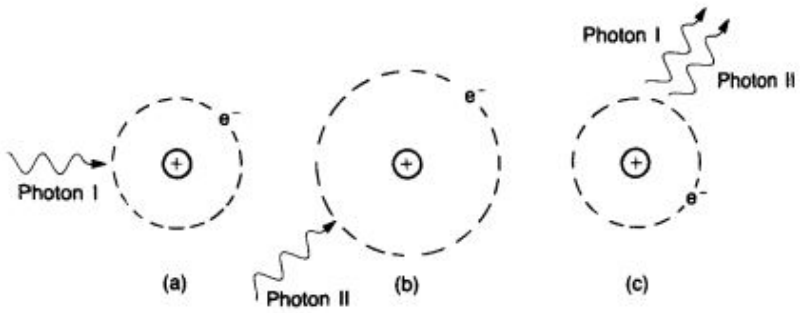

Figure 3.1: (a) An atom absorbs a photon. (b) An increase energy level atom absorbs a second photon. (c) The absorbed photon causes light to be emitted in the direction defined by the stimulating photon, so both photons leave traveling the same direction [6].

This light emitted from relaxation of atomic energy presents a uniquely characterized form of light ideal for localized material removal. Laser light is monochromatic, the photons emitted consist of a single wavelength (color) within a small bandwidth [46]. The light is considered to

be unidirectional in the direction of the excitation photon. This property is called directionality which is defined as a measurement, typically in milli radians, of beam divergence in the direction perpendicular to the light propagation [46],[6]. Cutting lasers can maintain the same diameter over several meters [8]. Laser light is termed spatially and temporally coherent, meaning the light has the same direction, wavelength, and phase. Coherence is term that encompasses monochromaticity, directionality, and phase consistency of the light. This descriptor is what makes laser light useful to cut material with a highly focused “heat spot" and limited thermal deterioration of the bulk material [6], [8].

3.2 Basics of Laser Machining

The preceding section described basic characterization of the laser mechanism to produce laser light and the corresponding properties of the ensuing light. The coming sections will describe laser beam parameters utilized in laser machining processes.

3.2.1 Laser Beam Parameter: Wavelength

The monochromatic light of a laser described earlier may be infrared, visible, or ultraviolet in the spectrum. Table 3.1 shows the wavelength of some common industrial lasers. The materials absorptivity will determine the appropriate wavelength. For example, metals have low absorptivity at 10.6μm, therefore the CO_2 laser will not cut the material and a Nd-YAG laser is a more appropriate choice [45]. At shorter wavelengths smaller spot sizes can be achieved, and in metals more photons can be absorbed causing the reflectivity to fall and the absorptivity of the surface to increases [47].

3.2.2 Laser Beam Parameter: Laser Mode

As stated earlier, laser light is spatially or temporally coherent in terms of phase. The temporal phase of laser light is categorized by either a continuous wave mode or a pulsed beam mode. The continuous wave mode, as the name implies, has emission without cessation. While, the pulsed beam mode is periodic emission of laser light [45]. Most commercially available laser-cutters operate on pulsed beam mode, which has the advantage of greater cutting depth with less power

Type of Laser	Wavelength	Areas of Application
Carbon dioxide	10.6 μm	Material processing, surgery, etc.
Carbon monoxide	2.4-4 μm	Material processing (engraving, welding, etc.)
Hydrogen fluoride	2.7-2.9 μm	Laser weapon
Nd-YAG	1.064 μm	Material processing
Nd-glass	1.062 μm	Velocity and length measurement
Excimer laser	193 nm	Laser surgery
Dye laser	390-460 nm	Medicine, birth mark removal
Ruby	694.3 nm	Tattoo removal, holography
Helium-neon	632.8 nm	Holography, spectroscopy
Argon	454.6 nm	Lithography, spectroscopy

Table 3.1: Wavelength of some industrial lasers [22].

requirement than continuous wave mode. The spatial phase of the laser light describes the laser beam profile. For laser machining purposes a Gaussian profile is ideal due to uniformity of the phase and the in turn formation of small spot sizes [45].

3.2.3 Laser Beam Parameter: Power and Intensity

The output power of the laser determines the type of material which can be machined with the system and the cost. Typically, the highest continuous was power is obtained from CO_2 lasers [45]. The intensity of the laser beam is the optical power per unit area, which is transmitted through an imagined surface perpendicular to the propagation direction with units of W/cm^2 [48]. The intensity may be calculated based on an average of at least oscillation cycle for a given mode of the beam.

3.2.4 Laser Beam Parameter: Focal Length and Beam Diameter

A commercial laser cutter consists of a belt driven x-y table with a stationary laser tube and a series of three angled mirrors. The third mirror is located on a moving head guided by the belt drive. This mirror angles the beam down at the work piece through a focusing lens and nozzle. An illustration of the operation of a laser-cutter is given in Figures 3.2-3.3. The parameters that determine the final spot size are the beam divergence, diffraction, and focal length. Industrial lasers can have beam diameters as small as 0.1-0.5 mm [49]. The focusing lens limits the beam diameter,

a parameter defined a central maximum measured between two points where the intensity has fallen to $1/e^2$ of the central value. For rectangular beams, the minimum beam diameter is given by Equation 3.1 and for single mode circular beams the diameter is given by Equation 3.2 [47].

$$d_{min} = 2f\lambda/\phi_{beam} \tag{3.1}$$

$$d_{min} = 2.44f\lambda/\phi_{beam} \tag{3.2}$$

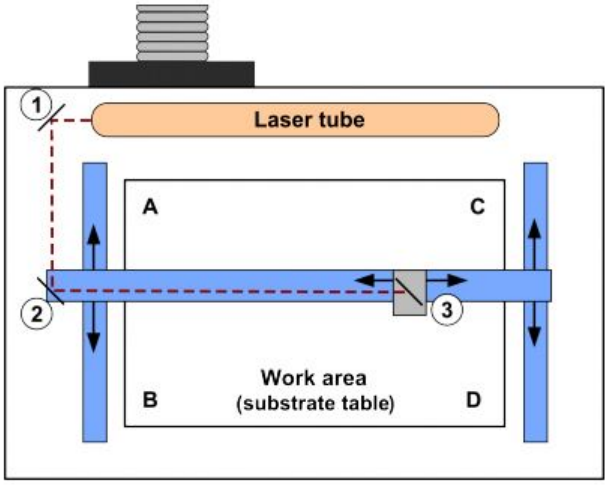

Figure 3.2: A schematic top view of a laser cutter. (The numbers 1-3 depict the location and angle of the mirrors for the laser represented by a red dotted line [7].)

For a beam with an ideal mode, a Gaussian distribution, the radius as a function of the distance from the beam waist diameter. The waist diameter, ω_0, again is the value where the intensity has decreased by $1/e^2$ or 13.5% of the peak value. The size of the Gaussian beam diameter at a distance z from the ω_0 is given by Equation 3.3. An approximation for the waist diameter and depth of focus for small numbers is given by Equations 3.4-3.5 [50],[51].

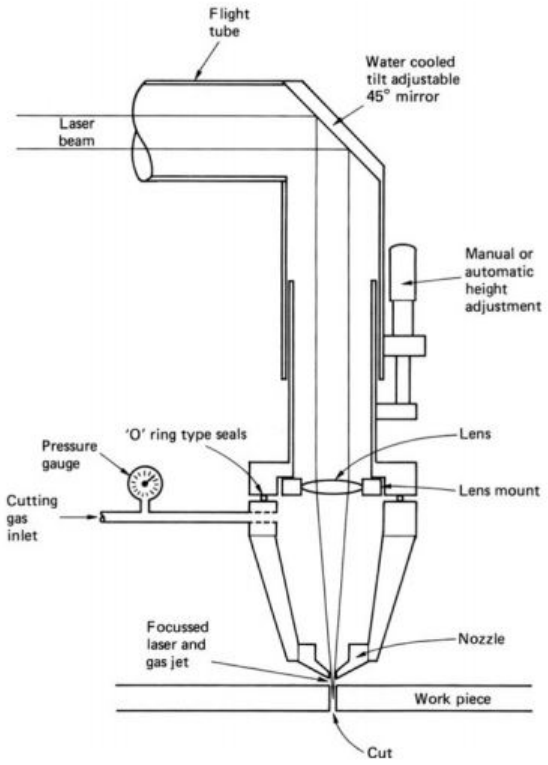

Figure 3.3: A schematic of the laser cutter head [8].

$$\omega(z)^2 = \omega_0^2 \left[1 + \left(\frac{\lambda z}{\pi \omega_0^2}\right)^2\right] \tag{3.3}$$

$$2\omega_0 = \left(\frac{4\lambda}{\pi}\right)\left(\frac{\phi_{lens}}{f}\right) \tag{3.4}$$

$$DOF = \left(\frac{8\lambda}{\pi}\right)\left(\frac{f}{\phi_{lens}}\right)^2 \tag{3.5}$$

3.2.5 Laser Type: CO_2 Laser

As described previously, laser light is beam of light due to the emission of photons from the exciting of atoms due to electrical energy [45],[6]. In the case of the CO_2 laser, the electrical energy is passed across a low pressure gas of CO_2 mixed with nitrogen and helium for additional

Category	Specification
Work Area	1220 x 610 mm (48 x 24")
Dimensions	1700 x 1170 x 360 mm (67 x 46 x 14.2")
Laser	120 W at 10.6 μm (100 W in long-life)
Resolution	0.1-0.03 mm (240-840 dpi)
Maximum Feed/Seekrate	6000 mm/min
Modes	vector, vector fills, raster

Table 3.2: Machine specifications for the Lasersaur [23].

efficiency in proportions of 1:5:20 [8]. The addition of nitrogen allows the CO_2 molecules to increase their excited energy state through collision with excited nitrogen molecules. The addition of helium returns partially excited CO_2 molecules to ground state due to the collision with these molecules [8].

3.3 Lasersaur: Building a Laser-cutter

As stated earlier, one of the objectives is to see if it is possible to create 3D structures from 2D SMP using laser-cutting and how does this processing affect the material. In order to accomplish this task a laser-cutter (Lasersaur) was built. The basics of laser-machining have been described in previous section to aide in the understanding of building the Lasersaur.

The Lasersaur is an open-source based laser-cutter project consisting of a rectangular frame, 120 W CO_2 laser, x-y belt driven gantry system with associated optics and air assist, and electronic controls and software [23]. A picture of the completed Lasersaur is given in Figure 3.4 and some associated specifications are given in Table 3.2. An overview of the build and the components is given here. The rectangular frame was assembled from aluminium extrusion pieces and connected together with brackets. The rectangular frame is divided into two compartments one for the x-y gantry system and separated compartment for the laser. A door opens to allow access to the bed of the laser cutter to place working pieces in the machine. Polycarbonate pieces separate the bed of the Lasersaur from the interior space containing the laser, as well as, cover the exterior frame and door.

After assembly of the frame which included the door, the top and bottom of the frame, and

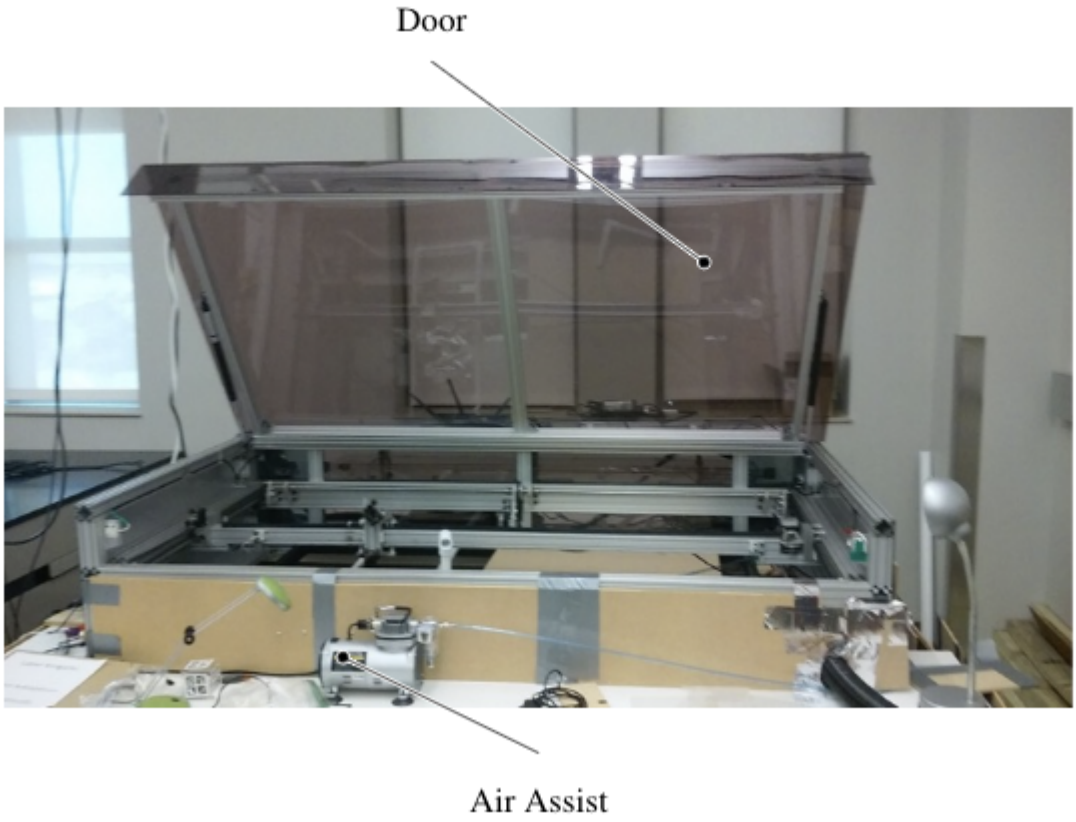

Figure 3.4: Lasersaur laser-cutter fully assembled.

exterior frame of the gantry and interior gantry components were added. Hydraulic pumps connect the door to the main frame and hold it in place when open. The system consists of a x-y gantry system having a rectangular outer frame that attaches to two belt-driven components. The interior y-axis cart was created made of an aluminium bar and attached to the laser cutter outer gantry frame by roller bearings. The y-cart is operated by a belt-driven system and has one optical mirror mounted on its exterior to direct the laser beam. This mirror corresponds to position 2 in Figure 3.2. The x-cart is an aluminum bar attached to the y-cart by roller bearings and holds the third mirror, corresponding to position 3 in Figure 3.2, as well the focusing components of the laser. The x-cart is also a belt-drive system. In the rear of the Lasersaur, the compartment for the laser is contained as well as the first mirror in Figure 3.2 which is attached to the aluminium frame. Some of these mechanical components are shown in Figure 3.5.

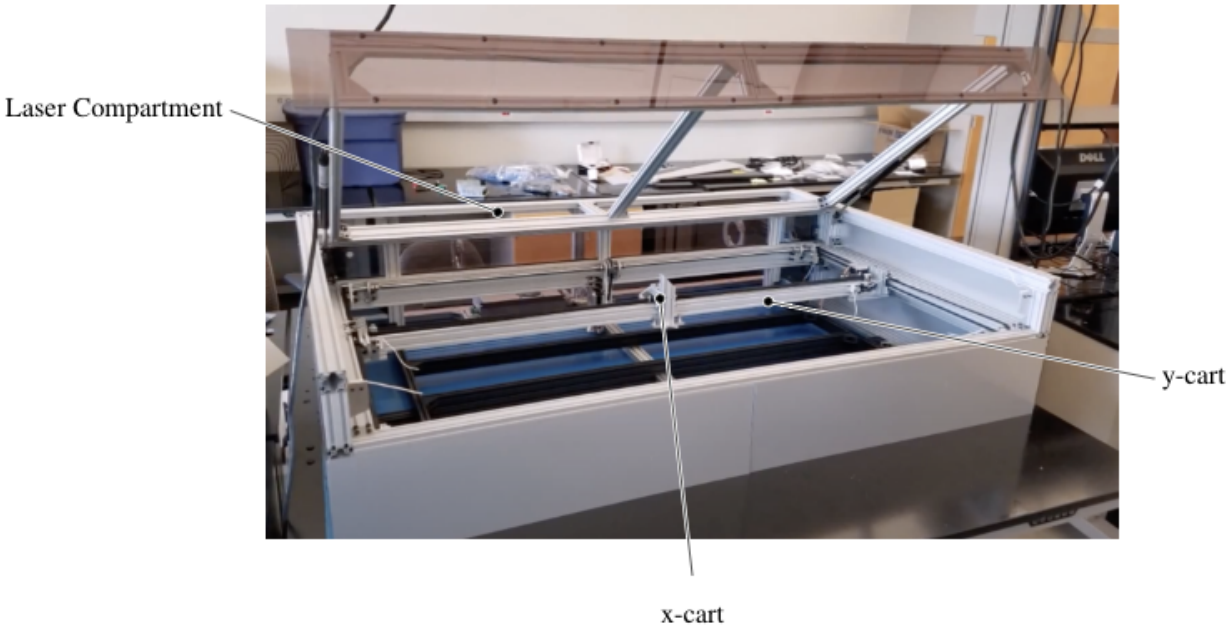

Figure 3.5: Lasersaur mechanical frame components.

The electronic system of the Lasersaur controls both the speed and position of the x and y belt driven drives, as well as, the laser power and the air assist. The electronic system is operated by g-code and contains a driver board to operate the stepper motors for the belt drives, the laser power, and the switches for the door, limit and chiller components. The air assist is a compressor based system attached with a tube to provide air pressure to stop flaming during the cutting process.

3.4 Review of Laser-Cutting Polymeric Materials

In laser-cutting of polymeric materials material removal occurs due to the mechanisms listed in Table 3.3. Melt shearing works by causing the material to reach a liquid phase transition. This molten liquid is blown away by the forced air output at the nozzle. In the melt vaporisation process, the material boils off the surface as a vapor phase. There is minimal chemical degradation as the process approximately a purely physical change from solid to liquid to vapor [8]. Chemical degradation as the name suggests break the chemical bonds within the material, and in general

Type of Degradation from Laser	Material Type
Melt shearing	Thermoplastics (polypropylene, polystyrene, polyethylene, polyamide and acrylonitrile-butadiene-styrene)
Vaporisation	Polymethyl methacrylate and polyacetal
Chemical Degradation	Thermosets (phenolic and epoxy resins, rubber, poly vinyl chloride, polycarbonate and polyurethane)

Table 3.3: Dominant material removal mechanisms for various polymers [8].

leave a layer of residual carbon dust along the cut edge [8]. The SMP is a thermoset epoxy/amine polymer system described in Chapter 2. Therefore, the mechanism for degradation within the structure is chemical degradation. From Figures 2.4 and Figure 2.5, one can infer the structure of the SMP as a three-dimensional network polymer composed of monomer linking units. Powell describes the chemical degradation of these thermosets stating that both chemical and physical work must be input into the system to break the bonds that make up the polymer matrix. This reduces the cutting speed and creates considerable temperatures in the cut zone [8].

Zhurkov and Korsukov categorized the atomic fracture mechanisms in polymers. Through the use of electroparamagnetic resonance to detect ruptured chemical bonds it was shown that under the action of mechanical stress a homolytic scission of macromolecular chains occurs and free radicals are formed. The rate of free-radical generation was found to increase exponentially with increasing tensile stress and temperature [52]. Stuart and Smith investigated the thermal degradation of epoxy-amine systems and suggested that homolytic chain scission may occur at aliphatic carbon-to-carbon, carbon-to-oxygen, and carbon-nitrogen bonds [53]. Davim et al. investigated the effect of CO_2 laser-cutting processing parameters (specifically power, cutting velocity, and gas pressure) and measured the size of the burr and the heat affected zone. Davim et al. included a glass/epoxy fiber system in the investigation and concluded that these systems present a deteriorate surface (burnout) and a high area related to the heat affected zone, consequently poor workability. For this study, the glass/epoxy system had burr dimension of approximately 0.1mm with a

heat affected zone as large as 0.6 mm [54]. Macan and Ivanković discuss the thermal degradation of epoxy/amine systems as very complex and consisting of numerous parallel reactions in which various gaseous and solid products are formed. They state that homolytic chain scission starts around $240°$C and is altogether progressed at $290°$C which causes changes in chemical composition, specifically, a recombination of the free radicals occurs to create new cross-links and a different randomized chemical structure [55]. Laser processing allows for sufficient thermal degradation to cause homolytic chain scission of free radical generation of the SMP. In order to change the T_g of the material, the structural components that inhibit rotation and translation are effected. The T_g of this epoxy/amine system is increased by the stiff backbone of the Epon 826 which contains the aromatic rings. The thermal degration causes restructuring of the backbone of the polymer or breaking of the bond segments and thus decreases the T_g of the material.

Although, several studies have presented characteristics of laser processed epoxy systems and machined epoxy systems there is little information for the affects of processing on SMP characteristics of these types of systems. Therefore, this study seeks to quantify the affect of processing parameters on SMP. In particular for laser-cutting, the size of the heat affected zone, the affect on Tg, and the amount of residual stress for various laser-cutting parameters.

3.5 Experimental Analysis of Laser-Cut SMP

In order the create self-assembling folding structures from SMP, understanding the concentration factors associated with machining the SMP and the impact on the chemical structure is essential. In image of the SMP being laser-cut is given in Figure 3.6. Laser-cutting appears to have an effect on the molecular structure of the polymer and create undesirable changes in specific material properties related to the essential function of the SMP. From the initial work in laser-cutting the SMP, it is apparent that the laser alters the chemical structure which causes a decrease in the T_g. A cast sample with a T_g of 60-70$°C$ which was laser-cut with the following parameters: power of 75 W, speed of 3.15 in/s, PPI of 1000. The resulting laser-cut shape appeared to be maellable in your hand A depiction of the maellable SMP is given Figure 3.7.

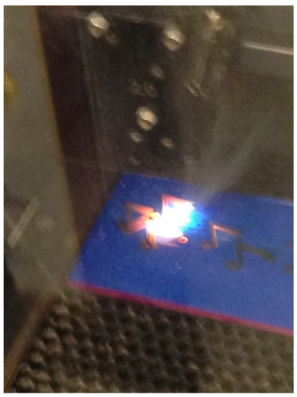

Figure 3.6: SMP being laser-cut using PLS6.150D laser-cutter by Universal Laser Systems.

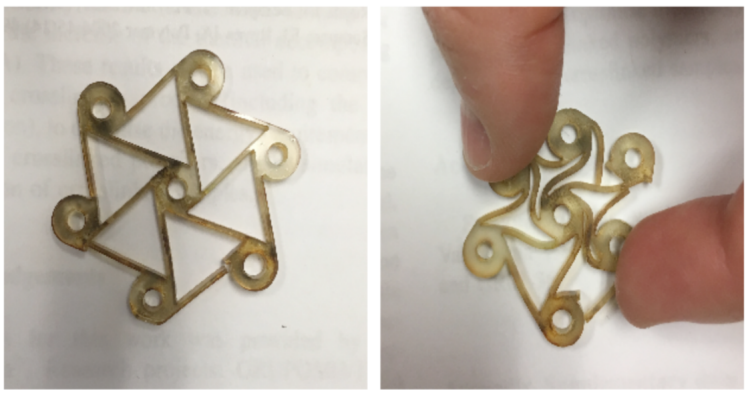

Figure 3.7: Maellable SMP after being laser-cut.

In succeeding sections seek to appropriately quantify the changes related to laser-cutting the SMP.

3.5.1 Microscope Measurements of Heated Affected Zone

Samples of SMP with a T_g of $50°C$ were made and cut. The samples were cast from a mold having dimensions of 50 mm by 50 mm by 3mm. A laser-cutter was used with a 120 W CO_2 laser. An image depicting the SMP before and after cutting, as well as the heat affect zone is given in Figure 3.8. The parameters were changed and the size of the heat affected zone was measured using a microscope.

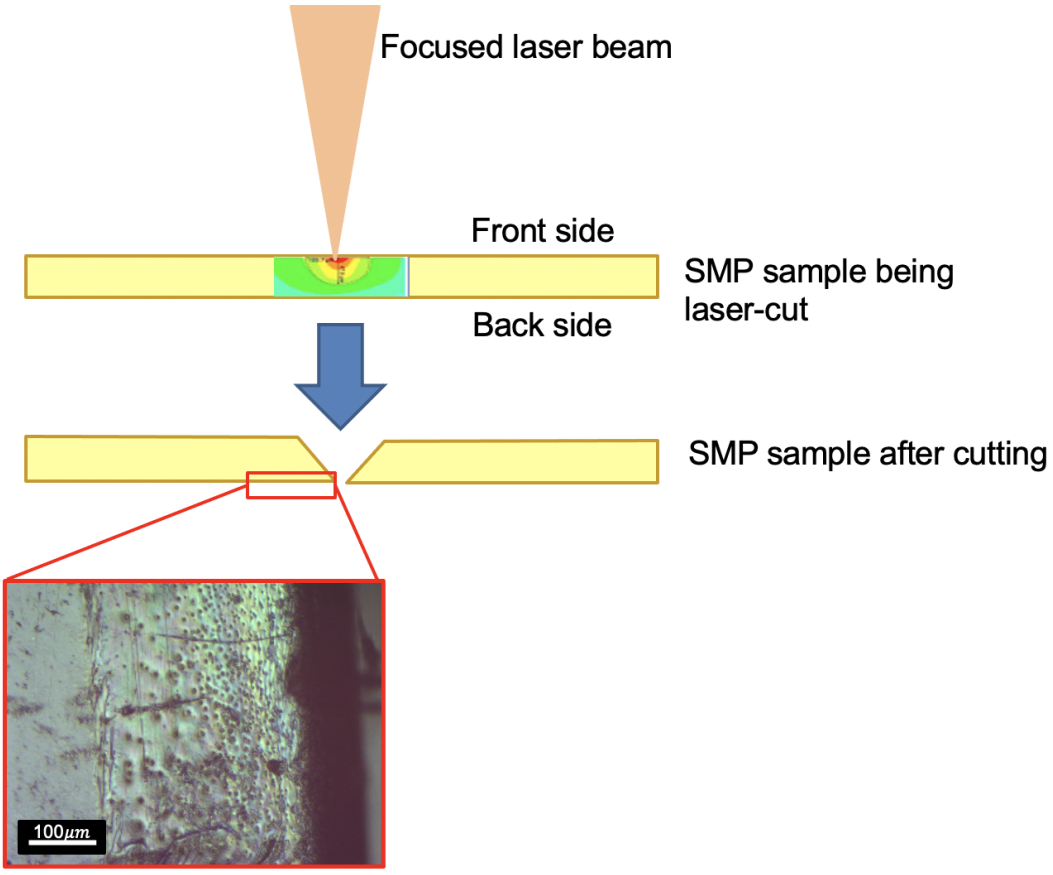

Figure 3.8: Schematic of a laser-cut SMP. (Notice the change in the smoothness of the material to a wavy boundary at the HAZ.)

The first experimental results are given in Table 3.4 were made by reducing the power from 90% incrementally until the power at which the specimen could not be cut was found, 55%. The other parameters were held constant at 70 mm focal length, a speed of 500 mm/min, and pressure of 3 bar during the power reduction. The second experimental results are given in Table 3.5-3.6 gives the HAZ for varying laser speeds at a set power, focal length, and pressure. For Table 3.5 results, the focal length was set at 70mm, the pressure was set at 3 bar, and the power was set at 90%. The speed of the laser was adjusted from 500 mm/min incrementally until the maximum speed at which a cut could be made was reached, 3000 mm/min. For Table 3.6 results, the focal length was set at 70mm, the pressure was set at 3 bar, and the power was set at 80%. The speed was again adjusted incrementally from 500 mm/min until the maximum cut speed was reached, 1000 mm/min. The third experimental results are given in Table 3.7 gives the HAZ and number of passes to cut the material associated with the variation in the focal length at a power of 90%, speed of 3000 mm/min, and pressure of 3 bar.

Sample Label	**Measured Thickness (in)**	**Power**	**HAZ (μm)**	**Groove Measurement (μm)**
1	0.124	90%	807.51	85.18
			789.81	56.42
			849.55	85.18
Average			815.62	75.59
2.1	0124	80%	1301	453.53
			1310	426.99
			1350	473.45
Average			1320	451.32
3	0.120	70%	940.25	59.73
			1070	59.73
			933.62	59.73
Average			981.29	59.73
3.1	0.150	60%	1110	307.52
			1070	293.14
			1090	303.19
Average			1090	301.28
4.2	0.150	57.5%	1010	686.94
			935.83	649.33
			861.72	669.24
Average			935.85	668.50
4.1	0.150	55%	785.39	349.55
			847.34	369.46
			803.09	411.50
Average			811.94	376.84

Table 3.4: HAZ associated with varying laser power at a focal length of 70 mm, speed of 500 mm/min, and pressure of 3 bar. (Below 55% the specimen could not be cut with the laser.)

Sample Label	**Measured Thickness (in)**	**Speed (mm/min)**	**HAZ (μm)**	**Groove Measurement (μm)**
1	0.124	500	807.51	85.18
			789.81	56.42
			849.55	85.18
Average			815.62	75.59
6	0.130	1000	228.98	181.41
			222.34	153.76
			226.77	170.35
Average			226.03	168.51
6.1	0.130	2000	202.43	384.95
			236.72	317.47
			214.60	327.47
Average			217.92	343.30
10.2	0.138	3000	198.01	323.00
			246.68	320.79
			224.55	283.18
Average			223.08	308.99

Table 3.5: HAZ associated with varying speed at a focal length of 70 mm, power of 90%, and a pressure of 3 bar. (Greater than 3000 mm/min, the head of the laser moved to quickly to cut through the material.)

Sample Label	**Measured Thickness (in)**	**Speed (mm/min)**	**HAZ (μm)**	**Groove Measurement (μm)**
20	0.144	500	859.50	360.62
			819.68	388.27
			717.90	366.15
Average			799.03	371.68
21	0.125	750	1090	51.14
			1080	53.34
			1100	50.05
Average			1090	51.51
22	0.126	900	896.01	551.98
			978.72	497.78
			809.72	549.77
Average			894.82	533.18
23	0.127	1000	740.04	412.61
			756.63	428.09
			735.61	428.09
Average			744.09	422.93

Table 3.6: HAZ associated with varying laser speed at a focal length of 70 mm, power of 80%, and a pressure of 3 bar. (Greater than 1000 mm/min, the head of the laser moved to quickly to cut through the material.)

Sample Label	**Measured Thickness (in)**	**Focal Length (mm)**	**Passes to Cut**	**HAZ (μm)**	**Groove Measurement (μm)**
26	0.125	80	1	134.94	234.51
				127.21	234.57
				139.38	238.94
Average				133.84	236.00
27	0.122	90	3	366.26	41.25
				376.16	51.14
				387.16	42.90
Average				376.53	45.01
30	0.120	100	5	556.41	128.69
				559.73	133.64
				560.83	135.84
Average				558.99	132.7
31	0.131	140	10	817.47	167.73
				825.21	166.08
				800.88	179.28
Average				814.52	171.03
32	0.120	120	8	982.20	97.98
				994.30	101.19
				1000	95.96
Average				992.17	98.38
33	0.127	110	5	887.16	118.79
				883.84	118.79
				896.10	124.29
Average				889.03	120.63
35	0.130	110	7	827.67	102.84
				814.47	122.64
				812.27	132.54
Average				818.14	119.34
36	0.127	130	9	1090	51.14
				1080	53.34
				1100	50.05
Average				1090	51.51

Table 3.7: HAZ associated with varying focal length at a power of 90%, speed of 3000 mm/min, and a pressure of 3 bar.

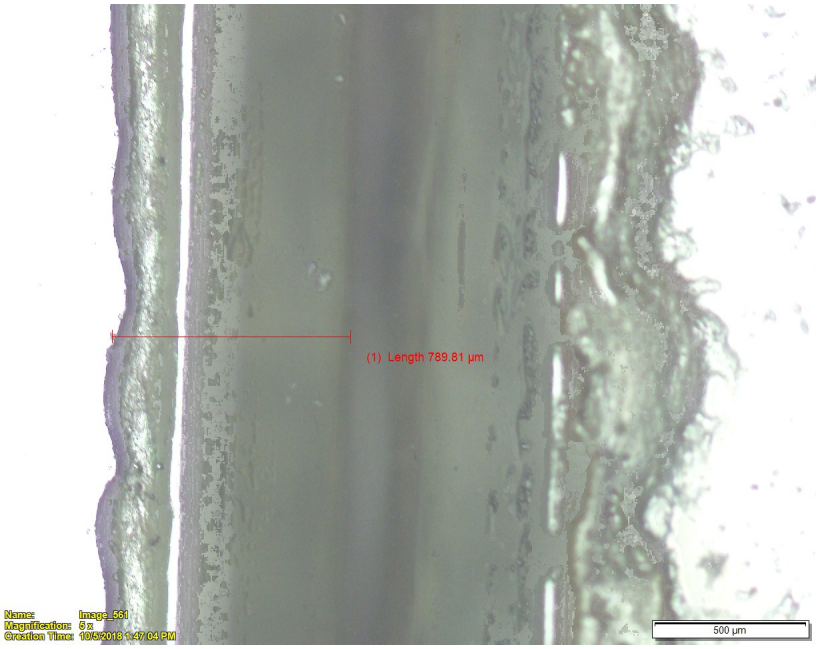

(a) HAZ of sample 1 (speed: 500 mm/min, focal length: 70 mm, power: 90%) in Table 3.5.

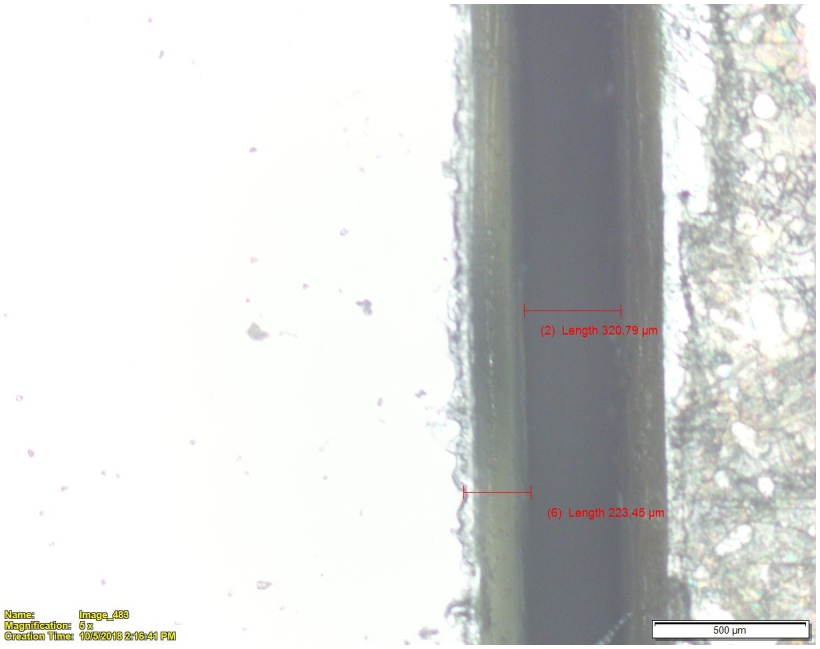

(b) HAZ of sample 10.2 (speed: 3000 mm/min, focal length: 70 mm, power: 90%) in Table 3.5.

Figure 3.9: The variation of HAZ due to different speeds at 500μm magnification. Notices the difference in thermal diffusion areas (waviness in the boundary and size of HAZ) due to variation in speed.

3.5.2 Measurements of T_g

The key to the design of any folding structure using SMPs is an understanding of how the processing involved in machining 2D sheets to create 3D structures, changes the underlying chemistry. Specifically, the effect on mechanical integrity and the T_g. This section will assess the local and bulk T_g of laser-cut SMP material. Specifically, the section will look at samples laser-cut using the Lasersaur machine. A table of the samples to be investigated is given in Table 3.8.

Sample Numbers	**Power**	**Speed (mm/min)**	**Focal Length (mm)**
16-20	80%	1000	70
36-40	70%	1000	70
46-50	60%	1000	70
71-75	90%	900	70
76-80	90%	800	70
81-85	90%	700	70
86-90	90%	600	70
91-95	90%	500	70
96-100	90%	400	70
101-105	90%	300	70
106-110	90%	200	70
26-30	*Control*		

Table 3.8: Sample laser-treatment to assess T_g.

3.5.2.1 Differential Scanning Calorimetry (DSC) Measurements of T_g

DSC measurement is used to assess first order (enthalpy) and second order (heat capacity) phase transformations [5]. The DSC used during these experiments a TA Instruments Q2500 was used which is a DSC that operates on *heat flux* principle. This *heat flux* DSC uses two samples an enclosed empty aluminum reference pan and an enclosed aluminum pan with with sample material in it. The pans sit on a thermoelectric disk that transfers heat to the pans at the same rate. The disk is surrounded by a furnace. The samples are measured using thermocouples and the difference in

temperature between them is recorded [5],[9]. An image of the DSC cell is given in Figure 3.10. The DSC measurements were performed based on the following procedure given in Table 3.9. The samples for the DSC were cut with scissors from the boundary layer next to the laser-cut edge. The sample and aluminum pan was weighed and record to place in the TA advanatge software for the DSC. Table 3.10 contains measurements of the T_g values for the laser-cut SMP found using the TRIOS software. Note the measurements of the bulk T_g remain approximately the same as the control measurements.

Figure 3.10: TA Instruments DSC Q2500 Cell showing the reference pan and sample pan in the cell where the heat is applied. Each pan has a thermocouple underneath it. The difference in temperature between the reference and sample thermocouple readings are recorded [9].

3.5.2.2 nano-AFM Measurements of T_g

Localized thermal analysis was done using nanoscale thermal analysis (nTA) using VITA module. This method provides a point specific T_g, while DSC or other thermal analysis methods provide a sample averaged T_g [56]. The nTA can provide localized transition temperatures on the surface. This is accomplished by a cantilever beam with a heated AFM probe tip. During the measurement, the probe is held at a fixed location on the surface of the sample. As the cantilever

Steps in Using the DSC
Ramp 10.00 °C/min to 0.00 °C
Isotherm for 1.00 min
Ramp 10.00 °C/min to 120.00 °C
Isotherm for 1.00 min
Ramp 10.00 °C/min to 0.00 °C
Isotherm for 1.00 min
Ramp 10.00 °C/min to 120.00 °C
Isotherm for 1.00 min
Ramp 10.00 °C/min to 0.00 °C
Isotherm for 1.00 min
Ramp 10.00 °C/min to 120.00 °C
Isotherm for 1.00 min
Ramp 10.00 °C/min to 0.00 °C

Table 3.9: Procedure for using the DSC.

Power	**Speed (mm/min)**	**Focal Length (mm)**	**T_g (°C)**
Control			49.56
80%	1000	70	47.49
70%	1000	70	45.07
60%	1000	70	47.52
90%	900	70	42.73
90%	800	70	45.09
90%	700	70	44.11
90%	600	70	46.79
90%	500	70	46.62
90%	400	70	42.42
90%	300	70	40.16
90%	200	70	46.76

Table 3.10: DSC T_g values of laser-cut SMP.

and, in turn, the sample heat up, the sample will expand, pushing the probe up and causing an increase in the vertical deflection signal. At a transition temperature, the material typically will soften such that the force applied by the cantilever can deform the surface of the sample, allowing the probe to penetrate the sample and decreasing the deflection of the cantilever [10]. An image of

the cantilever probe is provided in Figure 3.11. The result is output in terms of temperature (°C) versus deflection (mV).

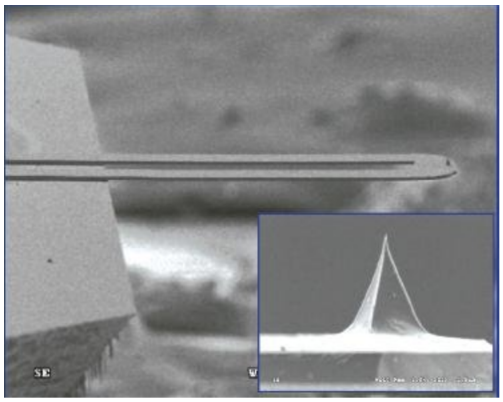

Figure 3.11: An SEM image of the microfabricated thermal probe used for nTA measurements. The inset is a zoom of the tip, which makes contact with the sample surface[10].

The bulk T_g of these tested laser-cut samples was 50°C. The nTA tests were performed at a consistent rate of 1°C/s up to 200°C, on the smooth surface of the sample, with a time interval of 5-10 minutes between each sample to eliminate the effect of slow heat dissipation. The results of the laser-cut samples show a cubic temperature verses deflection curve. The T_g measurements of the laser-cut surface of the SMP were taken at vertical and horizontal intervals. Figure 3.12 depicts the measurement coordinates for the T_g. The T_g values of these coordinates are given in Table 3.11.

	1	**2**	**3**	**4**	**5**
1	70.524	138.74	139.324	93.537	86.314
2	70.824	134.11	141.920	84.844	86.907
3	71.497	85.797	140.820	92.624	87.011
4	70.597	84.577	136.29	85.891	88.641
5	71.631	80.684	140.71	78.451	86.397

Table 3.11: Associated nTA T_g values, in °C, of laser-cut SMP corresponding to the positions in Figure 3.12.

Coordinates of each measured point

	1	2	3	4	5
1	(-55,0)	(-45,0)	(-35,0)	(-25,0)	(-5,0)
2	(-55,-10)	(-45,-10)	(-35,-10)	(-25,-10)	(-5,-10)
3	(-55,-20)	(-45,-20)	(-35,-20)	(-25,-20)	(-5,-20)
4	(-55,-30)	(-45,-30)	(-35,-30)	(-25,-30)	(-5,-30)
5	(-55,-40)	(-45,-40)	(-35,-40)	(-25,-40)	(-5,-40)

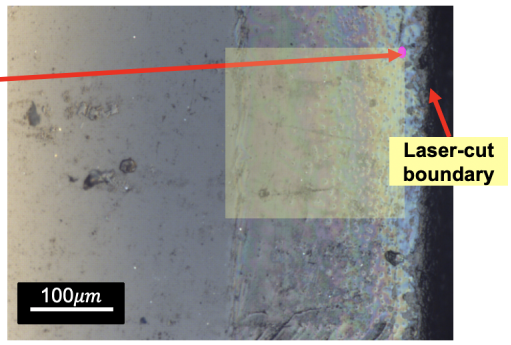

Unit is the division of the micrometer on the AFM base (1 div≈ 5 μm)

Figure 3.12: Coordinates of each measured point using nTA.

A summary of the nano-AFM T_g results is given below:

- The laser-cutting changes the local T_g for all 4 samples tested (4 with different machining paras).
- For laser-cutting with lower speed, the thermal diffusion areas could be observed. But when the laser-cutting speed increases to 1000 mm/min, diffusion areas are really minimal, let alone the variations of T_g values on the diffusion areas. An example of the variation in thermal diffusion areas due to speed can be seen in Figure 3.9.
- For the groups with lower speed, the changed in T_g is higher (sometimes 130 to 200 C on the diffusion areas).

3.5.2.3 Comparison of T_g Using DSC and nano-AFM

The nano-AFM was able to capture the thermal diffusion areas seen in Figure 3.9. The DSC is unable to detect the effect of local T_g. The nano-AFM was able to capture the greater HAZ zone that occurred at lower speeds, however the DSC was unable to capture this effect.

3.6 Summary

The measurement of the HAZ showed that the HAZ decreased nearly an order of magnitude (815.62 μm to 226.03 μm) when the speed was increased from 500 mm/min to 1000 mm/in for a

power level of 90%, focal length of 70 mm, and pressure of 3 bar. Beyond 1000 mm/min speed the HAZ was approximately the same. For cutting at 80% power level, focal length of 70 mm, pressure of 3 bar, and speeds of 500 mm/min, 750 mm/min, 900 mm/min, and 1000 mm/min the HAZ was quantitatively the same. This same result was seen when the speed was held constant at 500 mm/min, focal length of 70 mm, pressure of 3 bars, and varying the power levels of 0%, 80%, 70%, 60%, 57.5%, and 55%. As the focal length increased from 80 mm to 100 mm (power level of 90%, speed of 3000 mm/min, and pressure of 3 bar) the HAZ zone increased from 133.84 μm (80 mm) to 376.53 μm (90 mm) to 558.99 μm (100 mm) to 889.03 μm (110 mm). Once the focal length reached 110 mm the HAZ remained quantitatively the same for increased focal length.

The nano-AMF captures the effect on T_g in the HAZ. Specifically, the nano-AFM is able to depict a change in local T_g across the thermal diffusion boundary, while the DSC was not able to capture the change in bulk T_g. The DSC showed that the bulk T_g of the material remained approximately the same as the T_g of original material, except when the laser-cutting involves a significant portion of the material, like Figure 3.7. Laser-cutting provides an efficient way to machine SMP for the creation of origami structures. However, the thermal stress imposed breaks the chemical bonds of the material which in turn changes the local T_g by changing the connections between the “soft" segments and the “frozen" segments and altering the chemical composition. By changing the T_g laser-cutting can have an effect on the shape memory effect.

4. DRILLING AND MACHINING OF SMP

4.1 Review of Machining of Polymers

The previous chapter discussed the difficulties of creating self-folding structures using laser-cutting subtractive manufacturing. Another aspect of this research is to explore how to create origami structure using machining methods and the difficulties associated with those methods. In general, researchers have tried to categorize the influence of machining into three main sub-categories: environmental conditions (*i.e.* vibration isolation), machining and tooling conditions (rake angle, depth of cut, and cutting speed, ect.), and physical and chemical properties. Xiao and Zhang state that effects on physical and chemical properties in polymers are more pronounced than in metals, and it is more difficult to determine the relationship because of their viscoelastic nature [57]. Carr and Feger performed single-point diamond machining experiments on various polymeric materials. They noted that surface roughness corresponded to the molecular structure of polymers. Specifically, that crosslinked polymers are ruptured during removal, because of their inability to flow. Also, polymers with higher T_g behave as a glass when being cut with accompanying brittle fracture [58]. Alauddin et al. noted characteristics corresponding to cutting parameters for polyester resin, deemed as a representation thermoset. This research concluded that the cutting force components decrease as the rake angle turns from negative to positive. Secondly, transfiguration of the cutting force at positive rake angles originates from variation in chip formation [59]. These researchers showed that machining affects the molecular structure of the polymer not only by raising the temperature in the machined zone, but by imparting a high strain rate as well. This work seeks to assess how the thermoset SMP created in Chapter 2 is affected by machining, and how complex 3D structures can be created using machining methods.

4.2 Review of Folding Structures

Previous researchers have explored how to harness the principles of origami to construct complex 3D structures from 2D sheets. Liu, Genzer, and Dickey assess the current work in 2D shape

programming of polymers. They categorize the way shapes are created into the following four categories: (1) 2D substrates using additive or subtractive manufacturing; (2) 2D substrates that form wrinkles or creases in response to a stimulus; (3) 2D substrates that can form out-of-plane 3D shapes by bending; (4) 2D substrates that use hinges to achieve out-of-plane folding [43]. Tolley et al. created self-folding laminate structures with the use of polystyrene sheets (commercially available as ShrinkyDinks). The laminate structures consisted of a layer of polystyrene in between two structural layers connected by adhesive. The authors used predefined fold patterns on the laminate and adjusted the gap to achieve varying fold angles [11]. The resulting structures created from this work are given in Figure 4.1. Liu et al. also employed polystyrene sheets, however this work used black ink deposited on either side of the polymer in the areas associated with the bend. The ink coupled with light stimulus provides a localized heating above the T_g at the hinges causing the inked regions to relax and shrink to make a fold [60]. Yuan et al. use a bilayer SMP/elastomer laminate with a thermal strain mismatch to create folding structures. For these laminates the thermal strain difference was the driving mechanism, hence a larger the strain difference with a smaller total thickness an optimum thickness ratio creates increased bending curvature [61]. Ge et al. developed what they term as 4D printing of printed active composites (PACs). 4D printing is the concept of building self-assembling origami that works by 3D printing flat polymer sheets which are activated to a new shape by the fourth dimension, stimulus, creating active origami. In this case these PACs are are made using a multi-layer 3D printing and make up the hinges of the bend [62]. Deng et al. also used 4D printing, and printed silver ink traces on polystyrene. The silver ink acts as a current conductor causing the material to shrink and bend. The type of bend can be controlled by the current and resistance [12]. Neville et al. used polystyrene hinges and a technique termed Kirigami (origami with cutting allowed) to create depolyable polystyrene shape memory structures. The work uses Kirigami to create a proof of concept design for large volumetric deployment. This design is an open honeycomb configuration that has been designed by setting an initial three-dimensional re-entrant auxetic (negative Poisson's ratio) configuration, while the final honeycomb shape assume a convex (positive Poisson's ratio) layout [13]. A depiction of the ini-

tial and final shapes are given in Figure 4.3. Mansoori et al. studied adaptive architectural skins using wood/SMP composites. These structures are able to obtained their curved shape due to the geometry of wood. Their work combines a "kerfing" relief cutting method and the shape memory effect of the SMP to large deformation in the structure [63]. The review of 2D to 3D polymer sheets by Liu, Genzer, and Dickey concludes that there are still a large strides to be made in this area, in particular, decrease in complexity of fabrication of these structures without increasing the defects [43]. This work seeks to address gap by looking to employ simple machining practices on SMP to create complex 3D structures and assessing how these machining factors affect the material.

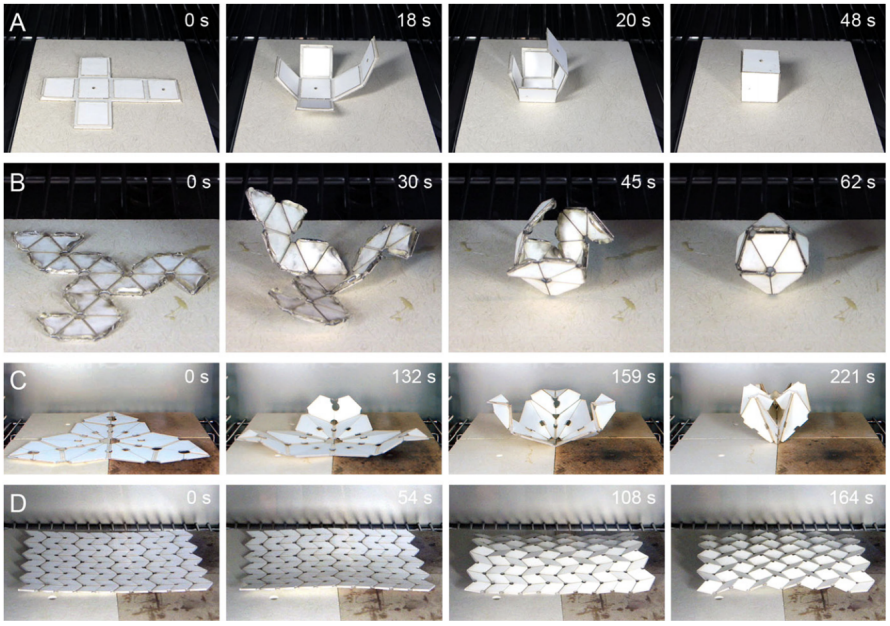

Figure 4.1: Time lapsed photos of self-folding structures created by Tolley et al. placed in an oven at 130°C (A) cube, (B) icosahdron, (C) Miura pattern, and (D) shapes [11].

4.3 Drilling of SMP

In order to assess how SMP behaved when it was machined, some initial work was done using an end milling machine on SMP sheets. Three types of specimens were investigated: SMP, SMP

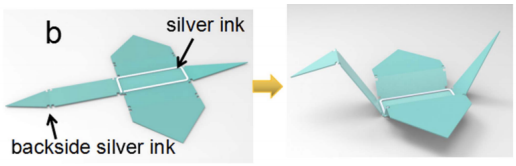

Figure 4.2: An origami crane using multiple circuits folding [12].

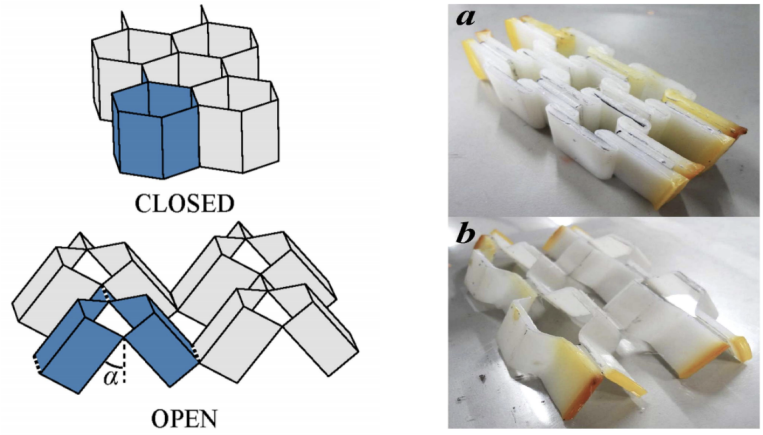

Figure 4.3: (a) Stowed configuration and (b) deployed configuration of the SMP honeycomb [13].

with thermochromatic powder incorporated into the matrix, and SMP with carbon black incorporated into the matrix. The tolerance of the machined specimens was measured using a microscope and the results are given in Table 4.1.

The table shows that the dimensions of the hole are approximately the same size as the bit. Therefore, it appears there is some thermal stress in the polymer causing the material to "shrink" inward. In order to provide an initial assessment of the thermal energy in the SMP, thermochromic powder was incorporated into the matrix. You can see from Figure 4.4 that the temperature within the specimen at least reaches that of thermochromic powder which is $30°$C.

Specimen Type	**Feed Type**	**RPM**	ϕ_{fh} **(mm)**	ϕ_{bh} **(mm)**	**Front Hole Circularity (mm)**	**Back Hole Circularity (mm)**
Clear	Low	450	4.097	4.149	0.048	0.046
	High	450	4.088	4.134	0.03	0.044
	Low	1000	4.082	4.149	0.034	0.046
	High	1000	-	-	-	-
Thermochromic Powder	Low	450	4.134	4.108	0.052	0.099
	High	450	4.067	3.996	0.093	0.09
	Low	1000	4.136	4.156	0.103	0.073
	High	1000	-	-	-	-
Carbon Black	Low	450	4.119	4.167	0.069	0.058
	High	450	4.09	4.136	0.077	0.041
	Low	1000	4.097	4.133	0.085	0.055
	High	1000	4.284	4.109	0.093	0.144

Table 4.1: Dimensions of SMP from drilling. (The drill bit used measured 4.0386 mm and 4.064 mm.)

Figure 4.4: Thermochromic heat sensing during machining.

The results of drilling using different speeds and feed types are given in Figures 4.5-4.8.

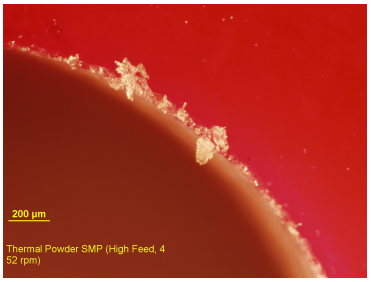

(a) 452 rpm and high feed.

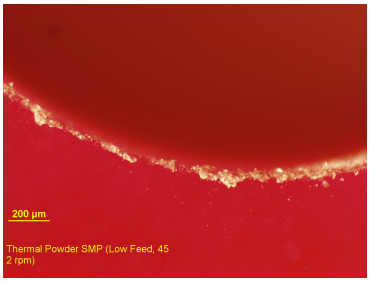

(b) 452 rpm and low feed.

Figure 4.5: SMP with thermochromic powder in matrix drilled at 452 rpm.

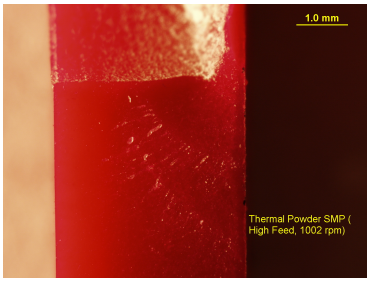

(a) 1002 rpm and high feed.

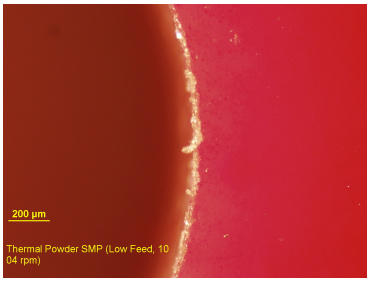

(b) 1000 rpm and low feed.

Figure 4.6: SMP with thermochromic powder in matrix drilled at 1000 rpm.

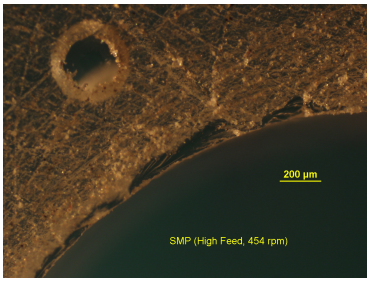

(a) 454 rpm and high feed.

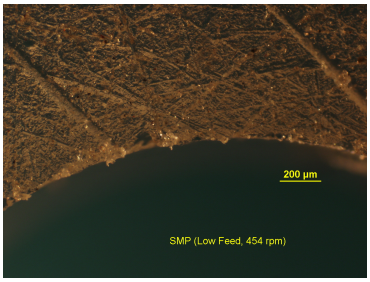

(b) 454 rpm and low feed.

Figure 4.7: SMP drilled at 454 rpm.

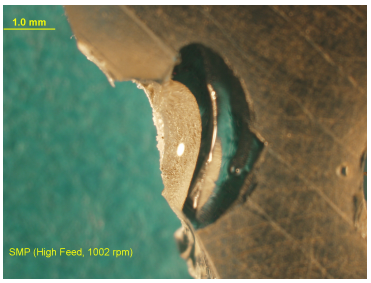

(a) 1002 rpm and high feed.

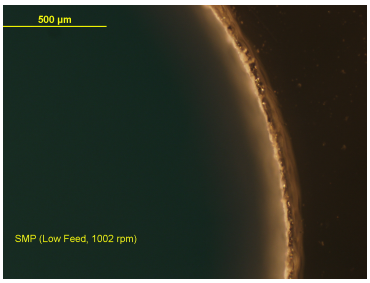

(b) 1002 rpm and low feed.

Figure 4.8: SMP drilled at 1002 rpm.

4.4 Folding of SMP Using Advanced Kirigami

In order to create origami structures using SMP sheets, a process called Advanced Kirigami was harnessed. Advanced Kirigami is the process of cutting and bending materials and creating 3D structures of high-strength materials such as polymer and metals. In order to investigate using Advanced Kirigami, CNC machining was used and the effect of the shape of the groove on the bend were investigated. Also, laser-cutting using a defocused laser and absorption was examined as an alternative means of Advanced Kirigami.

For this work, Ultra High Molecular Weight Polyethylene (UHMWPE) was compared to SMP for use in Advanced Kirigami structures. UHMWPE is a thermoplastic material made of long chains of polyethylene. Weak Van der Waals forces between these molecules provide a high intra-molecular strength due to the large overlaps between molecules. UHMWPE is a component used in joint replacement, such as knee, hip, and spine medical devices.

4.4.1 Geometry of a Bend

The bend angle of polymeric structures depends on the geometry of the folded state, as well as the folding torque and moment on the hinge. Here we look at the change in the width of the gap for a square gap, in relation to the bend angle. Figure 4.9 depicts the gap geometry of the folded and unfolded states for this case. In the figure, t_{smp} and t_{top} give the thickness of the SMP and top layer of the structure. The term δ describes the distance between the bottom of the SMP and the point of rotation. Therefore, the angle of bend is calculated according to Equation 4.1-4.2.

$$tan\left(\frac{\theta}{2}\right) = \frac{w_{gap}}{2(t_{smp}+\delta)} \tag{4.1}$$

$$(t_{smp}+\delta)^2 = \left(\frac{w_{gap}}{2}\right)^2 + \left(\delta + \left(\frac{t_{smp}}{2}\right)^2\right)^2 \tag{4.2}$$

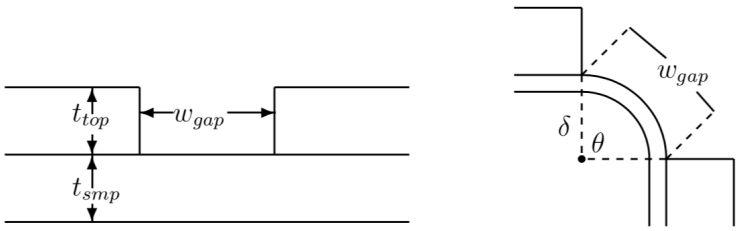

(a) Unbent state of SMP/epoxy composite. (b) Bent state of SMP/epoxy composite.

Figure 4.9: Schematic of the cross-section of SMP folding hinge geometry.

4.4.2 Single Hinge Folding with CNC Milling

Initially, a small CNC milling machine with a 24 volt spindle motor with a maximum speed of 7000 rpms was used. The machine had a frame size of 10.2" by 9.45" by 8.66" and a working area of 6.30" by 3.94" by 1.77". An image of the small CNC milling machine is given in Figure 4.10. With this machine, three types of bits, rounded, v-cut, rectangular, were used to investigate the type of cut made. These bits are given in Figure 4.11.

The initial analysis was performed using flat rectangular sheets and cutting with the three bits. Each sheet was cut so that the resulting groove was one third the original thickness of the sheet at the cut's lowest point. The results of this testing process give the "springback" or shape recovery angle. In order to obtain this angle, the material is heated for approximately 45 seconds, and then bent at a 90° angle by pushing with the hand. While holding this position, the material is then cooled for 60 seconds, and then the force is removed and the resulting angle is measured. The resulting springback angle from this simple shape memory cycle are given in Table 4.2. A second analysis was performed using only the weight of the object as a force. The force was applied at various time intervals of 60, 90, and 120 seconds. The results of this test are given in Table 4.3.

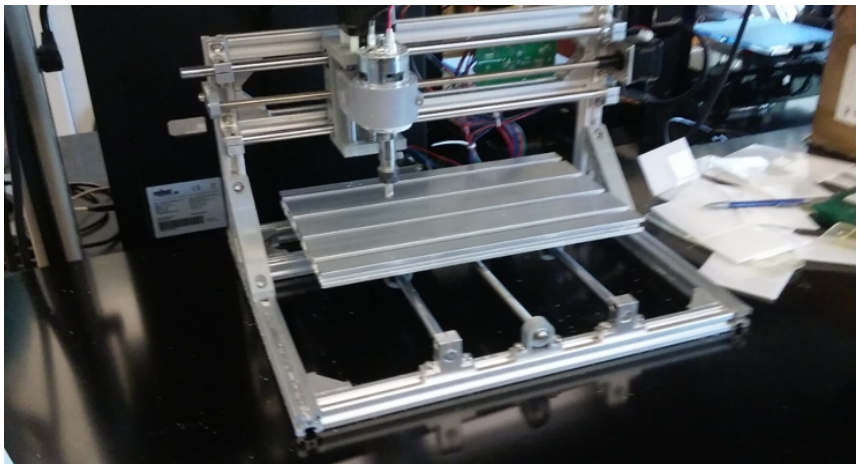

Figure 4.10: Small CNC milling machine.

(a) Rounded. (b) V-cut. (c) Rectangular.

Figure 4.11: CNC bits initially used to drill into SMP sheet.

Sample Number	**Material**	**Bit Type**	**Material Thickness (in)**	**Groove Height (in)**	**Springback Angle**	**Recovery Angle**
4	UHMWPE	Rounded	0.118	0.025	32°	2°
5	UHMWPE	Rectangular	0.118	0.03-0.05	34°	$< 1^\circ$
6	UHMWPE	V-Cut	0.118	0.045-0.05	34°	7°
10[1]	SMP	V-Cut	0.120	0.05-0.067	53°	n/a
11	SMP	Rounded	0.120	0.05	36°	n/a
12[2]	SMP	Rectangular	0.120	0.036	n/a	n/a

Table 4.2: Springback angle analysis from the small CNC mill and a simple shape memory cycle.

[1]This sample had a fracture with a small tear on both side.
[2]This sample had a fracture with a large tear in middle.

Sample Number	Material	Bit Type	Material Thickness (in)	Groove Height (in)	Bend Angle at given Time	Springback Angle	Recovery Angle
1	UHMWPE	Rounded	0.118	0.06-0.1	1°(60s), 3°(90s), 5°(120s)	8°	2°
2	UHMWPE	Rectangular	0.118	0.04	10°(60s), 35°(90s), 60°(120s)	19°	$< 1°$
3	UHMWPE	V-Cut	0.118	0.04	1°(60s), 2°(90s), 3°(120s)	11°	7°
7	SMP	Rounded	0.120	0.025-0.05	5°(60s), 15°(90s), 15°(120s)	2°	2°
8	SMP	Rectangular	0.120	0.035	10°(60s), 10°(90s), 10°(120s)	4°	$< 1°$
9[3]	SMP	V-Cut	0.120	0.05-0.06	32°(60s), 90°(90s), n/a (120s)	n/a	7°

Table 4.3: Springback angle analysis from the small CNC mill and a simple shape memory cycle and gravitational force.

[3]This sample had a complete fracture.

The UHMWPE performed without any fractures during the CNC milling testing. This resilience is due to higher fracture toughness, and the highly intricate overlapping bond forces. The rounded bit created some end effects in the UHMWPE. Specifically, the bit created a wider cutting surface at the ends of the cut. An example is given in Figure 4.12. The v-cut bit created a v-notch in the specimen and when bent resulted in increased number of fractures for the SMP, creating the most fragile shape. This increase in fractures is due to the fact that the tip of the notch creates a high localized stress concentration due to an asymptotic stress state at the apex. The v-notch acts as a crack-tip and the bend propagates the crack causing fracture at the notch. The rounded and square channels did not create the same high stress state as the v-notch channel and resulted in better flexure behavior.

Figure 4.12: UHMWPE cut with the rounded bit. (The ends have a larger, more rounded groove, while the middle portion maintains a more uniform width and thickness.)

4.4.3 Single Hinge Folding with Laser-Cutting

Laser-cutting was used to create single hinge folds of UHMWPE and SMP. The Lasersaur with specifications given in Chapter 3 is used. The bends are accomplished by de-focusing the laser to create a larger heat affected zone, and in turn melting the material. Surface treatment of a black dry erase marker comprised of SD Alcohol-40, an ethyl alcohol, isopropanol, and dark resin was applied to some of the samples to create better absorption.

These samples are again analyzed the same as in the previous section. Specifically to obtain the springback angle the material is heated for approximately 45 seconds, and then bent at a 90° angle by pushing with the hand. While holding this position, the material is then cooled for 60 seconds, and then the force is removed and the resulting angle is measured. These results are given Table 4.4. Also, the second analysis was performed using only the weight of the object as a force. The force was applied at various time intervals of 60, 90, and 120 seconds. These results are given in Table 4.5. The SMP with blackened surface had the lowest springback angle. This result is probably due to the large heat affected zone from greater surface absorption.

Sample Number	Material	Surface Treatment	Material Thickness (in)	Groove Height (in)	Springback Angle
14	SMP	n/a	0.120	0.06	15°
15[4]	SMP	n/a	0.120	0.032-0.05	8°
16	SMP	n/a	0.120	0.055-0.07	22°
17	SMP	blackend	0.120	0.04-0.05	6°
18[5]	SMP	blackend w/groove	0.120	0.04-0.05	6°
20	UHMWPE	n/a	0.118	0.075-0.08	40°
21	UHMWPE	n/a	0.118	0.075-0.085	49°
22	UHMWPE	n/a	0.118	0.075	45°
23	UHMWPE	blackend	0.118	0.075	45°
24	UHMWPE	blackend w/groove	0.118	0.075	37°

Table 4.4: Springback angle analysis from the laser-cutting and a simple shape memory cycle (power: 15, passes: 7, height: 0).

[4]This sample had a large tear in the middle.
[5]This sample had a small side tear.

Sample Number	**Material**	**Surface Treatment**	**Material Thickness (in)**	**Groove Height (in)**	**Bend Angle at given Time**	**Springback Angle**
13	SMP	n/a	0.120	0.05	10°(60s), 20°(90s), 24°(120s)	-5°
19	UHMWPE	n/a	0.118	0.07	7°(60s), 10°(90s), 12°(120s)	11°

Table 4.5: Springback angle analysis from the laser-cutting and a simple shape memory cycle and gravitational force (power: 15, passes: 7, height: 0).

4.4.4 Folding of Bilayer SMP

In order to create, folding structures for various applications, the folding of the bi-layer SMP described in Chapter 2 was investigated. First, the bi-layer SMP was cast according to the process given in Chapter 2 using a Trudeau 8" by 8" silicone square cake pan. Once, cured the part was removed from the mold and set in between two plates with and allowed to cool to give it a flatter final shape. Another method used to give it a flatter shape is after curing, the entire part was heated with a heat gun and set between two plates to flatten it out and allowed to cool prior to machining. The approximate minimum layer thickness that can be achieved with this mold is 0.125". Therefore, a two-layered structure with one layer having a T_g of 50-60°C and the other layer having a T_g of 80-100°C. From the previous equations it may be shown that the w_{gap} is approximately twice the thickness of the SMP layer for a bend angle of $90°$. Experimental testing was done to determine the angle of bend associated with varying the gap distance. All these experiments were performed using an Axiom Precision CNC router table. The results are given in Table 4.6. The chips created using the various bits are given in Figures 4.13-4.15.

Bit Size (in)	**Measure w_{gap} (in)**	**Measured t_{smp} (in)**	**Resulting Bend Angle**	**Spindle Speed (rpm)**	**Pass Depth (in)**	**Feed Rate (in/min)**	**Plunge Rate (in/min)**
1/4	0.2440	0.08750	$80°$	8,000	0.025	40	30
3/8	0.3790	0.0940	$100°$	10,000	0.025	40	30
1/2[6]	0.4935	0.110	$105°$	10,000	0.025	40	30

Table 4.6: Bend angle achieved using varying bit sizes.

[6]The 1/2" bit caused the material to melt.

Figure 4.13: Machine chips created using 1/4” bit.

Figure 4.14: Straight line machine chips created using 3/8” bit.

Figure 4.15: Fine powder machine chips created using 1/2” bit.

4.4.5 Folding Shapes Created Using CNC Milling

Once, the appropriate bit size was determined, several folding shapes were created using the SMP/Epoxy composite structure. Examples of these shapes are given in this section. The first shape created was a cube shape. Pictures of the cubic shape are given in Figure 4.16. The second shape created was a pyramid, whose picture is given in Figure 4.17.

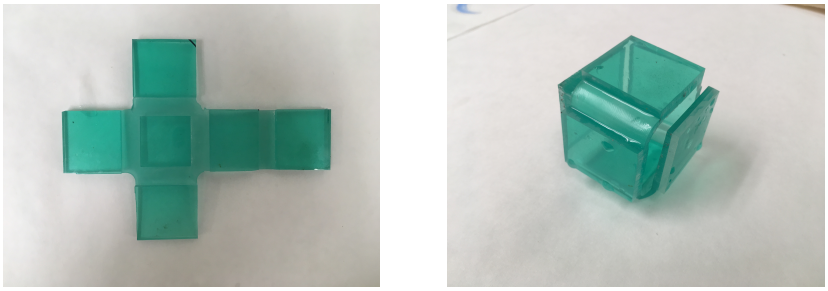

(a) Unfolded. (b) Folded.

Figure 4.16: SMP/epoxy origami cube shape created in this work from machining the bi-layer structure described in Chapter 2.

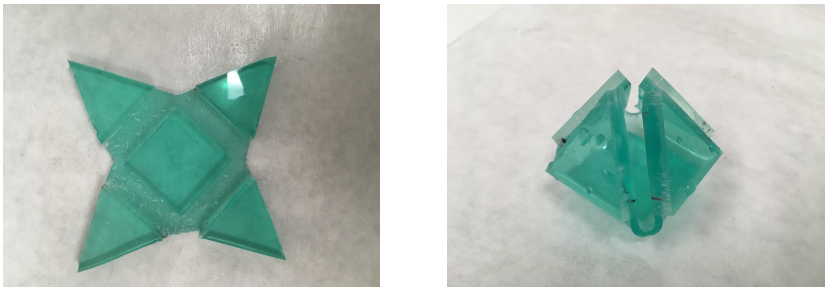

(a) Unfolded. (b) Folded.

Figure 4.17: SMP/epoxy origami pyramid shape created by myself from machining the bi-layer structure described in Chapter 2.

4.5 Summary

The shapes created using the folding bi-layer SMP are a workable prototype to creating a 3D structure that can be simply fabricated. Machining of the SMP does affect the material properties, specifically, the material shrinks back when drilled and some stress is induced.

5. SMPS IN TANGIBLE INTERACTIVE DESIGN *

5.1 Motivation for SMP Interactive Design

Typical applications of SMPs are adhesives, textiles, medical devices, cosmetics, and toys. The goal is to use the ability of SMPs to remember their permanent shape to build upon the idea of SMPs as “toys" to create a interactive pieces for learning purposes. SMPs’ ability to create new shapes based on an external stimulus provides a hands-on learning experience that can bridge complex concepts within nature into fully tactile interactive installations. The work presents two installations that take advantage of this aspect. One installation uses the shape memory effect and an auxetic shape coupled with thermochromic powder to showcase the shape and color change due to chromatophores occurring in cephalopods. These installations shows a practical context in switch the aspects of machining discussed in the previous chapters can be taken advantage of to create a reasonably complex end product.

5.2 SMPs as an Interactive Teaching Tool

Due to the shape memory effect, SMA and SMP present a unique opportunity to develop interactive artwork that represent different natural processes. Specifically, these materials provide a distinctive medium that engages the observer in a classical kinesthetic learning. Michael Eisenberg researched the impact of novel materials in “educational technology.” He provides three classifications of materials to be used of educational purposes: output or responsive materials; input, sensing, or communicative materials; and miscellaneous materials [64]. Eisenberg notes that several aspects of our engineered environment seem to the observer to work “like magic”and discourage the observer to understand the intricacies of a device. He suggests the application of material science in educational technology in that materials provide a medium that can be more informative of processes within a child’s environment through physical and tactile means [64]. Tan et al. explores

*The data reported in this chapter is reprinted with permission of the authors from “Incorporation of Shape Memory Polymers in Interactive Design" by Jessica Berry (Jessica Berry Reese) and Jinsil Hwaryoung Seo, July 2015. Proceedings of the 21st International Symposium on Electronic Art, (Vancouver, BC, Canada).

the use of an augmented reality tool that teaches students about materials. This paper presents two interactive teaching tools that provide a mechanism to teach students about classification of materials and microstructure. The preliminary study suggests that implementation of augmented reality to create a relationship between concrete object and a virtual object produces an enhanced hands-on method of representing difficult concepts [65]. Ishii et al. presented what is called the radical atoms concept for human-material interactions. Radical atoms seeks to overcome the challenges associated with graphical user interfaces and tangible user interfaces by using a dynamic material. This dynamic material responds to human interactions by changing physical form to reflect digital information [66]. The previous authors feature a key concept in classical learning that is lost when learning is solely through digital means. The concept that engaging the student's senses through the use of tangible objects in a palpable, real, and physical matter adds reinforcement of ideas that are absent with the increasing reliability on electronic devices.

5.2.1 Review of Prior Shape Memory Artworks

Several previous artists have explored the area of using "smart" materials as a medium. Elaine Ng Yan Liang has titled her work as "Naturology" which is the combination of nature and technology. Her works include a various shape memory veneers that incorporate color change according to humidity, temperature, and light. Also, she created a shape memory fabric, living furniture fabric, with wood veneer seen in Figure 5.1 [14]. She designed a "lace" roof for a seasonal depressive disorder which actuates in response to heat to allow light in winter months [67].

Figure 5.1: Living furniture fabric that responds through humidity [14].

Charolett Lelieveld created a SMA/SMP prototype for use as an adaptive building component. Lelieveld created shape memory composite system of SMA embedded in SMP that wrinkled when the SMA was heated. This structure utilized the rubbery state of the SMP that allowed accommodation for the force of the SMA when heated. She noted challenges of working with the SMA/SMP related to fatigue life, interface stresses, and environmental heating of the system [68]. Jie Qi actuated origami structures using SMA, see Figure 5.2. She investigated SMA electronic origami cranes as an educational tool for children ages 9 to 15 and assessed that SMA origami provided an enjoyable medium to teach circuitry, design, and soldering [15]. Some of her other works include animated vines, an interactive SMA installation that curls in the presence of the viewer and blooming paper flowers that open through SMA wire [69].

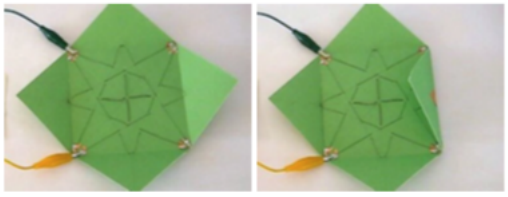

Figure 5.2: SMA folding flap [15].

Yvonne Y.F. Chan Vili created "smart" textile through the aesthetic engineering of SMA and SMP materials into woven structures. Her work employs SMA and SMP yarns to generate 3D fabric prototypes for uses as window treatments, partitions, or wall hangings that augment a space through their environmental responsiveness to stimulus [16]. An example of her "smart" textile is given in Figure 5.3.

The Texas Institute for Intelligent Materials and Structures (Ti-iMS) at Texas A&M University have installed a 'Pop-Op' which is a SMA wall installation composed of resin and C-glass fiber. The installation contains several components like flowers and flaps that are actuated by SMA and controlled by an Arduino [70]. These works provide the foundation for shape memory materials incorporated into artwork. This research explores an extension of previous shape memory artwork

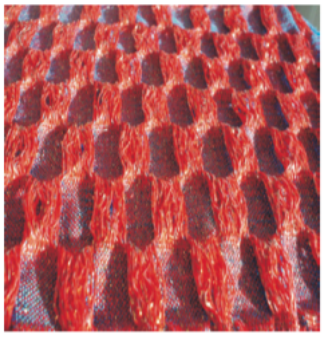

Figure 5.3: A simulated sample (in contracted state) solely woven with SMP yarn formations in regular floats. [16].

by incorporation of color changing material into SMP.

5.2.2 Review of Work in Biomimicry

Previous researchers and artists have found inspiration through nature in the creation of objects. Villanueva et al. created a robotic device from silicone and shape memory alloys that mimics the thrust and appearance of a jellyfish. The biomimicry design was chosen so that the device could conduct surveillance over distances for extensive periods of time and blend into the natural environment [71]. Menges et al. created a piece called "HygroSkin" which focuses on the concept that natural systems have embedded responsiveness. The work is an architectural wall that contains wooden apertures that open and close with changes in relative humidity [17]. An example of the "skin" is given in Figure 5.4. Morin et al. used the concepts of visual display that are exhibited in cephalopods and jellyfish to create a robot that can camouflage itself or display bright colors. The robot is made of an extensible elastomer and uses fluid channels coupled with colored and temperature-controlled fluids to create movement and visual communication [72]. Kolle et al. created a photonic fiber inspired by the seed coat of the *Margaritarie nobilis* fruit. These fibers were created by wrapping multiple layers of polymer around a glass core that is later removed by hydrofluoric acid etch. The end product is a fiber that exhibits various colors at different strain states due to the Bragg effect [18]. An image of the fiber is given in Figure 5.5. The following artworks seek to couple the concept of biomimicry and shape memory to create a tactile SMP

artwork that offers an enhanced learning experience.

Figure 5.4: A full-scale responsive prototype of “Hygroskin” in the open (top) and closed (bottom) positions [17].

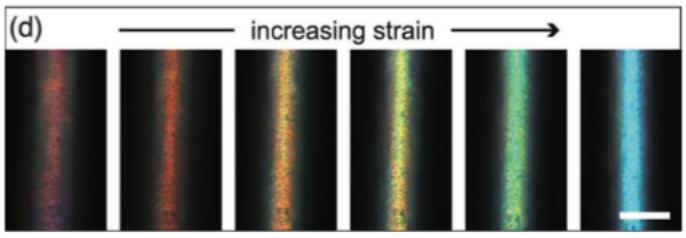

Figure 5.5: Color-tuned fiber [18].

5.3 Using Thermochromic SMPs for Interactive Art

This work expands biomimicry using SMPs combined with thermochromic powders during curing, described in Chapter 2, and fabricating structures using methods given in Chapter 3 to

create unique kinesthetic art. In this section, we will show two cases Auxesis that is based on thermally induced “expansion" somewhat similar to the chromatophores in biological cells, unlike the biochromatophoes that are actuated by muscles, these are heat actuated. We achieve this by creating "frame-like" structures with “spiral hinges" that open out causing a large planar expansion. The second case is called The Secret Garden. This application is based on the bending deformations of cantilevered structures that give rise to the "unfurling" structure somewhat like a flower.

5.3.1 Auxesis

This artwork was designed as a biomimicry concept for chromatophore cells which cause chameleons’ color change as a response to environmental factors to communicate mood, aggression, territorial instincts, or mating desires [73]. This color pattern happens due to specialized cells called chromatophores expanding and contracting on the skin’s surface. These chromatophores behave as flexible bags of color that is either stretched out to cover a large flat area or retracted back to a small, retracted point [73]. Each chromatophore is attached to radial muscle fibers at various points along its edge controlled by a nerve fiber. When a nerve impulse is sent, it causes these muscles to contract and expand the chromatophore. When the muscles relax, the chromatophore returns to a small, compact shape, thus reducing its area and making the pigmented area shrink [73]. The name for the artwork was chosen as “Auxesis” which is greek for growth, hence the “growth” of the chromatophore [19].

In order to mimic the cells of the chromatophore, a SMP was created using the formulation given in Chapter 2 for a transition temperature of 70°C. Color change was created, in this SMP, using the thermochormic powder and Castin’ Craft dye sonicated in the Jeffamine D-230 before being mixed with the NDGE and Epon 826. The mixture was then cast into 3 mm thick rectangular sheets and cured according to the steps given in Chapter 2, resulting in a sheet of color-changing SMP like the one given in Figure 2.7. A drawing of an auxetic shape was created using AutoCAD and the SMP was laser-cut into a chiral auxetic shape based on the work of Rossiter et. al. [74] [19]. An auxetic shape was chosen due to the negative Poisson ratio (the lateral width increases when stretched from either end) to represent the contraction of the cell. An example of the auxetic shape

is given in Figure 5.6 and associated dimensions from drawing file are given in Figure **??**.

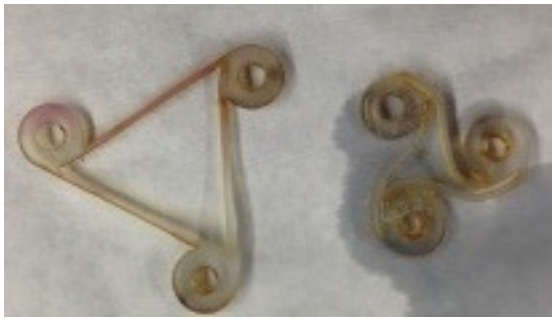

Figure 5.6: Contraction of chiral structure: expanded (left) and compressed (right) states [19].

The imitation of the pigmentation of the cell during the two states was accomplished by gluing fabric to the backside of the chiral along with previous mentioned materials that were incorporated into the matrix. An example of the chiral changing color and the fabric incorporation is given in Figures 5.7-5.8. The chiral was cut using a PLS6.150D laser-cutter by Universal Laser Systems. Painter's tape was placed on the surface of the SMP to provide some protection from charring during the laser-cutting process. The following parameters were used to laser-cut the SMP: power 75 W, speed 3.15 in/s, PPI of 1000. Some difficulty was encountered from the subtractive process to obtain the chiral. Specifically, design optimization was required to obtain struts that did not fracture with little effort. As mentioned previously, the heat from the CO_2 laser caused damage to the bonds in the polymer. When a lower T_g formulation was used several bonds within the system broke creating a lower number of bonds per area and resulting in a gummy polymer [19].

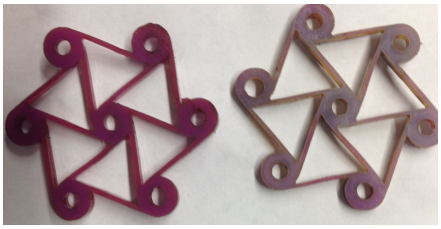

Figure 5.7: Chiral changes from purple to blue based on heat.

Figure 5.8: Colored shape memory chirals with fabric incorporated.

The actuation of the shapes was made by mounting the chirals on a canvas and using wire to attach the pieces to servo motors. The servo motors were triggered to move when a Lilypad thermal sensor (beside the chiral) detected a temperature change above the T_g. The observer used a hair dryer as the stimulus to create the change. Once the change was detected, using a temperature sensor, the Arduino was programmed to rotate the servo motor in the direction to close the chiral. The motor held this position until, the Lilypad detected that the temperature was sufficiently reduced below the T_g. Then the signal was sent to release the motor. The colder temperature was achieved by the observer using compressed air. The "cells" remained closed until another heat stimulus caused them to open [19]. A picture of the final product is given in Figure 5.9.

Figure 5.9: Front of "Auxesis" contains the color changing components [19].

Further experimentation is required in regards to the fatigue life of the chirals and streamlining the movement of the chirals. As stated before, the subtraction process markedly affects the fatigue life of the chiral struts. Therefore, greater assessment of the machining process parameters on residual stress is needed. Also, experimentation with regards to machining versus laser-cutting

the material versus direct casting of the shape. Furthermore, the Lilypad sensor seems to cease responding to the stimulus after a short period, possibly due to the extreme temperatures imposed by the two methods of stimulus. For future work, other methods of stimulus need to be explored.

5.3.2 The Secret Garden

This artwork is inspired by the process of an opening flower. The work seeks to mimic a flower unfolding into blossom. The conception of this piece comes from Chinese flowering tea, which is a tea in made by taking tea needles and binding them in a bundle around a flower. Once the tea is made to steep, the compressed leaves open to reveal a beautiful flower. The installation consists of three faucets that reveal hidden aspects of nature: the SMP flower activated by a clear bowl of water over a hot plate, the changing leaves, and the moss [19].

The color changing flower was created again using the formulation for a transition temperature of 70°C described in Chapter 2. The color change was created in this SMP by sonicating thermochromic powder into the Jeffamine D-230 and then mixing it with NDGE and Epon 826. The mixture was then cast and cured according to the steps given in Chapter 2. The creation of the "unfurling" flower, some experimentation was required. Initially, the flower was created by trying to mold the SMP using the silicone molds given in Figure 5.10. The resulting shape from one of these molds is given in Figure 5.11. The resulting flower from this mold did not create a flower that had a hinge-like structure to “unfurl," rather the flower structure consisted of a top surface with textured petals and a thick bottom base. The thick base is due to the fact that the mold fills over flat on the top surface, meaning the petals do not behave as individual hinges and unfurl. In order to create a hinged structure, the SMP mixture was cast into a 3 mm thick rectangular sheets and laser-cut using a PLS6.150D laser-cutter by Universal Laser Systems with the following parameters: power of 75 W, speed of 3.15 in/s, PPI of 1000. Painter’s tape was placed on the surface of the SMP to provide some protection from charring during the laser-cutting process. The final design of the flower for the installation was created using a sheet of SMP with thermochromic dye incorporated that was laser-cut in the shape of a flower which is given in Figure 5.12.

Another component of the installation is moss cast in thin layer of transparent resin with ther-

Figure 5.10: Silicone flower molds used to aide in iterative design of the Secret Garden.

Figure 5.11: SMP flower from previous iteration of the Secret Garden piece.

mochromic powder. When the thermal stimulus is applied, the minutiae of the moss is exposed to the observer, however in the non-activated state only partial aspects of the moss can be seen. The final aspect of this artwork utilize black thermochromic powder coated on leaves. These leaves mimic the fall season when heat is applied [19].

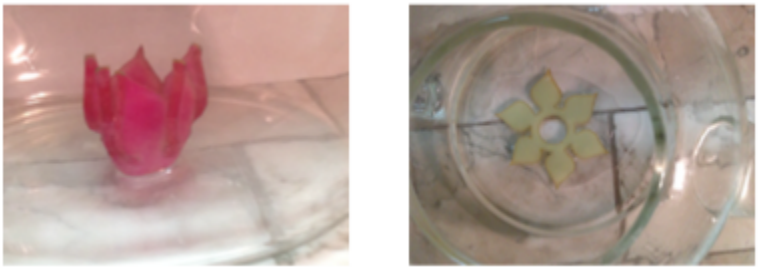

Figure 5.12: (Left) SMP flower before exposed to hot water. (Right) SMP flower after exposed to hot water [19].

This work provides an initial background for the creation of a more intricate hidden nature installation. Further experimentation in regards to creating a more intricate flowering shape and

casting the moss needs to be done [19]. The previous experimentation has shown that the thickness of the flower base is related to its compliance in the folding direction. A proposed model for a more intricate flower design is rendered in Figure 5.13 which mimics the bundles of the flowering tea and is molded after a lotus flower. This model appears to provide excellent folding behavior, however designing the mold to cast the SMP is challenging due to the varying levels of material with gap in between. In order to create this type of SMP flower, injection molding of the SMP should possibly be explored.

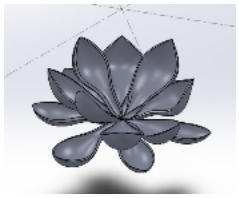

Figure 5.13: Proposed design for the Secret Garden flower.

5.4 Summary

The two artworks present a proof of concept in the creation of the tangible interactive structure for teaching using SMPs. The incorporation of the color changing component enhances the medium so there is both a visual and tactile component. These two artworks demonstrate ways to utilize SMP origami structures as a representation of hidden behavior of nature. Both works can demonstrate multiple phases of the structure represented. The results of this study builds on the work of the previous authors by including SMPs as a innovative tool to demonstrate educational concepts and make parts of our world tangible and not “magical” [64].

6. ORTHORIGAMI: SMPS IN CUSTOMIZED ORTHOTIC APPLICATIONS *

6.1 Motivation for Shape Memory Polymers in Design

In Chapter 5, it was discussed how the input/output nature of smart materials could be utilized as a teaching tool to represent complex concepts in a practical, tactile way. The ability of the materials to deform, sustain the deformed shape, and be reformed iteratively is an exceptional leveraging tool for a truly distinctive, interactive design. Designers desiring to use these materials must understand what applications would be most prudent to the materials' strength, and how to best harness the materials full capabilities for a given application. Several researchers have explored using smart materials for interactive design [75],[76],[77], [16], [78], [79]. This research emphasis structural design aspects including fabrication and engineering. Giles et al. in his work with "smart" e-textiles points out the gap in research excludes the tactile potential of the material to create interactive experiences, especially from the perspective of maker culture [80]. This chapter focuses on addressing this gap between smart materials and maker culture for a specific application, harnessing SMP sheets for use in Orthorigami (orthotics made using folding techniques) [20]. Explicitly, the goals of this section is to describe how to fabricate Orthorigami from a 2D sheet of SMP for specific design needs. The work investigates: designing Orthorigami for stroke patients, designing Orthorigami for children that can be adjusted as the child grows, and how children design Orthorigami.

6.1.1 Review of Customized Assistive Technology

One of the main motivations behind the exploration of the use of SMP in Orthorigami is that current orthotic devices on the market provide little to no customization in regards to size or aesthetics. Previous research in customized DIY assistive technologies (ATs) indicate user involvement during the design process increases the inclination for the individual to use the device [20].

*"Part of the data reported in this chapter is reprinted with permission of the authors from "Orthorigami: Implementing Shape-Memory Polymers for Customizing Orthotic Applications" by Jessica Reese, Jinsil Hwaryoung Seo, and Arun Srinivasa, Feb. 2020. Proceedings of the 14th International Conference on Tangible, Embedded, and Embodied Interaction, Sydney, Australia.

Generally, there are large percentages of traditional assistive devices that end up unused or abandoned [81],[82],[83]. Phillips and Zhao surveyed 227 adults about their use of AT. The device abandonment rate was 29.3% with large portion occurring in the first year or after five years due to change in needs or priorities. They showed that the abandonment rate of 66% for canes, braces, and walkers [83]. Hurst and Kane have identified some of the key factors from Phillips and Zhao surveys that influenced device abandonment [81],[83]:

1. *User involvement in device selection.* Users strongly desired to have influence over the selection of AT, and quotes one participant saying, "Listen to me! I know what works for me."

2. *Ease of procuring the device.* Devices that are easier to obtain, are more likely to be chosen, but do not necessarily provide the best performance with regards to needs.

3. *Device performance.* Participants cared about the reliability, comfort, ease of use, safety, and durability of AT.

4. *Change in ability (both improvement and decline) and preferences.* As a user's needs change, the device is unable to adapt to that change and therefore the technology does not work for a user's current lifestyle or priorities.

Scherer [82] points out that assistive devices are keen to assess the physical needs of the individual, but often neglect psychological and social aspects of using AT. Also, that until there is a comprehensive look at AT that considers environment, user preferences and expectations, and device features and functions, then usage and quality of life will not be enhanced.

DIY AT shows promise to address these current challenges with AT. Obstacles for making DIY AT remain: lack of tools for designing AT, lack of confidence, lack communication between users and designers of AT. Hook et al. sought to define the present challenges related to current DIY AT. In this study they interviewed occupational therapists, a medical physics practitioner, teachers at an additional needs school, and a person who makes DIY AT as a hobby. These interviews highlight

obstacles to designing DIY AT: lack of confidence in ability to build a device, time requirements to build a device outside of the normal care for a child, and uncertainty that the end product will suitable in strength, function, and aesthetics as a medical device [84],[20]. Buehler et al. surveyed makers (including both users and friends or loved ones, most without prior expertise) of 3D printed DIY AT on Thingverse. They identified the current trend in which designers of AT do not have disabilities or training in AT and suggest that DIY AT could benefit from creating more exposure to end-users and more communication between designers and users. The paper points out again that users with disabilities may not feel confident making their own DIY AT [85]. Hurst and Tobias in studies with adoptees and adoptive parents, showed AT users have specific ideas for design alteration and a willingness to learn how to create DIY technology [86]. McDonald et al. introduced 3D printing to physical therapists (PTs) for augmentation or making of AT. Their work demonstrated that PTs have unique knowledge of end users' medical needs and are accustomed to modifying existing AT for comfort. There were also certain limitations, specifically PTs' lack of background in 3D modeling, making the creation and design process of high fidelity customized devices more difficult, and that 3D printing materials also provide certain limitations in regards to comfort [87]. Baronio et al. sought to optimize production of a 3D printed customized hand orthosis. This research also points to the need for accurate hand geometry for a high fidelity model, and the trade-off between the cost of a scanning device and accuracy. Also, 3D printing has design limitations and that CAD technician and clinician expertise is necessary to create a suitable device [88],[20]. Chen *et. al.* did a pilot study (10 patients) with 3D printed casts for distal radius fractures. The design was able to sufficiently support the bones during alignment and all the patients preferred the customized design to traditional casting. The deficiencies reported include: the inability to acquire adequate scanned hand geometry, bio-incompatibility of the material (ABS) that lies next to the skin, fabrication cost in comparison to traditional casting methods, and odor of the cast after heavy sweating [89],[20]. Lin et al. looked at a single study that coupled designers with a quadriplegic patient to create a game controller and a mouse. The research implies that prototyping and digital fabrication techniques can help to create an accessible device that meets

specific needs and may be a preferable alternative when optimal fit and particular design details are necessary. However, additional training may be required to obtain the skills necessary to create a DIY AT [90]. Meissner et al. tries to address how people with disabilities experience DIY AT. Their results demonstrate that AT designers with disabilities feel empowered through making and see the benefit of learning maker skills for creating DIY AT for self-directed accessibility hacks [91]. Although, the work of creating a tailor-made device through DIY AT is encouraging to address the disadvantages with AT, there are still questions about what tools aid in making DIY AT, how to instill confidence (even if there is interest) in the makers of AT, and how to increase communication among makers and users of AT.

6.2 Implementing Shape Memory Polymers in Orthorigami

Since, work in the area of DIY AT has shown that user not only prefer customized devices, but are also more likely to use customized devices if they are involved in the design process and the device meets their specific needs now and in the future. In general, orthotic devices need to meet three criteria: aesthetically acceptable, lightweight and as simple as possible, and designed for easy adjustability [20],[92],[93]. This work answers how to design an orthotic that meets these criteria and is personally customizable using Orthorigami [20].

6.2.1 Designing SMP Orthorigami for Stroke Patients

Individuals who have suffered from stroke exhibit hypertonia, abnormal muscle tone. Therefore, a hand orthosis allows these people to perform daily tasks without assistance. Typically, a stroke patient would go to a physician's office to have the fit of their devices adjusted, because the commercially available material needs to be heated in the microwave. Posing a definite hazard to individuals who have loss of touch [20]. This process constrains the patient by always needing a physician to help with the device adjustment, and not being able to adjust their device to their own changing needs outside of a doctor's office. Orthorigami seeks to alleviate this obstacle, by having a material that can be heated with a hair dryer and provide visual feedback as to when the material is malleable enough to be formed.

In order to address this issue, several iterations of the prototypes were created. The initial prototype, sought to look at what size holes provide adequate “breathability" and what thickness provides "soundness" of the material without sacrificing comfort. For this initial prototype, no machining was introduced into the material. The research wanted to first focus purely on the material itself without any other factors influencing the design process. A variety of male molds were 3D printed. Then female silicone molds were made from these male molds to cast the SMP in. This process is the same fabrication process described in Chapter 2. A representation of some of the 3D printed molds used for casting is given in Figure 6.1. From these molds, a corresponding desired hole size that provided adequate “breathability" was selected and an initial prototype that incorporated Velcro straps, rayon-spandex pocket to hold and the SMP, and a finger plate in the outline of the patient’s fingers. This first prototype did not provide the desired comfortable fit for the finger plate area and the Velcro-straps proved to be loose-fitted [20].

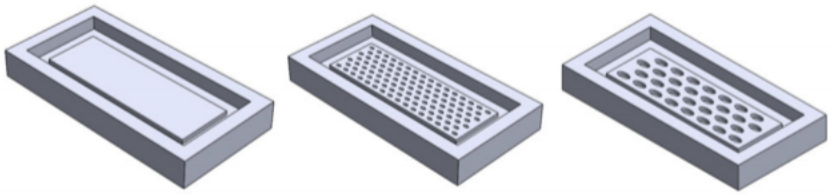

Figure 6.1: Prototypes for Breathability and Soundness [20]

The second prototype built upon the first prototype in that the finger plate was widened to better facilitate freedom of motion. The pocket for the SMP was removed in favor of a fully SMP plate design with the Velcro straps cured into the SMP and slots added to create adjustability with the velcro straps [20]. For this prototype, thermochromic powder as visual feedback was incorporated into the matrix. The powder was incorporated based on the procedure described in Chapter 2. The transition temperature of the powder was chosen to be equivalent to the transition temperature of the SMP. Therefore, the powder provided a visual feedback that coupled to the touch feedback

of the material. The prototype was reviewed by a local orthotist which assessed that the visual feedback was a significant improvement over current devices on the market allowing patients the ability to adjust the shape of their device without the need to come into a physician's office. The visual feedback, and the lower transition temperature, 50° C, which did not burn the patient when heated, was an advance in allowing patients with hypertonia to maintain independence with regards to device performance and change in ability [20].

A third prototype built upon a the second prototype, through further interaction with the orthotist. Through this interaction it was suggested that the finger outline be changed to a heavily contoured edge to allow for more uniform loading to the orthosis. The third prototype widen the support area around the wrist hand and fingers [20]. The plane geometry of this prototype proved to be acceptable, but the thickness was increased in a final fourth prototype. The molding for this final prototype is given in Figure 6.2.

Figure 6.2: (Left) 3D Printed ABS make mold to cast silicone. (Right) Silicone Female Mold to cast SMP [20].

A picture of the final Orthorigami design is given in Figure 6.3. The final design addresses two needs that lead to device abandonment discussed earlier: device performance and change in

ability. This design aides in usability and adaptability through the incorporation of thermochromic powder creating greater independence for the patient to make adjustments outside of a doctor's office. The device also increases safety due to the lower transition temperature needed for adjustment. This design addressed the needs related to hypertonia in stroke patients, however the design did not explore the incorporation of subtractive manufacturing to further improve on the ease of manufacturing the device [20]. Exploration of subtractive manufacturing in this application may further address user involvement in device selection and ease of procuring the device. If sheets of SMP are used with subtractive manufacturing, then a patient and a practitioner can work side by side to create many iterations of a design customized to the patient's individuals needs or wants.

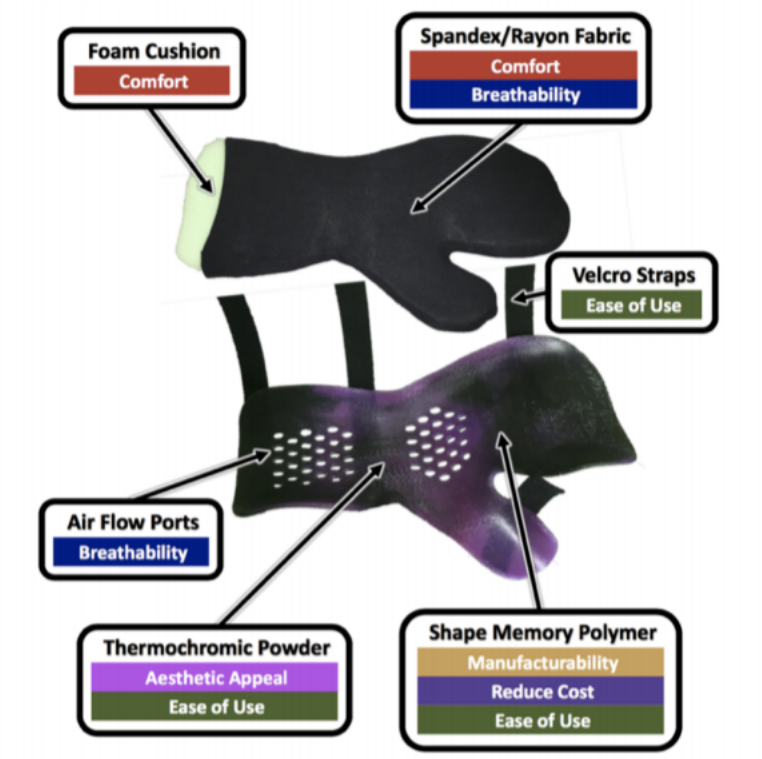

Figure 6.3: Final Design of the Orthotic Brace for Stroke Patients [20]

6.2.2 Designing SMP Orthorigami for Children

The second part of this work is to address how to design Orthorigami for children, specifically, change in ability needs with a device that can grow an adjust as a child grows. The second case study further explores incorporation of subtractive manufacturing in the process of the design to allow for ease of design iteration and ease of procurement of the device. Paper was chosen as the medium to create prototypes for this case study. The paper was hand-cut or laser-cut and then taped to the hand to address expeditious feedback in terms of fit, design, breathability, and aesthetics [20]. The paper prototyping allowed the designs to be selected for further investigation as final designs. Examples of the paper prototypes are given in Figure 6.4. The main insight from the paper prototyping was that the connection between the thumb and the finger needed consideration, as the area is sensitive with regards to motion of the hand.

Figure 6.4: (Left) Depiction of paper prototype of honeycomb design based on Chinese finger trap. (Middle) Depiction of paper prototype of strip strap design optimized for simplicity. (Right) Depiction of paper prototype of bosani design providing maximum support with minimal material [20].

This study sought to address how subtractive manufacturing could be beneficial in the design of Orthorigami. Also, the study sought to address the device how to make a device that is aesthetically pleasing. As the previous case study incorporated thermochromic powder to aide in functionality for a specific need, this study utilized both thermochromic and photochromic powders along with Castin' Craft epoxy dye to create an artistic visual effect. The method to incorporated the dye

and powder is again described in Chapter 2 with an image of a resulting sheet in Figure 2.7. Laser-cutting was the subtractive manufacturing method used to cut the SMP based on the paper designs. As explored in Chapter 3, the laser-cutting caused degradation and broke chemical bonds creating a significant decrease in thermal transition temperature for thin segments of SMP material. Therefore, it was determined that width of a supportive segment needed to be optimized for laser manufacturing in order to provide support with sacrificing structural integrity. This prototype sought to address comfort and breathability by incorporation of foam strips into the SMP matrix, allowing for the material not the adjacent to the skin and ventilation challenges for air to pass through [20]. Examples of some of the final designs with the thermochromic and photochromic effects are given in Figures 6.5-6.6.

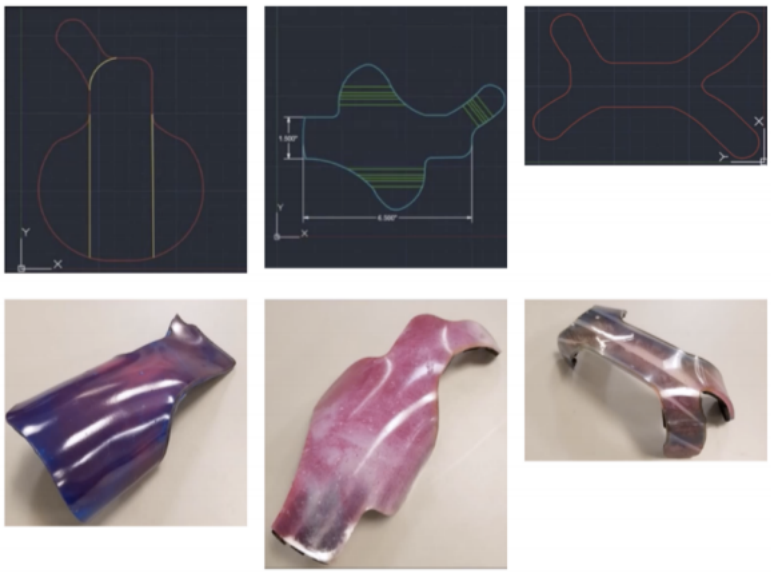

Figure 6.5: Final brace orthotic brace designs for children with 2D and 3D geometry [20]

This case study built upon the previous case study by adding and aesthetic component with thermochromic and photochromic powder and Castin' Craft dye. The paper prototype provided a valuable tool that allows for immediate tactile feedback on device design [20]. Specifically, paper prototyping helped address user involvement in device selection and device performance, by

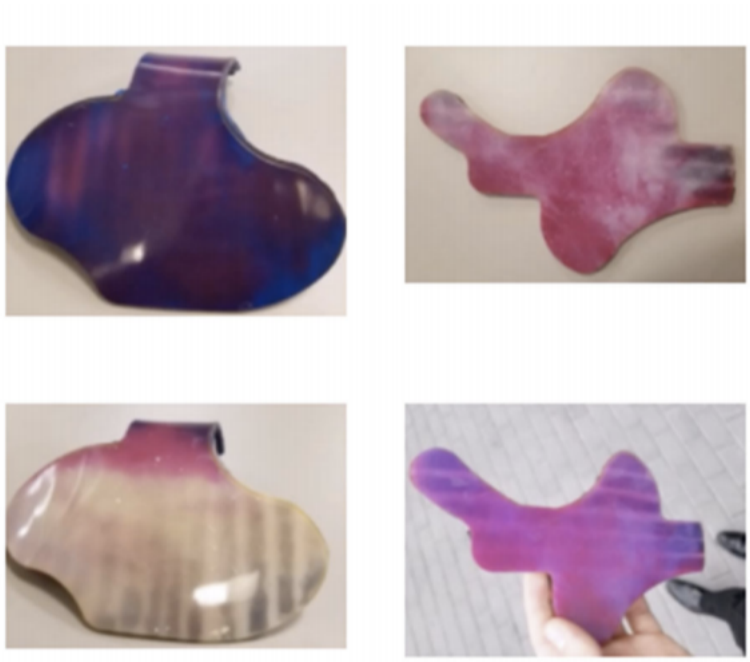

Figure 6.6: (Top left) Thermochromic design at room temperature. (Bottom Left) Thermochromic design heated. (Top Right) Photochromic design indoors, Bottom Right: Photochromic design outdoors [20].

allowing anyone with access to paper and scissors to begin to create and modify various prototype designs to their specific wants and needs. Subtractive manufacturing also aided in the ease of procuring the device by decreasing the amount of tools and time required to achieve a final design when using 3D printing [20]. The main disadvantage of this case study was seen due to the degradation imposed by the laser-machining. Both case studies address customization with regards to size and aesthetics for two different applications through the use of Orthorigami. The studies show that user involvement in design process is achievable even with very basic tools found in most homes. Also, the suggested design process: iterative paper prototyping with feedback/insight from individuals working with their practitioners followed by subtractive manufacturing with SMP sheets provides a straight-forward way that addresses the four components related to device abandonment identified earlier [81],[83]. A final case study was done to look at how children design Orthorigami and it also incorporated the use of CNC machining to alleviate the issues encountered with laser manufacturing.

6.3 Assistive Design through Children's Orthorigami Workshops

As stated earlier, Giles et. al. described the gap between smart materials and maker culture. Giles et. al. uses participatory workshops with visually impaired individuals and e-textiles, to create objects that are meaningful to them. The workshops also explore how crafting and making with e-textiles can be made more accessible to create an empowering experience for makers [80]. This work uses participatory design workshops to see how children create and design with SMP. Also, the workshops ask how making with SMP affects the children's confidence in their design capabilities to provide a positive, enabling experience.

6.3.1 Smart Materials and Children

Smart materials provide an active role with sensory feedback that can influence how makers create and design. A few previous researchers, have engaged children with these materials and assessed how children learn through this active/sensory design experience or how they design and create with these active materials. Qi and Buechley combined SMAs with paper origami techniques to create dynamic craft and art installation projects. In their workshop, 9-15 year olds created a SMA flapping crane. The activity fostered an increased interest in electronics and provided an exceptional method for teaching circuitry design [15]. Jacoby and Buechley explored how children can use capacitive touch with conductive ink, paper, and controllers for narrative storytelling and for stimulating creative interactive design. Their work showed that working with conductive ink was intuitive and comfortable for children. Children were able to use conductive ink in a versatile manner as a story-boarding tool, and some children able to combine function and aesthetics to fit a specific purpose within their design [94]. Takegawa *et. al.* asked children to design, discuss, and test the function a musical instrument by drawing different shapes on paper with conductive ink. Their system creates a musical instrument prototype that can be flexibly and intuitively customized by conductive ink [95]. Minuto focused on introducing smart material and building interfaces with these materials with children age 9. Workshops to guided the children in the creation of automated puppet plays by combining SMAs, origami, thermochromic paint, visual programming with

a modified type of Scratch programming, and a cardboard theater to display their work. Their results showed that children learned new skills related and methods of expression. Also, the use of smart materials fostered greater interest in storytelling [96]. Beuchley et al. examined how children work with computationally enriched e-textiles. They presented an electronic sewing kit, termed Sewing Circuits, in preliminary workshops with children and young adults ranging from ages 8-18. Almost every participant was able to construct a working circuit, and children expressed interest in integrating customized, fabric-based artifacts in their lives [97]. Kuznetsov et al. developed workshops for junior high youth and local adult artists that introduced DIY screen-printing fabrication with thermochromic, UV sensitive, and conductive ink. The researchers introduced a readily available medium for interactive art creation and storytelling. The youth viewed their work as "art and science" and they transitioned easily between screen-printing, traditional crafting, circuit prototyping, and use collaboration among their fellow participants create story lines. This work showed that screen-printing with smart inks is easy to access, reproducible, and naturally supports collaborative making [98]. These previous researchers show that the introduction of smart materials as a tool can provide an accessible medium with an "active" role in inspiring children toward innovative and collaborative thinking. Smart materials can also cultivate children's interest in science and help teach new, unfamiliar concepts.

6.3.2 Preliminary Orthorigami Workshops

To design an Orthorigami workshop several preliminary workshops were conducted. The purpose of these preliminary workshops was to explore and provide feedback on activities to determine which of these activities assisted and promoted students to think about the novel material and the task at hand. From these workshops, some conclusions were drawn with regards to the participants response from video transcribing and survey feedback.

To introduce the concept of SMP the children were allowed to design with a commercially available SMP (polystyrene) crafting material, "Shrinky-Dinks." Children designed bracelets using the "Shrinky-Dinks" material and colored pencils. Although the material does exhibit a shape memory effect, it does not do so in an equivocal way to the SMP created by the research team

because “Shrinky-Dinks" only appear to “recover" shape not “reform" shape. The choice was made to exclude this material as an introductory material, since crafting with this SMP proved to be too distinctly different in favor of only providing an introduction and demonstration of the SMP that the researchers created for use with the workshop.

Researchers introduced the concept of thermochromic painting as an added aesthetic design concept to assistive design. To make thermochromic paint, a generous amount of Solar Color Dust thermochromic powder was mixed with paint using a paintbrush. For example, blue thermochromic powder was mixed with red paint to create purple when cold and red when heated. Examples of painted scene were shown with 1-2 color changing components, to give a demo how the thermochromic painting works. Participants were also given a demonstration on color mixing/changing with paint coupled with thermochromic powders and how on primary and secondary color mixing can predict what color will appear as the thermochromic powder is heated when mixed with a certain type of paint. Color mixing and the notion of primary and secondary colors proved a more abstract concept to some children, so the research team decided to allot more time to this activity. For the final workshop, more time was allotted to explaining this activity to go through more examples of color mixing and what the resulting color would be when heated to give participants a greater understanding of color theory.

Researchers wanted to explore paper prototyping, since it provides a valuable medium for fast iterative and critical design thinking. During the first preliminary workshop, researchers created an example paper prototype thumb brace and then asked the children to design on their own a paper prototype brace for the thumb or wrist. Almost 50% of the participants chose to mimic the example thumb brace without modification. In future workshops, the example was excluded to force the children out of a “pattern-matching" behavior. Instead, the participants were given the opportunity to discuss any previous experience wearing a brace or experience with a close family or friend member who wore a brace. Reflecting on their discussion of experience, participants were again asked to design a paper prototype of a wrist brace using their own hand as a guide. Designing a freestyle paper prototype on their own body provided some challenges with not being

able to use two hands to create the full design. Also, there were challenges with mirroring aspects of 3D spatial design. In order to support 3D spatial design, the researchers decided to investigate the use of virtual reality and sculpting in subsequent preliminary workshops.

Participants were given the opportunity to design a wrist brace using a virtual reality tool, Google Tiltbrush with a hand model. Although some children had had previous experience using virtual reality, the environment proved to be far too removed from the tactile feedback of crafting. Therefore, the designs in virtual reality did not translate into physical designs and Tiltbrush was omitted as a fabrication technology.

To further inform 3D spatial design, participants were given the opportunity to wear a commercially available wrist brace used for a sprained wrist for 20-30 minutes. The brace gave participants the opportunity to think through certain essential design components, such as wrist support, and wrist attachment. After, students were able to reflect on their experience wearing a wrist brace, they were asked to design a wrist brace through sculpting with play-dough using their own hands as the template. The play-dough provided an improved medium for design, but designing trying to design for your body proved restrictive. The final workshop chose to use play-dough sculpting, because preliminary workshops showed participants found 3D design difficult on their own hand. A life cast of a hand for sculpting was prepared with Alja-Safe alginate by Smooth On. From the play-dough design, participants unfolded their 3D design and outlined on paper 2D brace design. These paper designs were input into a Glowforge laser-cutter that took a picture of the outlined design and laser-cut a paper-prototype to test the fit on the hand. The Glowforge, provided an efficient, easy way to iterate and adjust paper prototypes for the final design.

For the e-textile example, a sheet of SMP with holes on each side was created by same casting method in Chapter 2. An example e-textile was created by sanding the surface of the SMP and drawing a leopard face on the sanded surface. Fabric backing was added containing conductive thread and a coin cell battery connecting two green LEDs aligned behind the leopard eyes. This example to demonstrated how to connect electronic sewing and thinking through placement of LEDs to enhance aesthetic design.

The conclusions from these preliminary workshops showed that demonstrations and introductory material given by the researchers should be carefully chosen as to only inform as to function without creating a "pattern matching" behavior. For the final workshop, certain examples were withdrawn to allow for less unimpeded design results. An overview of the resulting final workshop activities and concepts is given in Table 6.2.

6.3.3 Orthorigami Workshop

6.3.3.1 Participants

For the Orthorigami workshops, participants were recruited through university email lists to participate in a creative assistive design workshop. The age range for the workshop was ages 9-12 with interest in arts and crafts and creating assistive design devices for medical applications. The design of the Orthorigami workshop took place over three days: Tuesday, Thursday, and Saturday within one week with each day consisting of a 2.5 hour session. Participants were given the option to attend either a morning or an afternoon workshop. The composition of the participants is given in Table 6.1. Upon entering the workshop, the parents and participants were given the chance to ask questions and parental consent and minor assent forms were obtained. At the beginning of the workshop, a pre-survey was administered to understand the participants background in with different artistic forms and assistive devices. The results of the background section of the Pre-study survey are given in Figure 6.7.

Participant ID	**Age**	**Gender**
ID17	11	F
ID18	11	M
ID19	12	F
ID20	9	M
ID21	10	M
ID22	11	M
ID23	10	F
ID24	9	F

Table 6.1: Participant background information.

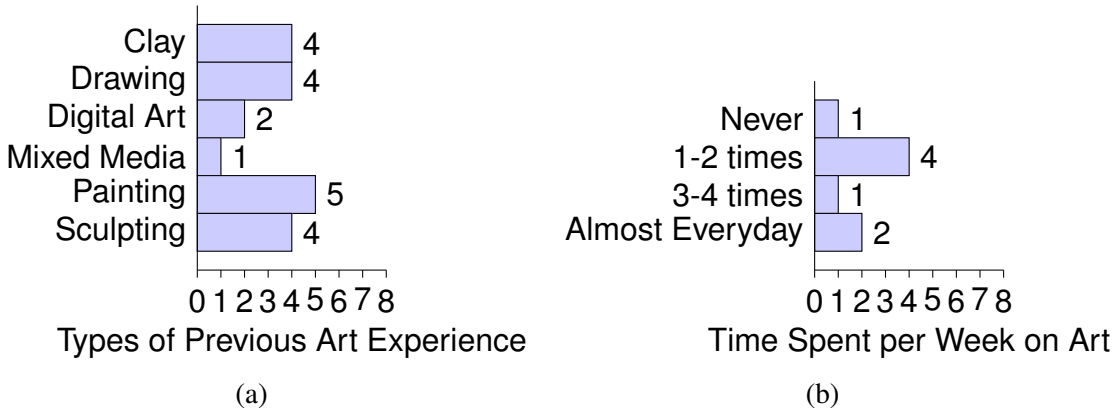

(a) (b)

Figure 6.7: Description of previous participant art experiences.

6.3.3.2 Workshop Structure and Materials

6.3.3.2.1 Day 1 Participants were introduced to the concepts of AT, wearable device and SMP. They started designing a wrist brace using play-dough, paper and 2D SMP sheets. In order to demonstrate the structure and function of a wrist, participants were given the opportunity to wear a commercially available wrist brace for approximately 30 minutes. The participants were allowed to reflect on how different available commercial braces had differing placement and types of metal support components and attachment. Next, participants were introduced to the concept of shape change within a SMP through a video demonstration that depicts the shape memory cycle of folding and unfolding through placing SMP in cups filled with different temperature water. Then participants were given pieces of the SMP material created by the researchers for a hands-on demo. These pieces heated with a warm hair dryer to become malleable, and participants were then allowed to bend the material and freeze the bent shape by holding the SMP under cold water or sticking it in the fridge. The material was again heated with a hair dryer in which it returned to its original shape.

The participants were asked to design a wrist brace that incorporates the SMP material. As a part of the design, participants were required to provide support for the wrist area, but free to choose whether to implement additional support for the fingers or not. Participants were given a cement cast hand asked to create a 3D design of the brace by sculpting with play-dough on the

Day	Activities	Design Concepts
1	Demo commercial wrist brace, Video demo of SMP, Material Experimentation with SMP, Design with Play-dough Sculpting on Hand, Laser-Cutting a Paper-Prototype, Iterative Adjustments of Paper Prototypes, Final Wrist Brace Design Sketch, CNC Machining of SMP Supports	Brainstorming, Material Experimentation, Crafting (Sculpting), Iterative Design, Fabrication Technology, Smart Material Design (SMP)
2	Laser-Cutting Fabric Design, Sewing Final Design, Reflection on Wrist Brace Design, Thermochromic Painting Demo, Color Mixing Introduction, Thermochromic Painting	Brainstorming, Fabrication Technology, Material Experimentation, Crafting (Painting, Sewing) Aesthetic Design Smart Material Design (Thermochromic)
3	E-textile Introduction and Demo, Simple Circuitry Introduction, Creation of E-textile Bracelet, Extrapolating New Designs from Workshop Activities	Brainstorming, Fabrication Technology, Material Experimentation, Crafting (Sewing), Smart Materials Design (E-textile, Conductive Thread), Integrative Thinking

Table 6.2: Orthorigami workshop activities.

hand. Once the design was done, the play-dough was removed from the hands carefully and laid out flat on paper and traced. The Glowforge laser-cutter took a picture of the traced design and then laser-cut a paper prototype. The paper prototypes were attached to the participants' hands using tape. After having the prototype on their hand, participants were asked to think about the fit of the paper on their hand and given the opportunity to cut and assess new prototypes based on iterative adjustments. Through this iterative process a final design was sketched out on paper. Participants were asked to include the specific details (aesthetic components, where the SMP will be positioned, how the device will attach, etc.) in the sketch of the final design. A depiction of the method of this design process is given in Figure 6.8a-6.8d. The shapes of the SMP in these final designs were scanned and converted into a drawing file to be used on a CNC machine. The CNC machine was used to cut the 2D SMP sheets in the shape of the final design of the support pieces.

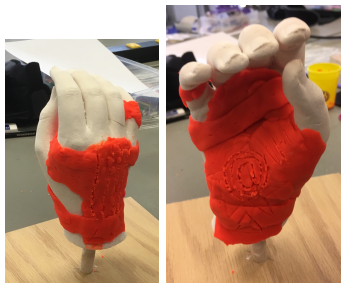

(a) Play-dough wrist brace design.

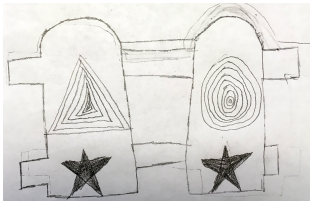

(b) Outlined Design to Scanned into Glowforge Laser-Cutter

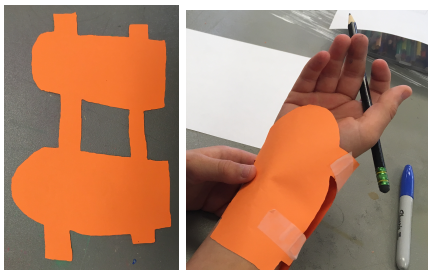

(c) Paper-Prototype of Wrist Brace Created Using Glowforge

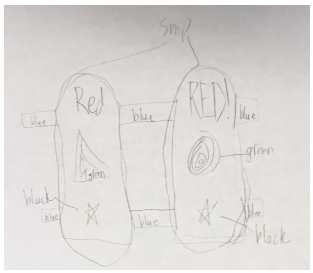

(d) Final SMP Wrist Brace Design Sketch from Paper Prototyping

Figure 6.8: Design Process for the Wrist Brace

6.3.3.2.2 Day 2 The second day children were given their machined SMP and the Glowforge was used with their final design sketches to cut the fabric components of the wrist brace. The participants, with help of the research team, sewed fabric for the design using sewing machines and the SMP was placed in the sewn brace. Participants were then introduced to the concept of thermochromic painting by showing videos of thermochromic materials, powder and paint, changing color with temperature. The participants were also given scenes painted by the research team and allowed to use the warm hair dryer to see how the thermochromic paint in the scene changed. Some of these example scenes included: a field of bluebonnets and Indian paintbrushes where the bluebonnets disappeared when heated, a cat caught in a rain cloud where the went away when heated, and a scene where the grass in a field turns from brown to green. Color mixing with regards to primary, secondary, and tertiary colors was explained in the context of thermochromic painting. The participants were asked to predict what colors would appear when the thermochromic paint mixture was cool or heated. For example, if blue thermochromic powder (that changes to

white when heated) is mixed with red paint, then the mixture will appear purple when cool and red when heated. After this introduction, participants were then asked to paint a scene containing 1-2 color changing components and to plan how the color will change within these components. Thermochromic powders of blue, yellow, magenta, green, and red were given to mix with various colors of paint. Participants were then given the choice of adding a color changing component to their final wrist brace design. After completion of the design, participants were allotted some time to discuss durability, practicality, fit, and aesthetics of their design with the group. Pictures of the participants final design is given in Figure 6.9.

Figure 6.9: Examples of participants final brace SMP designs: (Top Left) Breathable design with thermochromic clouds. (Middle Left) Space-themed design with a rocket ship, galaxy, and moon. (Bottom Left) Fashionable ninja blade design with thermochromic Pokémon masterball. (Top Right) Glove design from the design process in Figures 6.8a-6.8d. (Middle Right) SMP brace design with thermochromic initials. (Bottom Right) Design with layered laser-cut fabric depicting unicorn.

6.3.3.2.3 Day 3 The final day of the workshop participants were given the opportunity to expand their creation with a different smart material, e-textiles. Participants were introduced to what an e-textile was by being shown videos of interactive wearables, such as clothing and shoes with

LEDs incorporated and a phone operated LED necklace. The participants were also given an explanation of simple circuit design including how to connect a battery, switch, and LED. Participants were given a rectangular shaped fabric, rectangular shaped SMP, conductive thread, LEDs, and a coin-cell battery and asked to use soft-circuitry to design a shape-changing wearable bracelet. Pink, green, blue, yellow, or white Lilypad LEDs were available to be used in their design. Participants were given the choice to either draw on the surface of the SMP and integrate the LED into the fabric underneath the drawing or to leave the surface of the SMP clear and design a scene on the fabric with LEDs. Examples of the final design are given in Figure 6.10. Afterwards, participants were asked to discuss their design with the group. At the end of the workshop, a post-survey was given that asked about their experience in the workshop and asked them to extrapolate their design experience to the creation of new assistive devices or designs for themselves or others. The parent's of the participants were also given a survey to complete.

Figure 6.10: Examples of participants e-textiles: (Top Left) Doge internet meme with a halo on top. (Top Right) Clear SMP surface with fabric design of stars and threaded constellations. (Middle Left) Clear SMP surface with fabric design of rippling water and flower Lilypad. (Middle Right) Sanded SMP surface design of King Crimson from JoJo's Bizarre Adventure. (Bottom) Sanded SMP surface design of wand and Golden Snitch from Harry Potter.

6.3.4 Data Collection and Analysis Methods

The data collected for the study consisted of video interviews taken during the workshop, a pre-workshop survey, a post-workshop survey for participants and parents, and photos of the participants work. The video interviews were transcribed and placed into a spreadsheet. From the transcribed videos, the phrasing was coded. The coding for the elements attributed to the design process were derived from the categories described by Brown. Brown described as passing through three phases in design: inspiration (circumstances that motivate a search for solutions), ideation (the process of generating, developing, and testing ideas that lead to solutions), and implementation (charting a path to marketing) [99]. Coding was also used to describe the "designs" themselves have to do with the aesthetics of the design such as color, texture, structural support, and images. Further coding was also done to describe the emotional experience of the participants which included codes related to excitement, engagement, and empathy. These coding categories for the transcript are given in Table 6.3.

The words from the questionnaires were placed in an excel spreadsheet and descriptive notes of the drawings in the questionnaires were also collected in the spreadsheet. Pictures of the student's final work and drawing in the questionnaires were also analyzed. The analysis of these items included design coding descriptors listed earlier, as well as, using questions given by Clarke and Freeman and Mathison to analyze visual discourses [24, 25]. A summary of the questions used is given Table 6.4.

Coding Categories		
Design Process	**Design Aesthetics**	**Emotional**
Inspiration	Color	Excitement
Problem Definition	Texture	Engagement
Problem Observation	Images	Empathy
Role Playing	Structural Support	Sympathy
Ideation	Mimicry	
Brainstorm Sketching	Innovative Design	
Creative Framework	Innovative Performance	
Integrative Thinking		
Idea Categories		
Concept Selection		
Prototype		
Implementation		
Execution		

Table 6.3: Coding used in the Orthorigami workshop analysis.

Questions
What are the design features?
What values and knowledge are communicated by the creator?
What common experiences are invoked?
Can you determine whether the creation was aimed at a particular audience?
How is color used? What is bright and vivid and what is not? How does the variation in the color direct your attention?
Are there areas of different texture? What are they? What do they do to the overall image?
Are there symbolic or other references in the creation you can decode? What are they? Where do they come from? Why do you think they are there? What work do they do in the overall visual?

Table 6.4: Questions for assessment of visual aspects of the design [24, 25].

6.3.5 Results and Discussion

The participatory workshop was a success. All participants were able to create a customized wrist brace and e-textile of their own design using DIY concepts and SMP. Participants reporting an average (on a scale of 1-5) of 4.5 on how they felt about the workshop, of 4.1 on how they felt about the wrist brace they designed, and of 4.5 on how they felt about the e-textile they designed. Participants felt engaged in making process, felt aided by the use of fabrication technology, felt inspired to create new AT, and were able to bridge various crafting concepts presented in the workshop. Through our analysis we identified the following themes to discuss: (1) Participatory Making of DIY AT and (2) Creativity, Inspiration, and Integrative Thinking.

6.3.5.1 Participatory Making of DIY AT: Experience and Accessibility

The process of making is a complex process involving problem consideration, brainstorming, creation, iteration, evaluation, and integration of concepts. Even for highly motivated designers, there are still barriers due to lack of experience when creating a new functional product. Fabrication tools and techniques are needed that make unfamiliar design accessible to the average user. A major component of designing Orthorigami, is the ability to imagine a 2D to 3D origami shape change. Children and users of AT do not necessarily have experience with 3D spatial design or modeling software. Therefore, the introduction of sculpting with play-dough aided the participants in design of their AT. ID19 states that the play-dough aided in the design process, because it would have been tough to start with 2D first. The study of McDonald et al. also pointed out the preference to sculpting in aiding in design. The study found that 76.3% physical therapists who were taught how to use 3D modeling software, still preferred design with play-dough and 3D scanning of the design over 3D modeling of DIY AT. The Glowforge laser-cutter also provided a valuable tool for iterating multiple intricate prototypes to test against the participant's hand. Participant's were able to place the designs on their hands using tape and discuss with the researchers where the fit of the design was too lose or cutting into the skin too much. ID17 pointed out to the research team that the fit of the straps of the original paper prototype was too big on her hand and that the attachment

point where the velcro goes was too tiny. Based on this type of feedback new designs were able to be re-cut quickly with the laser-cutter or modified with scissors. The ease of use of the laser-cutter also foster how future designs were created or modified. For example, ID18 chose to use the laser-cutter in the e-textile design, Figure 6.10 (Middle Right), to cut the stars in the design, due to the fact they were small and intricate.

Children and users of AT do not necessarily possess medical knowledge or training to design AT. Designing AT with smart materials presented two main challenges to participants. The first challenge was to address how to provide adequate structural support with flexibility, wearability, and breathability. Second participants were challenged by designing with new and unfamiliar smart materials. Wearing the various commercial prototypes aided children in thinking through how typical devices addressed the first challenge. Also, children were able to consider, for their own design, how modifications could be made to create a better device. ID17 when reflecting on the final design stated, *"I feel like it could maybe like wider SMP because when you do this (places wrist in flexion), you can still move your wrist this way."* ID21 compares the SMP brace to design to one of the commercial braces, *"My brace is kind of like this (pointing out one of the commercial braces) except it has holes for each finger, so that it gives you more flexibility."* ID17 describes the SMP brace as, *"I think that mine is very durable. Like it's very wearable. Because like it's very simple and doesn't take a genius to understand how to function the whole thing. That's what I don't really like about some straps (pointing to the ones on the commercial braces) is that sometimes you have to weave them through the little loops. And then the loops rub against your arm and then all of that. So this is just felt and Velcro and a strip of plastic."*

The workshop and materials engaged participants and generated excitement in design. ID17 described her experience as *"all of it being fun"*. ID23 when asked what their perception of the material was said *"I like it. It's a really fun material."*. At the beginning of the workshop, ID20 seemed disinterested in participating in the workshop, stating they couldn't make a brace, and felt compelled to be there because their parent signed them up. By the end of the workshop, ID20 was able to share how they designed their brace, felt the skill level was not as difficult as originally per-

ceived, and was motivated to integrate a favorite D&D concept, a bag of holding, into a new design. The workshop also encouraged them to co-design and collaborate with the researchers, as well as, their peers participating in the workshop. Few of the participants had experience with sewing, the researchers helped in sewing co-design with regards to advising participants on stitching space requirements for placement of aesthetic or electronic components and for seams. The researchers also taught techniques and assisted participants in thinking through how to make mixes for their thermochromic color changing choices and using the appropriate amount of thermochromic powder to create a significant change. For example, ID19 stated they wanted to do a Pokéball on their SMP brace design. The researchers encouraged the participant to think color change options that like red to white, through a collaborative discussion ID19 decided to use a Pokémon masterball changing from purple to red. The workshop motivated participants to consult the research team and each other on how to take their designs from an idea phase to a product phase. During the brace design, ID20 asked to see ID22's SMP brace design because it gave him an idea. ID22 proceeded to explain how they created the sculpted the face component to aid in execution of ID20's idea. ID24 created a galaxy (swirl) on the play-dough model of the SMP brace design. Through co-design with the research team a fabric equivalent of the galaxy was created to add texture.

6.3.5.2 Creativity, Inspiration, and Integrative Thinking

Each participant's work represented a unique, tailor-made wearable AT or e-textile. Participants chose personal preferences to integrate into their final designs such as nature; favorite animals, characters, or themes; colors; and textures. In Figure 6.9 (Middle Left) ID24's design is an inspired favorite space theme: *"And I'm doing mine like space theme...like that's a rocket ship, that's supposed to be a shark and then that's a [inaudible]."* In Figure 6.10 (Middle Left) ID19's design is a favorite anime character, King Crimson, from the series Jojo's Bizarres Adventures. Figure 6.9 (Bottom Right) ID23 incorporated a character, a unicorn, by textured layering of laser-cut felt materials in the SMP wrist brace design. In Figure 6.10 (Middle Left), ID17's design uses texture to depict a lily pad and rippling water. ID17 describes the work as *"So, this was a lily pad cut out like a little lily. This was something a lot of people thought was a flower. Well some people*

also thought it...but it's just the ripples in the water that you see when you drop something in there and you just touch the water when you just see the wave and reflection.".

Their designs also represented creative integration of between smart materials, such as thermochromic components or SMP, electronics, and design. In Figure 6.9 (Bottom Left) ID19's design incorporates a ninja blade and thermochromic Pokémon ball that changes from a purple Masterball to a standard red Poké ball. In Figure 6.9 (Middle Right) ID17's final design uses favorite colors and thermochromic paint that changes from purple to pink to place an initial on the SMP brace design. In Figure 6.9 (Top Left) ID18's SMP brace design uses thermochromic clouds changing from pink to white. In Figure 6.10 (Bottom), ID23's design incorporates a Harry Potter wand and golden snitch as a favorite theme, but accentuates the wand and snitch using LEDs. ID18's e-textile design, in the same figure (top right), integrates LEDs to light up the stars and conductive thread as a representation of constellations. ID22's design is a favorite internet character, Doge, with a halo above it's head illuminated by a white LED. These final designs of the SMP brace and e-textile represent a merging of purpose, functionality, and fashion.

Participants were inspired to share their work with friends and family, discussing what they had created, how the device was created, and how the material worked. Parents were asked if their children were interested in discussing the workshop with themselves or peers. ID23's parent stated, *"Yes, she showed her friend how her design worked and how it was made (polymer, play-dough, laser-cutter)."* ID17's parent stated the participant discussed, *"more the experience and the thermo-sensitive nature of the polymer. She talked about designing the brace and also painting with heat sensitive paint."* ID20's parent responded, *Yes, ID20 is so excited about this workshop. He discussed with me and his dad, and his brother. He kept saying, "We learned cool stuff like cutter with laser and polymer smart shape."*

Participants were motivated to an increased interest in art or exploration of design. ID17's parent stated when asked if there were any changes in their art creativity or activity post-workshop, *"She has already been very interested in home made 'goo', playing substances like 'play-dough', 'oobleck' types and this will certainly keep that interest active.".* ID19's parent said *"He tried to*

use light bulb and sun light to see the color painted shift from purple to red." ID24's parent said *"Already interested in slime, and now really wants to make devices."*

At the end of the workshop, all the participants expressed they felt confident to design and make things. On the post-survey participants were asked to brainstorm by bridging the materials they have used in the workshop to design new innovative creations. Examples of their brainstorming based creations with LEDs are given in Figure 6.11. The designs represent the integration of LEDs into wearables, AT, and personalized dishware to enhance fashion or functionality.

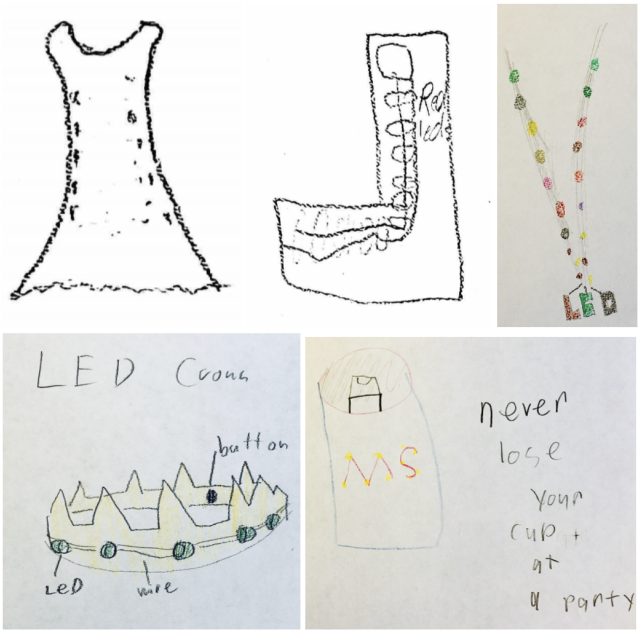

Figure 6.11: Examples of participants brainstorming design with LEDs: (Top Left) LED dress. (Top Middle) Ankle brace with red LEDs. (Top Right) LED necklace. (Bottom Left) LED crown. and (Bottom right) LED koozie.

Participants were also asked if they could think of other uses for SMP outside of AT or wearable design. Their responses demonstrated integrative critical thinking with regards to the material functionality. ID19 said, *"We could make something out of this and then you compress it and then heat it up again and it turns back again. Like you can make stuff portable, because like if you*

make a uh bowl and you take the bowl and you turn it into a ball and then if you heat it up again. Then you've got your bowl." ID17 suggested making a small water bottle that can be stretched out. ID17 describes the device as, *"Like if we had the same bottle or if we had a bottle this size, like we just thought I don't want this big a bottle because I don't want to carry it around just squish it together. Or you just want to carry a small little emergency water bottle, because you don't have water carrier you can, because I've seen these people who carry something like that and then they make their own little filter and they just attach it on like if they are tired or something."*

6.3.6 Conclusions from the Orthorigami Workshop

The Orthorigami workshop addressed these questions: How children make and design with smart materials, specifically SMP? How children create and design with SMP to make DIY AT? How using SMP in design can affect children's creativity and confidence and provide a positive, enabling experience? What types of tools or fabrication or crafting technology aid children in design of DIY AT? The workshop showed participants felt confident to create designs with SMP. Specifically, the participants were able to brainstorm new designs that incorporated the concepts introduced in the workshop. Participants were innovative in their choices regarding implementation of smart materials into the design. They created unique artefacts of intricate personalized designs, and they were excited to share their work and experience with friends and family members. The workshop stimulated an increased interest in art. The materials and activities in the workshop helped participants to have a positive outlook with regards to their ability to design DIY AT. Smart materials proved to be an accessible medium and an "active" participant in aiding in design with children. The experience cultivated bringing together different aspects of design and encouraged further inspiration of art and design.

The tools used in the workshop, showed that low-tech DIY design through crafting helped participants feel confident and understand how to design. Observing commercial braces and learning about the materials assisted participants in thinking through designing with smart materials and a device that was functional. The activities in the workshop engaged the participants fostering creativity and excitement in the design process. Participants actively discussed with others how to

execute their ideas in a final design.

Although, over half the participants had worn a brace or had a close family member with a disability, this preliminary work was not able to include individuals with extensive experience with AT. Future participatory workshops would involve users of AT in co-design with children or involve children who use AT in design. Future work would build on this workshop to assess if involving users of AT might require different fabrication technology or techniques to aid in co-design. Also, to assess how children's perception about user's of AT may change through the co-design process. Do children show an increased awareness of challenges or needs of those with disabilities? Do children understand what questions are appropriate to ask users of AT to help aid in the design of AT? How will children's design change when considering input from those with disabilities?

6.4 Summary

This chapter examined how to design a personally customizable orthotic device using DIY technique, Orthorigami, for stroke patients, adjusted as a child grows, and how children design these devices. DIY AT addresses the challenges of users involvement in device selection, performance, and design to accommodate change in ability or preferences. The chapter outlines design considerations and design methods to assist in DIY AT. In particular, designers should consider: breathability, comfort, fit, support, aesthetics, and adaptability. To design DIY AT for stroke patients, thermochromic powder, having the same transition temperature as the SMP was introduced. This incorporation created greater independence over traditional commercial devices due to the ability to heat the device at a safe temperature with a hair dryer and not in the microwave. These commercial devices required patients to go to a practitioner whenever adjustment was needed. The chapter addressed how to design a device that can be adjusted as the child grows. The case study showed that iterative paper prototyping provided an accessible tool to create greater user involvement in device selection and performance. The study also presented an alternative ventilation method foam strips to provide protection from placing the device directly against the skin. The addition of photochromic powder added another aesthetic component. The last study address how

children design DIY AT and how the process of designing DIY AT makes them feel. The study showed that children were inspired to think of new designs and felt empowered in their ability to design DIY AT. Also, as with the second case study, that crafting aided in thinking through complex 2D to 3D design. Future work should build upon each of these case studies by involving a greater number of users of AT, practitioners, and DIY designers in collaboration. New work should seek to look at the insights co-design would bring to the design process and the designs themselves may change to reflect the AT user's needs.

7. SUMMARY AND CONCLUSION

This work sought to answer the research questions given in Chapter 1. Specifically, these questions can be summarized in four major areas: How can complex 3D structures be created from 2D SMP sheets using origami techniques? What are the effects of the manufacturing processes in creating these structures? How can structures for interactive design and DIY AT be made using origami or other techniques? How do children create and design with smart materials? The work assesses two avenues to create complex 3D structures from 2D SMP sheets: machining and laser cutting.

7.1 Laser-Cutting of SMP

The work presented showed that laser-cutting the SMP created a significant HAZ at speeds lower than 1000 mm/min for a power level of 90% and focal length of 70 mm. However, the HAZ remained quantitatively the same for a power of 80%, focal length of 70 mm, and speeds of 500 mm/min, 750 mm/min, 900 mm/min, and 1000 mm/min. The HAZ was also quantitatively the same for speed of 500 mm/min, focal length of 70 mm, and power levels of 90%, 80%, 70%, 60%, 57.5%, and 55%. The HAZ showed an increase with each change in the focal length from 80 mm to 90 mm to 100 mm at a power level of 90% and a speed of 3000 mm/min. Once the focal length reached 110 mm, with HAZ was approximately the same for increased focal lengths greater than 110 mm. The nano-AFM was able to capture the effect of the processing on the SMP. Specifically, the nano-AFM showed the effect of the HAZ on local T_g, while the DSC was unable to capture the change the in the bulk T_g. Laser-cutting is an efficient way to machine SMPs, however the thermal stressed induced on the part could potentially cause localized problems in utilizing the shape memory effect. The DSC is unable to capture the effect of the change in local T_g, unless the effect spans a significant portion of the bulk material. (This is seen in Figure 3.7 where two boundaries are cut on a thin strut creating an overlapping thermal diffusion layer.) Therefore, laser-cutting imposes thermal stress due to the breaking of chemical bonds with the material and should

be utilized with caution in designing structures with performance based on a specific T_g.

7.2 Machining of SMP

The work presented in Chapter 4 shows that creating folding structures with SMP using a process called Advanced Kirigami is possible. Specifically, the work shows that a process defocusing the laser and laser-cutting to create origami structures is not feasible. The chapter provides details of the associated spring-back angle, bend angle, and recovery angle using a laser-cutter and a CNC-machining for various bit sizes and depths of grooves for UHMWPE and SMP. These details can provide the parameters to create various advanced Kirigami structures. Finally, the chapter presents an advanced kirigami prototype based on creating grooves using a CNC machine in bi-layer SMP. Future work would seek to expand the bi-layer simple advanced Kirigami bi-layer SMP structures into more complex shapes. Also, future work would seek to create advanced Kirigami structures using UHMWPE and compare the use of SMP to UHMWPE within these structures.

7.3 SMP in Interactive Design

The set of results presented in Chapter 5 is a proof of concept for using SMPs in interactive design. The use of SMP in interactive design was presented in terms of two artworks: one representing a flower unfolding in a secret garden and another the nature of the chromatophore through an auxetic shape. Both works represent how complex ideas can be revealed through the tactile and visual nature of SMP and thermochromic smart materials. Future work would seek to build upon this work through involving children in workshops with smart materials and using interactive installations to teach abstract concepts. The workshops would assess how the tactile nature of the material aides in children's learning of new unfamiliar concepts.

7.4 SMPs in Orthorigami

The Orthorigami in Chapter 6 explored three case studies for designing DIY AT. These studies presented here have limitations, such as small sample size. Although, the sample size is acceptable for design, future work should include a larger pool of participants for each of the case studies. The case studies displayed that crafting techniques such as paper prototyping and sculpting aided in the

creation of DIY AT. Further, the studies presented methods of creating breathability and comfort (strips and holes) within these orthotic devices. The studies present how aesthetic and functional components can incorporated into DIY AT using photochromic and thermochromic powder. The final Orthorigami workshops with children reveal that the process of designing DIY AT makes children feel confident in their design capabilities and fosters innovative thinking. Future work would seek to involve users of AT with DIY AT designers or have users of AT design DIY AT. Future work should look at what users of AT can bring to the design of DIY AT. Do the same design tools, methods, and fabrication technology work for users of AT or co-designers? How does the design vary with input from users of AT? Future work would also seek to see children who co-design with users of AT have an increased awareness or empathy for those individuals with disabilities.

REFERENCES

[1] A. Lendlein and S. Kelch, "Shape-memory polymers," *Angewandte Chemie International Edition*, vol. 41, pp. 2034–2057, 2002.

[2] J. Hu, *Shape Memory Polymers and Textiles*. CRC Press, 2007.

[3] A. Lendlein and R. Langer, "Biodegradable, elastic shape-memory polymers for potential biomedical applications," *Science*, vol. 296, pp. 1673–1676, 2002.

[4] S. Mueller, B. Kruck, and P. Baudisch, "Laserorigami: Laser-cutting 3d objects," in *Proceedings of the SIGCHI Conference on Human Factors in Computing Systems*, (Paris, France), pp. 2585–2592, April 2013.

[5] R. J. Young and P. A. Lovell, *Introduction to Polymers*. CRC Press, 2011.

[6] B. Hitz, J. Ewing, and J. Hecht, *Introduction to Laser Technology*. Piscataway, New Jersey: IEEE Press, 3 ed., 2000.

[7] "Laos laser: How does a laser-cutter work." Web, 2016.

[8] J. Powell, CO_2 *Laser-Cutting*. London, United Kingdom: Springer, 2 ed., 1998.

[9] "Dsc differential scanning calorimeter." Web, 2007.

[10] B. N. Surfaces, "Bruker's thermal analysis (vita) module enables nanoscale thermal analysis of polymers," *AZO Nano*, 2009.

[11] M. T. Tolley, S. M. Felton, S. Miyashita, D. Aukes, D. Rus, and R. J. Wood, "Self-folding origami: Shape memory composites activated by uniform heating," *Smart Materials and Structures*, vol. 23, pp. 1–9, 2014.

[12] D. Deng, Y. Yang, Y. Chen, X. Lan, and J. Tice, "Accurately controlled sequential self-folding structures by polystyrene film," *Smart Materials and Structures*, vol. 26, pp. 1–13, 2017.

[13] R. M. Neville, J. Chen, X. Guo, F. Zhang, W. Wang, Y. Dobah, F. Scarpa, J. Leng, and H.-X. Peng, "A kirigami shape memory polymer honeycomb concept for deployment," *Smart Materials and Structures*, vol. 26, pp. 1–10, 2017.

[14] E. N. Y. Ling, "Naturology," in *Cheers 2011–UK Chine Art and Design Festival*, (London, United Kingdom), September 2011.

[15] J. Qi and L. Buechley, "Animating paper with shape memory alloys," in *Proceedings of the SIGCHI Conference on Human Factors in Computing Systems*, (Austin, TX), pp. 749–752, May 2012.

[16] Y. Y. C. Vili, "Investigating smart textiles based on shape memory materials," *Textile Research Journal*, vol. 77, pp. 290–300, 2007.

[17] A. Menges and S. Reichert, "Material capacity: Embedded responsiveness," *Architectural Design*, vol. 82, pp. 52–59, 2012.

[18] M. Kolle, A. Lethbridge, M. Kreysing, J. Baumberg, J. Aizenberg, and P. Vukusic, "Bio-inspired band-gap tunable elastic optical multi-layer fibers," *Advanced Materials*, vol. 25, pp. 2239–2245, 2013.

[19] J. Berry and J. H. Seo, "Incorporation of shape memory polymers in interactive design," in *Proceedings of the 21st International Symposium on Electronic Art*, (Vancouver, BC, Canada), July 2015.

[20] J. Reese, J. H. Seo, and A. Srinavasa, "Orthorigami: Implementing shape-memory polymers for customizing orthotic applications," in *Proceedings of the Fourteenth International Conference on Tangible, Embedded, and Embodied Interaction*, TEI '20, (New York, NY, USA), p. 123–130, Association for Computing Machinery, 2020.

[21] T. Xie and I. A. Rousseau, "Facile tailoring of thermal transition temperatures of epoxy shape memory polymers," *Polymer*, vol. 50, pp. 1852–1856, 2009.

[22] E. T. Akinlabi, R. M. Mahamood, and S. A. Akinlabi, *Advanced Manufacturing Techniques Using Laser Material Processing*. Hershey, Pennsylvania: IGI Global, 1 ed., 2016.

[23] "Lasersaur." Web, 2007.

[24] A. E. Clarke, *Situational analysis : grounded theory after the postmodern turn. Adele E. Clarke.* SAGE, 2005.

[25] M. Freeman and S. Mathison, *Researching children's experiences. Melissa Freeman, Sandra Mathison.* Guilford Press, 2009.

[26] P. Ghosh, "Thermomechanical modeling of a shape memory polymer," Master's thesis, Texas A&M University, College Station, TX, December 2008.

[27] C. Liu, H. Qin, and P. T. Mather, "Review of progess in shape-memory polymers," *Journal of Materials Chemistry*, vol. 17, pp. 1543–1558, 2007.

[28] F. Li, A. Perrenoud, and R. C. Larock, "Thermophysical and mechanical properties of novel polymers prepared by the cationic copolymerization of fish oils, styrene and divinylbenzene," *Polymer*, vol. 42, pp. 10133–10145, 2001.

[29] F. Li and R. C. Larock, "New soybean oil–styrene–divinylbenzene thermosetting copolymers. v. shape memory effect," *Journal of Applied Polymer Science*, vol. 84, pp. 1533–1543, 2002.

[30] K. Gall, M. L. Dunn, Y. Liu, D. Finch, M. Lake, and N. A. Munshi, "Shape memory polymer nanocomposites," *Acta Materialia*, vol. 50, pp. 5115–5126, 2002.

[31] Y. Osada and J. Gong, "Stimul-responisve polymer gels and their application to chemomechnical systems," *Progress in Polymer Science*, vol. 18, pp. 187–226, 1993.

[32] J. M. Ortega, W. Small, T. S. Wilson, W. J. Benett, J. M. Loge, and D. J. Maitland, "A shape memory polymer dialysis needle adapter for the reduction of hemodynamic stress within arteriovenous grafts," *IEEE Transactions on Biomedical Engineering*, vol. 54, no. 9, pp. 1722–1724, 2007.

[33] P. R. Buckley, G. H. Mckinley, T. S. Wilson, W. Small, W. J. Benett, J. P. Bearinger, M. W. Mcelfresh, and D. J. Maitland, "Inductively heated shape memory polymer for the magnetic

actuation of medical devices," *IEEE Transactions on Biomedical Engineering*, vol. 53, no. 10, pp. 2075–2083, 2006.

[34] T. S. Wilson, W. S. IV, W. J. Benett, J. P. Bearinger, and D. J. Maitland, "Shape memory polymer therapeutic devices for stroke," in *Smart Medical and Biomedical Sensor Technology III* (B. M. Cullum and J. C. Carter, eds.), vol. 6007, pp. 157 – 164, International Society for Optics and Photonics, SPIE, 2005.

[35] W. Lehmann, H. Skupin, C. Tolksdorf, E. Gebhard, R. Zentel, P. Krüger, M. Lösche, and F. Kremer, "Giant lateral electrostriction in ferroelectric liquid-crystalline elastomers," *Nature*, vol. 410, pp. 447–450, 2001.

[36] D. L. T. III, P. Keller, J. Naciri, R. Pink, H. Jeon, D. Shenoy, and B. R. Ratna, "Liquid crystal elastomers with mechnical properties of a muscle," *Macromolecules*, vol. 34, pp. 5868–5875, 2001.

[37] I. A. Rousseau and P. T. Mather, "Shape memory effect exhibited by smectic-c liquid crystalline elastomers," *J. Am. Chem. Soc.*, vol. 125, no. 50, pp. 15300–15301, 2003.

[38] C. Liu, I. Rousseau, H. Qin, and P. Mather, "Tailored shape memory polymers: not all smps are created equal," 01 2002.

[39] H. Jeon, P. Mather, and T. Haddad, "Shape memory and nanostructure in poly(norbornyl-poss) copolymers," 2000.

[40] C. Liu and P. T. Mather, "Thermomechanical characterization of blends of poly (vinyl acetate) with semicrystalline polymers for shape memory applications," in *ANTEC-CONFERENCE PROCEEDINGS-*, vol. 2, pp. 1962–1966, UNKNOWN, 2003.

[41] J. Kruth, M. Leu, and T. Nakagawa, "Process in additive manufacturing and rapid prototyping," *Annuals of the CIRP*, vol. 47, pp. 525–541, 1998.

[42] K. V. Wong and A. Hernandez, "A review of additive manufacturing," *ISRN Mechanical Engineering*, vol. 2012, pp. 1–10, 2012.

[43] Y. Liu, J. Genzer, and M. D. Dickey, ""2d or not 2d": Shape-programming polymer sheets," *Progress in Polymer Science*, vol. 52, pp. 79–106, 2016.

[44] T. Xie, X. Xiao, and Y.-T. Cheng, "Revealing triple-shape memory effect by polymer bilayers," *Macromolecular Rapid Communications*, vol. 30, pp. 1823–1827, 2009.

[45] G. Chryssolouris, *Laser Machining: Theory and Practice*. New York, New York: Springer-Verlang New York, Inc., 1 ed., 1991.

[46] A. K. Maini, *Lasers and Optoelectronics: Fundamentals, Devices, Applications*. Chichester, West Sussex, United Kingdom: John Wiley & Sons Ltd., 1 ed., 2013.

[47] W. M. Steen and J. Mazumder, *Laser Material Processing*. London, United Kingdom: Springer-Verlang London Limited, 4 ed., 2010.

[48] "Rp photonics encyclopedia: Optical intensity." Web, 2016.

[49] R. Crafer and P. J. Oakley, eds., *Laser Processing in Manufacturing*. Springer Science + Business Media Dordrecht, 1 ed., 1993.

[50] A. E. Siegman, *Lasers*. Mill Valley, California: University Science Books, 1 ed., 1986.

[51] "Technical note: Gaussian beam optics." Web, 2018.

[52] S. Zhurkov and V. Korsukov, "Atomic mechanism of fracture of solid polymers," *Polymer Physics*, vol. 12, pp. 385–398, 1974.

[53] J. Stuart and D. Smith, "Some aspects of the degradation of epoxide resins," *Journal of Applied Polymer Science*, vol. 9, pp. 3195–3214, 1964.

[54] J. P. Davim, N. Barricas, M. Conceição, and C. Oliveira, "Some experimental studies on co_2 laser cutting quality of polymeric materials," *Journal of Materials Processing Technology*, vol. 198, pp. 99–104, 2008.

[55] J. Macan and M. Ivanković, "Influence of epoxy-amine ratio on degradation of epoxy-silica hybrid materials," in *Progress in Polymer Degradation and Stability Research* (H. W. Moeller, ed.), pp. 209–231, New York, NY: Nova Science Publishers, Inc., 2008.

[56] G. Meyers, A. Pastzor, and K. Kjoller, "Localized thermal analysis: From the micto- to the nanoscale," *American Laboratory*, 2007.

[57] K. Xiao and L. Zhang, "The role of viscous deformation in the machining of polymers," *International Journal of Mechanical Sciences*, vol. 44, pp. 2317–2336, 2002.

[58] J. W. Carr and C. Feger, "Ultraprecision machning of polymers," *Precision Engineering*, vol. 15, pp. 222–237, 1993.

[59] M. Alauddin, I. Choudhury, M. E. Baradie, and M. J. Hashmi, "Plastics and their machining: A review," *Journal of Materials Processing Technology*, vol. 54, pp. 40–46, 1995.

[60] Y. Liu, J. K. Boyles, J. Genzer, and M. D. Dickey, "Self-folding of polymer sheets using local light absorption," *Soft Matter*, vol. 8, pp. 1764–1769, 2012.

[61] C. Yuan, Z. Ding, T. Wang, M. L. Dunn, and H. J. Qi, "Shape forming by thermal expansion mismatch and shape memory locking in polymer/elastomer laminates," *Smart Materials and Structures*, vol. 26, pp. 1–12, 2017.

[62] Q. Ge, C. K. Dunn, H. J. Qi, and M. Dunn, "Active origami by 4d printing," *Smart Materials and Structures*, vol. 23, pp. 1–15, 2014.

[63] M. Mansoori, N. Kalantar, T. Creasy, and Z. Rybkowski, "Toward adative architectural skins. designing temperature-responsive curvilinear surfaces," in *International Conference on Computer-Aided Architectural Design Research in Asia (CAADRIA) 2018*, (Tsinghua University, Beijing, China), May 2018.

[64] M. Eisenber, "Tangible ideas for children: Materials science as the future of educational technology," in *Proceedings of the 2004 conference on Interaction design and children: building a community*, (Baltimore, Maryland), pp. 19–26, June 2004.

[65] K. Tan, E. Lewis, N. Avis, and P. Withers, "Using augmented reality to promote an understanding of materials science to school children," in *ACM SIGGRAPH ASIA 2008*, (Singapore), December 2008.

[66] H. Ishii, D. Lakatos, L. Bonanni, and J.-B. Labrune, "Radical atoms: beyond tangible bits, towards transformable materials," *Interactions*, vol. 19, pp. 38–51, 2012.

[67] F. G. A. S.p.A., "Techno naturology, design "au natural"," *Lancia TrendVisions | Fashion, design and lifestyle magazine*, November 2010.

[68] C. Lelieveld, *Smart Materials for the Realization of an Adaptive Building Component*. PhD thesis, Delft University of Technology, Delft, Netherlands, February 2013.

[69] J. Qi, "Jie qi."

[70] G. Esquivel, D. Weiser, D. Hartl, and D. Whitten, "A shape memory-based morphing wall," *International Journal of Architectural Computing*, vol. 11, pp. 347–362, 2013.

[71] A. Villanueva, C. Smith, and S. Priya, "A biomimetic robotic jellyfish (robojelly) actuated by shape memory alloy composite actuators," *Bioinspiration & Biomimetics*, vol. 6, 2011.

[72] S. Morin, R. Shepherd, S. W. Kwok, A. Stokes, A. Nemiroski, and G. Whitesides, "Camouflage and display for soft machines," *Science*, vol. 337, pp. 828–832, 2012.

[73] M. B. Laboratory, "The long-finned squid (loligo pealei)," 2008.

[74] J. Rossiter, K. Takashima, F. Scarpa, P. Walters, and T. Mukai, "Shape memory polymer hexachiral auxetic structures with tunable stiffness," *Smart Materials and Structures*, vol. 23, 2014.

[75] T. Kaihou and A. Wakita, "Electronic origami with the color-changing function," in *Proceedings of the Second International Workshop on Smart Material Interfaces: Another Step to a Material Future*, SMI '13, (New York, NY, USA), p. 7–12, Association for Computing Machinery, 2013.

[76] J. Du, P. Markopoulos, Q. Wang, M. Toeters, and T. Gong, "Shapetex: Implementing shape-changing structures in fabric for wearable actuation," in *Proceedings of the Twelfth International Conference on Tangible, Embedded, and Embodied Interaction*, TEI '18, (New York, NY, USA), p. 166–176, Association for Computing Machinery, 2018.

[77] M. Coelho and P. Maes, "Sprout i/o: A texturally rich interface," in *Proceedings of the 2nd International Conference on Tangible and Embedded Interaction*, TEI '08, (New York, NY, USA), p. 221–222, Association for Computing Machinery, 2008.

[78] J. Ou, L. Yao, D. Tauber, J. Steimle, R. Niiyama, and H. Ishii, "Jamsheets: Thin interfaces with tunable stiffness enabled by layer jamming," in *Proceedings of the 8th International Conference on Tangible, Embedded and Embodied Interaction*, TEI '14, (New York, NY, USA), p. 65–72, Association for Computing Machinery, 2014.

[79] D. Groeger, E. Chong Loo, and J. Steimle, "Hotflex: Post-print customization of 3d prints using embedded state change," in *Proceedings of the 2016 CHI Conference on Human Factors in Computing Systems*, CHI '16, (New York, NY, USA), p. 420–432, Association for Computing Machinery, 2016.

[80] E. Giles, J. van der Linden, and M. Petre, "Weaving lighthouses and stitching stories: Blind and visually impaired people designing e-textiles," in *Proceedings of the 2018 CHI Conference on Human Factors in Computing Systems*, CHI '18, (New York, NY, USA), p. 1–12, Association for Computing Machinery, 2018.

[81] A. Hurst and S. Kane, "Making "making" accessible," in *Proceedings of the 12th International Conference on Interaction Design and Children*, IDC '13, (New York, NY, USA), p. 635–638, Association for Computing Machinery, 2013.

[82] M. J. Scherer, "Outcomes of assistive technology use on quality of life," *Disability and Rehabilitation*, vol. 18, no. 9, pp. 439–448, 1996. PMID: 8877302.

[83] B. Phillips and H. Zhao, "Predictors of assistive technology abandonment," *Assistive Technology*, vol. 5, no. 1, pp. 36–45, 1993. PMID: 10171664.

[84] J. Hook, S. Verbaan, A. Durrant, P. Olivier, and P. Wright, "A study of the challenges related to diy assistive technology in the context of children with disabilities," in *Proceedings of the 2014 Conference on Designing Interactive Systems*, DIS '14, (New York, NY, USA), p. 597–606, Association for Computing Machinery, 2014.

[85] E. Buehler, S. Branham, A. Ali, J. J. Chang, M. K. Hofmann, A. Hurst, and S. K. Kane, *Sharing is Caring: Assistive Technology Designs on Thingiverse*, p. 525–534. New York, NY, USA: Association for Computing Machinery, 2015.

[86] A. Hurst and J. Tobias, "Empowering individuals with do-it-yourself assistive technology," in *The Proceedings of the 13th International ACM SIGACCESS Conference on Computers and Accessibility*, ASSETS '11, (New York, NY, USA), p. 11–18, Association for Computing Machinery, 2011.

[87] S. McDonald, N. Comrie, E. Buehler, N. Carter, B. Dubin, K. Gordes, S. McCombe-Waller, and A. Hurst, "Uncovering challenges and opportunities for 3d printing assistive technology with physical therapists," in *Proceedings of the 18th International ACM SIGACCESS Conference on Computers and Accessibility*, ASSETS '16, (New York, NY, USA), p. 131–139, Association for Computing Machinery, 2016.

[88] G. Baronio, S. Harran, and A. Signornoi, "A critical analysis of a hand orthosis reverse engineering and 3d printing process," *Applied Bionics and Biomechanics*, vol. 2016, pp. 1–7, 2016.

[89] Y.-J. Chen, H. Lin, X. Zhang, W. Huang, L. Shi, and D. Wang, "Application of 3d-printed and patient-specific cast for the treatment of distal radius fractures: Initial experience," *3D Printing in Medicine*, vol. 3, no. 11, 2017.

[90] H. W. Lin, L. Aflatoony, and R. Wakkary, "Design for one: A game controller for a quadriplegic gamer," in *CHI '14 Extended Abstracts on Human Factors in Computing Systems*, CHI EA '14, (New York, NY, USA), p. 1243–1248, Association for Computing Machinery, 2014.

[91] J. L. Meissner, J. Vines, J. McLaughlin, T. Nappey, J. Maksimova, and P. Wright, "Do-it-yourself empowerment as experienced by novice makers with disabilities," in *Proceedings of the 2017 Conference on Designing Interactive Systems*, DIS '17, (New York, NY, USA), p. 1053–1065, Association for Computing Machinery, 2017.

[92] P. McKee and L. Morgan, *Orthotics in Rehabilitation: Splinting the Hand and Body: An Instructor's Guide*. F.A. Davis Company, 1997, 1997.

[93] A. A. Portnova, G. Mukherjee, K. M. Peters, A. Yamane, and K. M. Steele, "Design of a 3d-printed, open-source wrist-driven orthosis for individuals with spinal cord injury," *PloS ONE*, vol. 13, no. 2, 2018.

[94] S. Jacoby and L. Buechley, "Drawing the electric: Storytelling with conductive ink," in *Proceedings of the 12th International Conference on Interaction Design and Children*, IDC '13, (New York, NY, USA), p. 265–268, Association for Computing Machinery, 2013.

[95] Y. Takegawa, K. Fukushi, T. Machover, T. Terada, and M. Tsukamoto, "Construction of a prototyping support system for painted musical instruments," in *Advances in Computer Entertainment* (A. Nijholt, T. Romão, and D. Reidsma, eds.), (Berlin, Heidelberg), pp. 384–397, Springer Berlin Heidelberg, 2012.

[96] A. Minuto, *Materials that matter: Smart materials meet art interaction design*. PhD thesis, University of Twente, Netherlands, Oct. 2016. SIKS dissertation series no. 2016-38.

[97] L. Buechley, N. Elumeze, and M. Eisenberg, "Electronic/computational textiles and children's crafts," in *Proceedings of the 2006 Conference on Interaction Design and Children*, IDC '06, (New York, NY, USA), p. 49–56, Association for Computing Machinery, 2006.

[98] S. Kuznetsov, P. Fernando, E. Ritter, C. Barrett, J. Weiler, and M. Rohr, "Screenprinting and tei: Supporting engagement with steam through diy fabrication of smart materials," in *Proceedings of the Twelfth International Conference on Tangible, Embedded, and Embodied Interaction*, TEI '18, (New York, NY, USA), p. 211–220, Association for Computing Machinery, 2018.

[99] T. Brown *et al.*, "Design thinking," *Harvard business review*, vol. 86, no. 6, p. 84, 2008.